UNIVERZITA KARLOVA V PRAZE

Přírodovědecká fakulta

Studijní obor: Fyzikální chemie

RNDr. Martina Riesová

SYSTÉMOVÉ ZÓNY V KAPILÁRNÍ ELEKTROFORÉZE

System Zones in Capillary Electrophoresis

Dizertační práce

Vedoucí práce: prof. RNDr. Bohuslav Gaš, CSc.

Praha 2013

Předkládaná dizertační práce shrnuje výsledky získané během mého doktorského studia ve Skupině elektroforetických a chromatografických separačních metod (ECHMET) na Katedře fyzikální a makromolekulární chemie Přírodovědecké fakulty Univerzity Karlovy v Praze.

Práce byla financována v souvislosti s řešením projektů GA UK, č. grantu 51009, GAČR projekt č. 203/08/1428, CEEPUS CIII-RO-0010-07-1213-M-61693 a výzkumného záměru MŠMT, projekt MSM0021620857.

Prohlášení

Prohlašuji, že jsem tuto dizertační práci zpracovala samostatně, pod vedením školitele prof. RNDr. Bohuslava Gaše, CSc. a že jsem uvedla všechny použité informační zdroje a literaturu. Tato práce ani její podstatná část nebyla předložena k získání jiného nebo stejného akademického titulu.

V Praze dne ……

……..

podpis

Poděkování

Nevím, čím jsem si to zasloužila, ale v mém studijním, pracovním i osobním životě mě obklopují samí úžasní lidé, které mám ráda, kterých si vážím a kteří (troufnu si tvrdit) mají rádi mě, podporují mě, fandí mi, ale hlavně je tu všechny mám, když potřebuji poradit a podržet. Na tomto místě bych jim všem ráda poděkovala.

Raději tu nebudu všem těm úžasným Frájám a Frájám, Květuškám, Vilíkům, Jirkům, Radímkům, Bobům, Pavlům, Echmeťákům, Dětem, Chemikům, Pítroušům, babičkám, tatíkům, ségrám a rozhodně také ne Ťuťasům děkovat jmenovitě a konkrétně - mohlo by mě to zbytečně dojmout☺

Díky !!!

Klíčová slova

kapilární zónová elektroforéza, systémové píky, lineární model elektromigrace PeakMaster, komplexační činidlo, komplexační rovnováha

Keywords

capillary zone electrophoresis, system peaks, linear theory of electromigration, PeakMaster, complexation agent, complexation equilibrium

Souhrn

Kapilární elektroforéza je účinná, spolehlivá a rychlá separační metoda s nízkou spotřebou chemikálií a tedy i nízkými náklady na analýzu. Systémové zóny, které tato práce studuje, jsou nevyhnutelnou součástí každého elektroforetického systému a v nepříznivých případech mohou značně ovlivnit elektroforetické výsledky, znehodnotit je, nebo vést k jejich špatnému výkladu.

Pomocí predikčních počítačových programů vystavěných na základě teoretického popisu elektromigrace lze v jednoduchých systémech dobře a spolehlivě předpovídat pozice systémových píků. Tato předpověď však nemusí být dostatečná a nemusí zaručit jednoznačnou identifikaci systémových píků v získaných záznamech. V rámci předkládané práce byl proto rozšířen současný teoretický model elektromigrace a vznikla nová verze 5.3 predikčního programu PeakMaster, která umožňuje předpovídat nejen pozice, ale i tvary a polarity systémových zón. Pomocí nového PeakMasteru 5.3 lze tak lépe předpovídat případnou interakci nebo překryv systémových píků s píky analytů a nově může být také optimalizováno složení vzorku právě s ohledem na polaritu a tvary systémových píků. Program PeakMaster má široké využití v běžné analytické praxi při efektivním výběru separačních systémů a predikce elektroforetických výsledků.

Aplikovatelnost kapilární zónové elektroforézy může být rozšířena tím, že se použije komplexační činidlo jako přídavek do základního elektrolytu za účelem cílené interakce s analyty. Přesto však nelze vyloučit (zejména při nevhodné volbě pufru) ani současnou interakci komplexačního činidla se složkou základního elektrolytu. Ukázali jsme, že tato nechtěná interakce může mít značný vliv na vlastnosti elektroforetického systému (pH, vodivost, iontovou sílu) nebo na chování systémových zón. Teoreticky i experimentálně jsme vyšetřili změny vlastností v systémech, kde komplexuje neutrální komplexační činidlo s pufrující složkou základního elektrolytu a ukázali jsme možný dopad na elektroforetické výsledky. Dále jsme prokázali, že chování systémových píků v komplexujících systémech se liší od chování, které předpovídá klasická teorie elektromigrace. Jednoduchým testem k odhalení nechtěné komplexace může být kontrolování hodnoty pH po přídavku (třeba i neutrálního) komplexačního činidla do základního elektrolytu.

Abstract

Capillary electrophoresis is a method of choice in many analytical laboratories for its high separation efficiency, rapidity, low consumption of chemicals and therefore low costs. Inherent to each electrophoretic separation system are system peaks, which can significantly affect or confuse the electrophoretic results.

In capillary zone electrophoresis, position of system zones can be predicted easily and reliably by means of prediction software based on a theoretical description of electromigration. However, the prediction of only position of a system zone may not be sufficient for identification of system peaks in obtained electropherograms. Therefore, an existing theoretical model was significantly extended and new version of PeakMaster software (PeakMaster 5.3) was introduced in the framework of this thesis. PeakMaster 5.3 enables to predict not only the positions of system zones, but also their shapes and polarity. Thus, PeakMaster 5.3 improves the prediction possibility of overlapping or interaction of system peaks with analyte peaks. Moreover, composition of the sample can be optimized in order to obtain convenient shapes and amplitudes of system peaks.

The applicability of capillary zone electrophoresis can be extended by addition of a complexation agent into the background electrolyte. Complexation additives are primarily intended to offer additional interactions for analytes. Nevertheless, simultaneous interactions of background constituents with complexation agents may occur. We demonstrated that such unwanted interactions seriously influence properties of the background electrolyte (pH, ionic strength or conductivity) or behavior of system peaks. We investigated changes of fundamental buffer properties caused by complexation, both theoretically and experimentally, in systems where a neutral complexation agent interacts with buffering constituents of several background electrolytes. We also showed how these changes impact on electrophoretic results in practice. Further, we revealed that behavior of system peaks differs from the behavior predicted by classical theory of electromigration in such systems. We proposed to measure pH changes after addition of neutral complexation agent as a simple method for detection of unwanted complexation.

Obsah

Seznam použitých zkratek a symbolů

A	analyt
BGE	základní elektrolyt (*background electrolyte*)
C	komplexační činidlo
CD	cyklodextrin
CZE	kapilární zónová elektroforéza
CHES	*N*-cyclohexyl-2-aminoethansulfonová kyselina
HVL	Haarhoff – van der Lindeho funkce
LTE	lineární teorie elektromigrace
SP	systémový pík
β-CD	beta-cyklodextrin

b_x	molární vodivostní odezva
c_i	molární koncentrace *i*-té složky
$c_{i,z}$	molární koncentrace *z*-té formy *i*-té složky
c_i^{in}	počáteční molární koncentrace *i*-té složky
$\vec{c}$	vektor molárních koncentrací
$\tilde{c}_i$	porucha v koncentraci *i*-té složky
$\vec{\tilde{c}}$	vektor poruch v koncentracích
C_i	konstantní hodnota molární koncentrace *i*-té složky
J	proudová hustota
$\boldsymbol{M}$	čtvercová matice mobilit
n_i	nejmenší sytnost *i*-té složky
p_i	nejvyšší sytnost *i*-té složky
S_x	*velocity slope*
T	čas
TR	*transfer ratio*
u_i	iontová mobilita *i*-té složky
$u_{i,z}$	iontová mobilita *z*-té iontové formy *i*-té složky
X	podélná osa kapiláry ve směru vnějšího elektrického pole
Z	nábojové číslo
κ	specifická vodivost
κ_{BGE}	specifická vodivost neporušeného základního elektrolytu

Předmluva

Systémové píky provázejí celé mé vysokoškolské studium. Na začátku, v bakalářském stupni, jsem se věnovala miniaturizované elektroforéze na čipu a systémovým zónám v komerčně prodávaných základních elektrolytech pro analýzu proteinů. Později jsem se zabývala výjimečnými základními elektrolyty, jež vykazují oscilační chování, které je způsobeno komplexními hodnotami mobilit systémových zón. Získané zkušenosti a vědomosti o problematice systémových zón a píků jsem využila a hlavně prohloubila i v rámci mého doktorského studia.

Předmětem této práce bylo v prvním kroku zlepšování možností predikce a identifikace systémových píků v kapilární elektroforéze – rozšíření počítačového programu PeakMaster vyvinutého v naší pracovní skupině pro předpovídání výsledků kapilární zónové elektroforézy. O této etapě pojednávají dvě publikace v předkládané práci označené jako Publikace 2 a Publikace 3.

Další velikou kapitolou, která byla v rámci mé dizertační práce započata a které doposud v literatuře nebyla věnována téměř žádná pozornost, je chování systémových píků v elektroforetických systémech obsahujících komplexační činidlo. Náš zájem o komplexační činidla v separačních metodách vyústil v publikaci souhrnného článku (Publikace 1), kterou v této práci přikládám jakou součást kapitoly Úvod. Účelem přítomnosti komplexačního činidla v základním elektrolytu bývá cílená interakce činidla s analytem a zlepšení selektivity separace nebo dosažení chirálních separací. Přítomnost komplexačního činidla může ale také výrazně ovlivnit vlastnosti základních elektrolytů a značně ovlivnit elektroforetické výsledky. Této problematice přísluší Publikace 4 a 5.

V závěru práce jsou zařazeny Kapitola 4.3 a Publikace 6 jako ukázky praktického využití kapilární zónové elektroforézy, při kterých jsem zúročila a uplatnila nabyté zkušenosti. Díky predikčním programům jsem byla schopna velmi rychle vybrat vhodné separační systémy a to nejen z hlediska základních vlastností základního elektrolytu, ale i s ohledem na počty a pozice systémových zón.

1. Úvod

Od dob svého vzniku ušla elektroforéza dlouhou cestu. Vyvíjela se, brala na sebe různé podoby, díky nimž překonávala mnohé výzvy a splňovala nejrůznější cíle. V dnešních dnech, ve své „kapilární“ podobě, vyzrála v excelentní techniku, hojně používanou v mnoha moderních analytických laboratořích po celém světě. Vyniká vysokou účinností, rychlostí a především nízkou spotřebou chemikálií, tedy nízkými náklady. Použitelnost kapilární elektroforézy dále rozšiřují její nejrůznější modifikace. Lze ji proto využít k analýzám široké škály anorganických i organických látek, nejen ionických, ale i neutrálních, k achirálním i chirálním separacím. Směle tak konkuruje a velmi často i nepostradatelně doplňuje ostatní účinné separační metody, zejména vysokoúčinnou kapalinovou chromatografii.

Nezpochybnitelnou výhodou kapilární elektroforézy oproti ostatním metodám je její ucelený teoretický popis. Příslušné matematické modely, implementovány do počítačových programů, umožňují předpovídat elektroforetické výsledky a tak snadno hledat a optimalizovat vhodné separační systémy. Mnohdy také tyto simulační programy pomáhají vysvětlit experimentálně pozorované jevy nebo jimi lze předpovědět neobvyklé chování některých elektroforetických systémů.

Některé jevy, které elektroforetické experimenty doprovázejí, však mohou uživatelům život značně znepříjemnit. V kapilární zónové elektroforéze je jedním z těchto jevů přítomnost systémových zón, která může v krajních případech vést ke špatnému výkladu elektroforetických výsledků nebo k jejich úplnému znehodnocení. Systémové zóny, v detektoru zaznamenané jako systémové píky, mohou být totiž mylně považovány za píky analytů nebo s nimi mohou interagovat. Tato interakce pak vede k deformaci píků analytů, které pak často není možné vyhodnotit. Systémové zóny jsou ale vlastní každému elektroforetickému sytému a jsou tak nevyhnutelnou součástí kapilární zónové elektroforézy. Vyšetřování jejich chování v jednoduchých i stále složitějších systémech, zlepšování možností jejich předpovědí a rozeznávání ve výsledných elektroferogramech je tedy smysluplným úkolem.

1.1 Systémové zóny v kapilární zónové elektroforéze

Systémové zóny vznikají v kapilární zónové elektroforéze (CZE) při nadávkování vzorku. Jelikož se složení zóny vzorku liší od složení základního elektrolytu (i když třeba jen nepatrně), dojde při nadávkování k porušení koncentračních profilů složek základního elektrolytu (BGE). Po vložení napětí pak mohou tyto poruchy – systémové zóny, podobně jako zóny analytů, putovat kapilárou. Pokud migrují směrem k detektoru, mohou být detektorem zaznamenány jako píky, které ale nepříslušejí žádnému z přítomných analytů. Pro takové píky se ustálil název systémové píky.

Pojem systémový pík byl poprvé použit pro obdobný jev v kapalinové chromatografii [1]. V chromatografii se také jako první objevily pokusy o vysvětlení základních principů vzniku a výskytu systémových píků a popis vztahů systémových píků k termodynamice a kinetice procesů v chromatografické koloně [2-4]. V CZE stoupl zájem o systémové píky později a je spojen s rozvojem nepřímé UV detekce [5]. Systémové píky lze totiž detekovat pouze v případě, že použitý detektor reaguje alespoň na jednu složku základního elektrolytu. To je v CZE nejčastěji případ vodivostní nebo právě nepřímé UV detekce.

Ačkoliv jsou systémové píky považovány spíše za rušivý jev, lze je využít například ke stanovení kritické micelární koncentrace [6]. Jisté, i když ne příliš přesvědčivé, je využití systémových píků také v podobě vakantní afinitní kapilární elektroforézy, například při stanovení konstant stability [7,8]. Problematika systémových píků byla několikrát shrnuta v pracích Gebauera a Beckerse [9,10] a později v přehledových článcích Gaše a kol. [11,12].

Zpočátku byly systémové zóny zkoumány zejména experimentálně, autoři však správně soudili, že existenci systémových zón, popřípadě jejich počet i mobility musí plynout ze správného teoretického popisu zónové elektroforézy nebo procesů kapalinové chromatografie [4].

1.2 Matematické přístupy k popisu CZE a systémových zón

Elektroforéza má ve srovnání s chromatografií výhodu v jednoduchosti uspořádání, v němž probíhá separační proces. To umožňuje dobře a v principu jednoduše matematicky popsat elektromigrační proces pomocí (i) rovnice kontinuity (ii) podmínky elektroneutrality a (iii) rovnic pro příslušné rovnováhy (acidobazické, komplexační). Sadu rovnic, nabízejících úplný popis elektromigračních procesů, lze řešit pouze numericky pomocí počítačových programů. Numerické simulační programy [13-17] tak nabízejí detailní náhled do dynamiky elektromigračních procesů. Simulace jsou ale náročné na čas i výkon počítačů a neumožňují počítat kvantitativní charakteristiky elektroforetických systémů, na základě kterých by bylo možné vyslovovat některá obecná pravidla například o počtu a mobilitě systémových zón, parametrech zón analytů a podobně. Proto se autoři již v minulosti zaměřili na hledání popisu kapilární zónové elektroforézy majícího analytické řešení.

1.2.1 Hmotnostní bilance na pohyblivých rozhraních

Prvním přístupem k řešení elektromigračního chování zón byla formulace rovnic hmotnostní bilance na pohyblivých rozhraních. Prvními, kdo představil tento koncept pro kapilární zónovou elektroforézu, byli Longsworth [18] a Alberty [19] již v polovině 20. století. Na tyto základy navázal později Beckers, který se rozsáhle věnoval popisu vzniku systémových zón i teoretickému popisu zónové elektroforézy samotné. Použil model stacionárního stavu využívaný v izotachoforéze a nestacionární procesy kapilární zónové elektroforézy řešil opakovanou aplikací tohoto stacionárního modelu. Na základě takového přístupu ukázal, že systémové píky a pohybující se rozhraní vznikají z poruch koncentrace a pH základního elektrolytu a popsal základní zákonitosti jejich mobilit v jednoduchých systémech [20]. Stejný postup následně použil pro výpočty složení zón analytů, včetně pH a koncentrace koiontů a protiiontů. Byl tedy schopen předpovědět i záznamy pro nepřímou a vodivostní detekci. Z vypočítaných změn pH a elektrického pole v zóně vzorku a z mobilit koiontů také určoval tvar (*fronting* nebo *tailing*) a polaritu píků analytů a odvodil některá obecná pravidla pro výskyt daného tvaru a polarity píku v daných typech jednoduchých základních elektrolytů s jedním

koiontem [21,22]. Tento model byl pak rozšířen i pro systém s dvěma a více koionty nebo protiionty, kdy už ale složitost sytému a výpočtů neumožňovala taková obecná pravidla určit. Obecný popis byl v takovém případě nahrazen sadou diagramů, tzv. SystChart, které zobrazovaly vztahy mezi mobilitou analytu a jednotlivými parametry (pH, koncentrace kationtů a aniontů v BGE) pro konkrétní základní elektrolyt. Pomocí diagramů SystChart bylo možné alespoň odhadovat asymetrii a polaritu píků v konkrétních BGE [23,24].

Někteří autoři studovali systémové píky a zejména jejich počet pomocí vakantní elektroforézy [25,26]. Při popisu píků analytů dávají Gebauer a Boček do spojitosti *fronting* a *tailing* píků se záporným či kladným znaménkem veličiny *velocity slope* S_x a sestavují diagramy tvarů píků (*Peak Shape Diagram*) pro daný BGE [27]. V přístupu zavedeném Beckersem bylo dále možné formulovat pro jednoduché systémy veličiny důležité pro vodivostní a nepřímou detekci – limitní molární vodivostní odezvu b_x [28] a *transfer ratio TR* [29]. Tento přístup uměl předpovídat existenci některých systémových píků nebo interakci systémových zón se zónou analytu, způsobující neobvyklou nebo tzv. schizofrenní disperzi píku analytu [30,31]. Často diskutovaným tématem v problematice systémových píků byl jejich počet. Z modelu pohybujících se rozhraní nevyplývá jednoznačné pravidlo o počtu systémových píků a předpovědi se často opíraly jen o experimentální zkušenosti pro dané typy BGE [10,32-34] a tzv. galerie systémových zón [35]. Na základě tohoto přístupu nebylo možné charakterizovat obecný systém (*N* složek, slabých či silných, jednosytných či vícesytných, kyselin, zásad či amfolytů).

1.2.2 Lineární teorie elektromigrace

Druhý přístup k teoretickému popisu kapilární zónové elektroforézy zavedl Poppe [36,37], když vysvětlil existenci systémového píku a možnost nepřímé detekce na základě matematického modelu linearizovaných transportních rovnic. Tento matematický model ústil v řešení problému vlastních hodnot matice (*eigenvalues problem*) a Poppe proto nazval systémové píky eigenpíky. Jako první také vyslovil předpověď, že systém s *N* stupni volnosti (*N* složek systému) bude mít *N* eigenpíků. Každému z píků přísluší jedna vlastní hodnota matice s rozměrem mobility a vlastní

vektor, který popisuje relativní intenzity poruchy každé složky v dané zóně. Pro tento model se později vžil název lineární teorie elektromigrace (LTE). V dalších pracích skupina Poppeho úspěšně objasňovala, na základě LTE, jevy související s nepřímou detekcí [38], s předávkovanými systémy [36] nebo předpovídala pozice a intenzitu systémových píků [39].

Na tento model navázala Gašova skupina. Zabývala se systémy silných jednosytných elektrolytů [40], slabých jednosytných elektrolytů [41] a postupně zobecnila lineární teorii elektromigrace pro *N* složek, slabých či silných kyselin, zásad nebo amfolytů libovolné sytnosti [42]. Z jevů spojených se systémovými píky se tato skupina ve svých pracích zabývala rezonancí, tedy jevem nastávajícím v případě rovnosti mobilit analytu a systémového píku [40], vysvětlila existenci stacionárního píku [41] a předpověděla systémy, které zmíněný pík nemají [42]. Z LTE také vyplynulo, že mobility systémových zón mohou být v principu komplexní čísla. Takové systémy pak byly skutečně nalezeny a vykazují neobvyklé, oscilační, chování [43,44]. Dále bylo prokázáno, že i v rámci tohoto přístupu lze získat veličiny: molární vodivostní odezvu, *transfer ratio* a *relative velocity slope*, a předpovídat tak odezvy vodivostní i nepřímé spektrofotometrické detekce [42]. Spektrálním rozkladem matice mobilit byla získána matice amplitud systémových píků [45]. Z lineární teorie elektromigrace jednoznačně vyplývá, že počet eigenmobilit systému, tedy i počet systémových zón, je roven počtu složek systému. Ionty OH^- a H_3O^+ nejsou považovány za složky systému, jejich koncentrace je dána acidobazickými rovnováhami a podmínkou elektroneutrality. Přesto tyto ionty mohou výrazně ovlivnit chování systémových zón. Lineární teorie elektromigrace předčila přístup hmotnostní bilance na pohyblivém rozhraní a nabízí ucelený matematický model pro kapilární zónovou elektroforézu.

1.3 Simulační program PeakMaster

V předchozí kapitole byly shrnuty základní přístupy matematického popisu kapilární zónové elektroforézy. Tyto matematické modely byly od počátku implementovány do počítačových programů, které měly za cíl předpovídat výsledky

elektroforetických experimentů. Lineární teorie elektromigrace se stala základem pro simulační program PeakMaster, který byl vyvinut v naší skupině [46].

PeakMaster je volně a zdarma dostupný na stránkách naší skupiny [47] a je široce využíván v mnoha laboratořích, nejen v elektroforetických. V Tabulce 1 jsou přehledně shrnuty požadované vstupní parametry a nejdůležitější výstupní parametry, které může program PeakMaster, verze 5.2, poskytnout.

Tabulka 1. *Vstupní parametry potřebné pro výpočty v programu PeakMaster 5.2 a přehled nejvýznamnějších výstupních parametrů*

Vstupní parametry		**Výstupní parametry**	
BGE	• složení/koncentrace • disociační konstanty[b] • limitní mobility[b]	**BGE**	• pH • vodivost • iontová síla • pufrační kapacita
Analyty	• množství (S,M,L, XL)[a] • disociační konstanty[b] • limitní mobility[b]	**Analyty**	• efektivní mobilita • *TR* [29] (nepřímá detekce) • b_x [28] (vodivostní detekce) • S_x [27] (elektromigrační disperze)
Experimentální podmínky	• celková délka kapiláry • délka kapiláry k detektoru • vkládané napětí • mobilita/pozice markeru elektroosmotického toku	**Systémové zóny**	• mobility • amplitudy[c][45]

TR - transfer ratio; b_x - molární vodivostní odezva*;* S_x *- velocity slope*

[a]v případě analytů se v základním nastavení nezadává jejich přesná koncentrace, ale vybírá se jedno z možných množství: S (small), M (medium), L (large) nebo XL (extra large)

[b]pro širokou škálu látek je možné je vyhledat přímo v databázi programu PeakMaster; databáze jsou založeny na datech T. Hirokawy

[c]dostupné v podokně „*Amplitudes*“ po zadání přesného složení dávkovaného vzorku

Výsledky výpočtů jsou dány jak číselnými hodnotami jednotlivých parametrů, tak i v podobě simulovaného elektroferogramu. Celá simulace a výpočet jsou oproti numerickým simulátorům velmi rychlé (v řádu vteřin). Limitní mobility jsou v PeakMasteru korigovány na iontovou sílu pomocí Onsagerova a Fuossova vztahu

[48], disociační konstanty pomocí McInnesovy aproximace Debye-Hückelova zákona s lineárním členem.

1.3.1 Výpočet mobilit systémových zón v rámci LTE

Uvažujme obecný elektroforetický systém složený z *N* složek rozpuštěných ve vodě, umístěný v kapiláře o konstantním průřezu a s konstantní radiální distribucí všech složek. Zanedbána je také difúze způsobená gradientem chemického potenciálu a teplotní a sorpční efekty. Kapilára je umístěna podél osy *x* a koncentrace $c(x,t)$ je pak tedy funkcí prostorové proměnné *x* a času *t*. Výchozím bodem je rovnice kontinuity popisující jednorozměrnou elektromigraci:

$$\frac{\partial c_i}{\partial t} = -j\sum_{z=n_i}^{p_i} \mathrm{sgn}(z)\frac{\partial}{\partial x}\left(\frac{u_{i,z}c_{i,z}}{\kappa}\right) \qquad i = 1,\ldots,N \qquad (1)$$

kde specifická vodivost κ je dána

$$\kappa = \left(\sum_{i=1}^{N}\sum_{z=n_i}^{p_i}|z|\,u_{i,z}c_{i,z} + u_{OH}c_{OH} + u_{H}c_{H}\right) \qquad (2)$$

c_i je analytická koncentrace *i*-té složky, *t* je čas, *j* značí proudovou hustotu, *z* nábojové číslo, n_i a p_i je nejnižší a nejvyšší sytnost *i*-té složky, *x* je podélná osa kapiláry ve směru vnějšího elektrického pole, $u_{i,z}$ udává iontovou mobilitu *z*-té iontové formy *i*-té složky a $c_{i,z}$ její koncentraci. Sadu rovnic (1) lze upravit a zapsat ji v maticovém tvaru:

$$\frac{\partial \vec{c}}{\partial t} = -\frac{j}{\kappa_{BGE}}\boldsymbol{M}(\vec{c})\times\frac{\partial \vec{c}}{\partial x} \qquad (3)$$

kde $\vec{c} = (c_1,\ldots,c_N)^T$ je sloupcový vektor koncentrací složek (index T značí transponovanou matici), $\boldsymbol{M}$ je čtvercová matice typu $N \times N$, jejíž členy závisejí na $\vec{c}(x,t)$. κ_{BGE} je specifická vodivost původního neporušeného BGE. Tuto maticovou

rovnici lze díky vhodnému uspořádání CZE linearizovat. Uvažuje se, že koncentrace složek základního elektrolytu jsou podél kapiláry rovnoměrně rozloženy a v průběhu separace se koncentrace i-té složky mění jen málo, tedy zůstává blízká konstantní hodnotě koncentrace C_i. Potom tuto změnu koncentrace můžeme označit jako poruchu, $\tilde{c}_i$, kde $\tilde{c}_i = c_i - C_i$. Takto lze uvažovat i o analytech, které jsou dávkovány v malých koncentracích (mnohem menších než jsou koncentrace složek základního elektrolytu) a pro které tedy uvažujeme, že podél kapiláry mají $C_i = 0$ a porucha v místě dávkování odpovídá nadávkované koncentraci. Poruchy jsou malá čísla blízká nule a rovnici (3) lze tedy přepsat do linearizovaného tvaru:

$$\frac{\partial \vec{\tilde{c}}}{\partial t} = -\frac{j}{\kappa_{BGE}} \boldsymbol{M} \times \frac{\partial \vec{\tilde{c}}}{\partial x} \qquad (4)$$

Vektor $\vec{\tilde{c}}$ je vektor poruch koncentrací složek, $\vec{\tilde{c}} = (\tilde{c}_1, \ldots, \tilde{c}_N)^T$. Matice ***M*** je Jacobiho matice a je zde již konstantní maticí. Řešení této maticové rovnice vede na problém vlastních čísel (*eigenvalues*). Vlastní čísla matice ***M*** mají rozměr mobilit a naše skupina pro ně zavedla název eigenmobility (vlastní mobility). Existence eigenmobility naznačuje, že jistý jev, zóna, se může pohybovat separačním kanálem s právě takovou mobilitou. Pokud je jednou či více složkami systému analyt, pak je patřičný počet vlastních čísel (vlastních mobilit) roven příslušným efektivním mobilitám analytů. Ostatní (tedy vlastní hodnoty pro složky BGE) odpovídají mobilitám systémových zón.

Spektrálním rozkladem matice ***M*** lze získat matice amplitud systémových píků [45].

1.3.2 Použitelnost programu PeakMaster

Na rozdíl od numerických simulátorů nelze PeakMaster využít pro různé elektromigrační techniky (izotachoforéza, izoelektrická fokusace, apod.). Jak z podstaty LTE vyplývá, PeakMaster může predikovat výsledky pouze pro kapilární zónovou elektroforézu. CZE je dnes nejběžnější elektromigrační technikou, kterou lze navíc

vhodně modifikovat přídavkem látek poskytujících analytům různé cílené interakce. PeakMaster je určen pro vodné prostředí, ačkoliv po drobné modifikaci a se správnými vstupními údaji může být využit např. i pro methanolické základní elektrolyty [49]. Disperze píků analytů předpovídaná programem je dána jen elektromigrační disperzí, difúze není uvažována. Vrátíme-li se k Tabulce 1, je patrné, že dosavadní verze PeakMasteru nebyly schopné předpovídat tvary systémových píků. Rozšíření linearizovaného modelu, jeho implementace do PeakMasteru, stejně jako experimentální ověření schopnosti nové verze programu předpovídat tvary systémových píků, jsou uvedeny v Publikacích 2 a 3 této práce.

V současné době se v naší skupině snažíme rozšířit pole použitelnosti PeakMasteru také na systémy kapilární elektroforézy, kde se uplatňují kromě acidobazických rovnováh také rovnováhy komplexační. Zatím byla publikována první verze PeakMasteru 5.3 Complex, schopná předpovídat elektromigrační disperzi silného elektrolytu dávkovaného jako analyt do systému obsahujícího jedno neutrální komplexační činidlo tvořící s daným analytem komplex [50,51]. Kompletní linearizovaný model elektromigrace zahrnující komplexační rovnováhy všech složek systému zatím není dostupný. Proto mohou být systémový píky v těchto systémech studovány pouze experimentálně nebo simulovány některými z numerických simulátorů – např. Simul 5 Complex [52] nebo GENTRANS [53].

1.4 Komplexační rovnováhy v kapilární elektroforéze

Rychlé komplexační rovnováhy se v kapilární elektroforéze využívají čím dál častěji. Přítomnost komplexujícího činidla v BGE má za cíl poskytnout analytům dodatečné interakční možnosti a zvýšit tak selektivitu daného separačního sytému. Pokud je komplexačním činidlem chirální selektor, pak je navíc možné dosáhnout enantioseparace chirálních analytů. Toto využití komplexačních rovnováh v CZE lze z důvodu velkých nároků na enantiomerní čistotu léčiv a potravinových doplňků [54,55] považovat v současnosti za nejrozšířenější. Přehled chirálních selektorů

používaných v HPLC a kapilární elektroforéze je zařazen na konci této kapitoly v Publikaci 1.

I pro tyto elektroforetické systémy se vyvíjely teoretické modely zaměřené na optimalizaci separačních podmínek pro enantioselektivní separace. Tyto modely se soustředily hlavně na analyty a předpovídání jejich efektivních mobilit v systémech, kde interagují s přítomným komplexačním činidlem (chirálním selektorem). Cílem prací bylo najít separační podmínky poskytující co možná největší selektivitu enantiomerů [56-58].

Komplexace analytu s komplexačním činidlem je v dnešní době již detailně popsána. Velmi malou pozornost však autoři věnovali a věnují možné nechtěné komplexaci daného komplexačního činidla se složkami použitého základního elektrolytu. Práce některých autorů napovídají, že v důsledku komplexace komplexačního činidla s BGE může docházet k výrazným změnám ve vlastnostech BGE. Chen a kol. [59] zaznamenali vznik systémových píků v důsledku interakce nativních cyklodextrinů s použitým CHES pufrem při separaci nederivatizovaných gangliosidů. Podobně Fang a kol. [60] detekovali dodatečný systémový pík, pokud byly v BGE současně přítomny acetonitril a sulfatovaný β-cyklodextrin.

Chování systémových píků v komplexujících systémech i změny fyzikálně-chemických vlastností základních elektrolytů v důsledku nechtěné komplexace BGE s komplexujícím činidlem a případný vliv na elektroforetické výsledky byly předmětem Publikací 4 a 5 v Kapitole 4.2.

Publikace 1

Recent chiral selectors in HPLC and CE

*Kalíková K., **Riesová M.**, Tesařová E.*

Central European Journal of Chemistry, 2012, 10, 450-471

VERSITA

Cent. Eur. J. Chem. • 10(3) • 2012 • 450-471
DOI: 10.2478/s11532-011-0142-3

Central European Journal of **Chemistry**

Recent chiral selectors for separation in HPLC and CE

Review Article

Květa Kalíková, Martina Riesová, Eva Tesařová*

Charles University in Prague, Faculty of Science, Department of Physical and Macromolecular Chemistry, 128 43 Prague 2, Czech Republic

Received 13 September 2011; Accepted 14 November 2011

Abstract: Enantiomers (stereoisomers) can exhibit substantially different properties if present in chiral environments. Since chirality is a basic property of nature, the different behaviors of the individual enantiomers must be carefully studied and properly treated. Therefore, enantioselective separations are a very important part of separation science.

To achieve the separation of enantiomers, an enantioselective environment must be created by the addition of a chiral selector to the separation system. Many chiral selectors have been designed and used in various fields, such as the analyses of drugs, food constituents and agrochemicals. The most popular have become the chiral selectors and/or chiral stationary phases that are of general use, *i.e.*, are applicable in various separation systems and allow for chiral separation of structurally different compounds.

This review covers the most important chiral selectors / chiral stationary phases described and applied in high performance liquid chromatography and capillary electrophoresis during the period of the last three years (2008-2011).

Keywords: *High performance liquid chromatography • Capillary electrophoresis • Chiral selector • Chiral stationary phase • Enantioselective separation*

1. Introduction

Many reviews dealing with enantioselective separations have been published over the last few years. Based on the topic they focused on, the reviews can be roughly categorized as reviews on various chiral selectors (CSs) or chiral stationary phases (CSPs), on enantioselective separation mechanism, and application. Often it is a combination of these topics. Some reviews are published annually, some every two or three years. These papers are mostly entitled "fundamental" reviews but other papers, also fundamental, appear in the literature, as well.

As we do not wish to repeat the information which has been already reviewed, and considering the tremendous number of papers covering the topic, we decided to focus on papers that have not been reviewed previously, *i.e.*, published between January 2010 and May 2011. The reviews published between January 2008 and May 2011 (according Web of Science) are summarized in Table 1 (liquid chromatography) and Table 2 (capillary electrophoresis). Basic research papers contribute to the explanation of chiral recognition mechanism and analytical applications are of interest to analysts from commercial laboratories. Therefore, we have included both aspects in this review.

As CSPs play the most important role in chiral high performance liquid chromatography (HPLC) separations, the HPLC part of this review has been divided into subchapters based on the various CS/CSP types used. In addition, different separation modes that can be used are discussed.

The capillary electrophoresis (CE) is more difficult to categorize. The variety of chiral selectors, as well as the different electromigration methods, such as capillary zone electrophoresis (CZE), micellar electrokinetic chromatography (MEKC) or capillary electrochromatoghraphy (CEC) can be used and contribute to diverse separation mechanisms.

2. HPLC

Table 1 summarizes the recent reviews relating to chiral HPLC separations using different chiral stationary phases.

* *E-mail: tesarove@natur.cuni.cz*

All authors contributed to this review paper to the same extent.

Table 1. An overview of the review articles dealing with enantioselective separation in HPLC published in the period between January 2008 and May 2011.

CS/CSP*	Topic	Analytes	Ref.
	LEC, CZE and CEC		[1,2]
	preparation of new CSPs by click chemistry, application		[3]
polymeric, macrocyclic, brush type, ligand exchange CSPs	silica-based CSPs		[4]
	development of new CSPs, application		[5]
major commercially available CSPs	application	active pharmaceutical ingredients	[6]
	application	pharmaceuticals	[7]
	application	organophosphorus pesticides	[8]
	application	fluoroquinolones antibiotics	[9]
	application	biologically important small epimeric peptides and their amino acid components	[10]
	application	pyrethroids	[11]
	chiral modified silica monolithic columns		[12]
	monolithic CSPs, application		[13]
modern CS/CSPs	separation mechanism		[14]
	indirect LC, application	D,L-penicillamine	[15]
	application	pharmaceuticals in aquatic environment	[16]
macrocyclic glycopeptide-based CSPs	separation mechanism, physicochemical properties		[17]
polysaccharide derivatives	CSPs, application		[18]
tartrates and metal-tartrates CS	CS, application		[19]
coated/immobilized polysaccharide CSPs	CSPs, application	chiral pharmaceuticals	[20]
	application	antidepressant drugs and their metabolites in biological samples	[21]
	application	pesticides	[22]
	application	triptans	[23]
	application	amino acids in biological samples	[24]
	reversed CSPs, application	pharmaceutical compounds	[25]
Pirkle-type, polysaccharide-based CSPs	CSPs, application	pharmaceutical compounds	[26]
penicillin G acylase CS	CS		[27]
	ion-pair chromatography, application		[28]
	application	pharmaceutical formulations	[29]
vancomycin and its degradation products	CS, application		[30]
	CS/CSPs, application		[31]
macrocyclic antibiotics	recognition mechanism, application		[32]
	chiral separations since 1998 to 2008		[33]
protein/glycoprotein CSPs	recognition mechanism		[34]
chitosan phenyl carbamate derivatives	CSPs		[35]
	chiral and achiral methods, application	thalidomide and its metabolites	[36]
	application	adrenergic drugs	[37]
	CSPs, application		[38]
	CSPs		[39]
Chiralpak IA, Chiralpak IB, Chiralpak IC	application, methods compatible with MS		[40]
polysaccharide-, macrocyclic glycopeptide-, protein-, cyclodextrin-based CSPs	application, methods compatible with MS/MS	chiral drugs and/or their metabolites	[41]
	application	antimalarial drugs and their metabolites	[42]

**If the CSs/CSPs are not stated the review gives an overview of various types.*

2.1. Recent chiral HPLC

The majority of enantioselective HPLC systems are composed of a chiral stationary phase and an achiral mobile phase. This fact is reflected in this review.

2.1.1. Cyclodextrin-based CSPs

Cyclodextrin (CD) CSPs are still widely used in chiral and achiral HPLC as confirmed by the number of papers published since 2010. Commercially available or newly modified (derivatized with various groups) CD CSPs are remaining popular in both basic research and applications.

ChiraDex Beta (β-CD CSP) and ChiraDex Gamma (γ-CD CSP) columns were used for an achiral separation of 9,10-antraquinone derivatives in reversed phase (RP) mode with gradient elution [43]. An off-line two-dimensional reversed phase/reversed phase liquid chromatography (2-D RP/RPLC) method combining stationary phase C18 and β-CD CSP was developed for achiral separation of more than 500 components in extracts of *Fructus schisandrae chinensis*, which represent traditional Chinese medicine [44]. Two new CSPs were prepared by bonding mono[6-deoxy-(*R*)-(−)-N-1-(2-hydroxyl)-4-chlorophenylethylimino]-β-cyclodextrin (*R*-CPGCD) and mono[6-deoxy-(*R*)-(−)-N-1-(2-hydroxyl)-4-hydroxy-methylphenylacetate-imino]-β-cyclodextrin (*R*-HMPGCD) to silica gel, chiral nitro aromatic alcohol derivatives were separated on these CSPs in RP and polar organic (PO) modes [45]. Another novel CD-based CSPs containing mono(6(A)-N-(omega-alkenylamino)-6(A)-deoxy) perphenylcarbamoylated β-cyclodextrin with spacers of three different lengths were prepared, compared and applied for enantioseparation of various racemates in normal phase (NP) mode [46]. Four novel ionic liquids functionalized β-CDs CSPs were prepared and their enantioselectivities were tested with 16 chiral aromatic alcohol derivatives and 2 racemic drugs in PO mode [47]. Hydrobenzoin and structurally related compounds (benzoin and α-phenetyl alcohol) were successfully separated on β-CD and hydroxypropyl-β-cyclodextrin (HP-β-CD) in RP HPLC [48]. The new synthesized CD-based CSPs: heptakis(6-deoxy-6-azido)-β-CD and heptakis(6-deoxy-6-azido-phenylcarbamoylated) β-CD showed good enantioselectivity with over forty pairs of different enantiomers [49]. Another novel CD derivative, mono(6(A)-azido-6(A)-deoxy)-per(p-chlorophenyl carbamoylated) β-CD immobilized onto an amino-functionalized silica gel with different pore and particle sizes was examined by enantioseparation of variety of racemates in NP and RP modes [50]. A series of imino-modified β-CD derivatives were bonded to silica gel to form a new CD-based CSPs; their separation performance was examined with the separation of different compounds, *i.e.,* amino acids, chiral aromatic alcohol *etc*. [51]. A click chemistry strategy was used in the preparation of a new CD-based CSs and evaluated by chiral separation of various analytes, *i.e.,* aryl alcohols, flavonoids, atropine, β-blockers *etc*. [52]. A click chemistry-derived β-cyclodextrin (CD-click-sil and CD-click-RAM) CSPs were evaluated by enantioseparation of mandelic acid and chlorthalidone in human plasma [53], and a novel chiral-CD-RAM CSP prepared via atom transfer radical polymerization was tested on enantioseparation of some chiral drugs [54]. Newly prepared ethylenecliamine-β-cyclodextrin functionalized poly(glycidyl methacrylate-co-ethyleneglycol dimethacrylate) monoliths were characterized by scanning electron microscopy, differential scanning calorimetry and X-ray photoelectron spectroscopy and used for the chiral separation of racemic ibuprofen [55]. Two new types of substituted β-CD CSPs, which actually combined two powerful CSs (macrocyclic antibiotics and CD), vancomycin-capped β-CD-bonded silica particles and rifamycin-capped β-CD-bonded silica particles, were developed, characterized and tested with separation of achiral disubstituted benzenes and chiral drugs [56]. Bromine-containing β-CD-bonded stationary phase (BACD-HPS, bromoacetate-substituted [3-(2-O-β-CD)-2-hydroxypropoxy]propylsilyl-appended silica particles) were prepared and evaluated by separation of achiral disubstituted benzenes and some chiral drug compounds [57]. Native and derivatized CD CSPs (high performance hydroxypropylether-β-CD, hydroxypropylether-β-CD, acetylated β-CD, *R*- and *S*- naphthylethylcarbamate-β-CDs, dimethylphenylcarbamate-β-CD, 2,6-dinitro-4-trifluoromethylphenylether-β-CD, dimethylated β-CD) were chosen for enantioseparation of fifteen racemic 4,5-disubstituted imidazole compounds, and the mechanism of chiral recognition was discussed [58]. π-acidic and π-basic perphenylcarbamoylated β-CDs were synthesized and their enantioselectivities were examined and compared using a set of 2-piperazine-1,2-dihydronaphthaline derivatives and other chiral compounds in NP and RP modes [59]. Enantioseparation of a set of β-lactams was predicted and confirmed on three β-CD based CSPs, permethyl-β-CD, β-CD and *R,S*-HP-β-CD [60,61].

In addition to their excellent enantioseparation abilities CD CSPs show interesting capabilities for achiral application in hydrophilic interaction liquid chromatography (HILIC). Wang *et al*. carried out an achiral separation of a series of three cycloinulooligosaccharides (cyclofructans) on the Cyclobond I 2000 column (β-CD

CSP) in HILIC mode [62]. Cyclobond I 2000 (native β-CD CSP) and Cyclobond I 2000AC (acetylated β-CD CSP) columns exhibited great potential for achiral separation of estrogen and estrogen conjugated compounds in HILIC mode [63]. However, CD-based CSPs are mostly applied in RP separation mode or with PO mobile phase. Under these conditions they yield the best results.

Cyclodextrins were also used as mobile phase additives for chiral and achiral separations in HPLC [64-69]. However, this way of creating a separation environment is less popular than the use of CD-based stationary phases.

2.1.2. Polysaccharide CSPs

Recently, polysaccharide-based CSPs are the most frequently used group of CSPs used in chiral HPLC method development. Many studies reported during the review period discuss the enantiorecognition mechanism.

These CSPs are commercially available as either immobilized or coated on a support surface. The limited stability of coated CSPs could be a disadvantage as compared with CD CSPs that can resist repeatable changes among all known separation modes. The coated CSPs can be used with a rather limited number of eluents (alkane/alcohol mixtures) in NP chromatography and water/acetonitrile mixtures in RP chromatography. Solvents with intermediate polarities (*e.g.* ethyl acetate, tetrahydrofuran (THF), 1,4-dioxane, acetone) can partially or totally dissolve the chiral polymer. Chemically bonded (immobilized) polysaccharide CSPs have been developed to overcome the drawbacks of the coated CSPs and broaden the range of applicable solvents [70].

Immobilized Chiralpak IC, Chiralpak IA and coated Lux Cellulose-1, Lux Cellulose-2 and Lux Amylose-2 CSPs were used for the enantioseparation of 1-phenyl-1,2,3,4-tetrahydroisoquinoline, all three separation modes (RP, NP and PO) were tested [71]. Chiral separation of eight racemic atropisomers of biphenyl was investigated on six polysaccharide CSPs in NP and PO modes [72]. Enantioselectivity of four recently commercialized CSPs, *i.e.,* Lux (R) Cellulose-1, Lux (R) Cellulose-2, Lux (R) Amylose-2 and Lux (R) Cellulose-4 were tested on a set of 61 racemic compounds in normal phase mode [73]. Preparative enantioseparation of substituted 4-oxo-1,4-dihydroquinoline-3-carboxamide derivatives (new potential selective agonists of the cannabinoid CB2 receptor) was performed on a Chiralpak AD-H column (amylose tris(3,5-dimethylphenylcarbamate) CSP) in NP mode [74]. Three chlorine containing cellulose-based CSPs, *i.e.,* cellulose tris(3-chloro-4-methylphenylcarbamate) (Sepapak-2s column), cellulose tris(4-chloro-3-methylphenylcarbamate) (Sepapak-4s column) and cellulose tris(3,5-dichlorophenylcarbamate) (Sepapak-5s) were evaluated by the separation of basic amino-drug enantiomers in PO mode [75]. Neonicotinoid insecticides were enantioseparated on Chiralcel OD-H, Chiralpak AD-H and Chiralpak IB columns in NP mode, but also using supercritical fluid chromatography (SFC) [76]. The types of interactions play a role in the mechanism of enantioselective recognition and the thermodynamic parameters affecting the process were discussed. Amylose tris(3,5-dimethylphenylcarbamate) CSPs was used for the enantioseparation of newly synthesized triazole fungicides in NP mode [77]. The 3,5-dimethylphenylcarbamate derivatized amylose and cellulose CSPs in systems with PO eluents were compared in terms of the enantioseparation of coumarin-based compounds [78]. The 2-D RP HPLC method using a C8 RAM BSA column as the first step followed by amylose tris(3,5-dimethoxyphenylcarbamate) CSP for the determination of lansoprazole in human plasma was developed and validated [79]. The enantioseparation of eight novel (*R,S*)-N-mexiletine derivatives with different alkyl chain lengths were performed on both a Chiralcel OD-H column and a Chiralcel OJ-H column under NP conditions [80]. Chiralpak IA and Chiralpak IC columns were used for the enantioseparation of new quinazoline derivatives bearing an α-aminophosphonate moiety under NP conditions; the chiral recognition mechanism was also discussed [81]. Chiralpak IA and Chiralpak IC columns were also applied to the enantioseparation of hypericin, pseudohypericin and protohypericin in PO mode; optimized HPLC conditions were used for determination of stereodynamic parameters of interconversion of the enantiomers [82]. HPLC methods were developed for the enantioseparation of five new aminonaphthol analogs in systems with amylose tris(3,5-dimethylphenylcarbamate) CSP (Kromasil ®AmyCoat ™ column) or cellulose tris(3,5-dimethylphenylcarbamate) CSP (Kromasil ® CelluCoat ™ column), the influence of the mobile phase composition on enantioseparation was tested [83]. Relative content of (2*S*)- and (2*R*)-naringin in the albedo of pummelo during maturation during the entire season was determined by a NP HPLC using Chiralpak IB column [84]. The enantioseparation of α-arylthiocarboxylic acids (*i.e.,* pirinixic acid derivatives) with different substitution patterns were performed on amylase tris(3,5-dimethylphenylcarbamate)-coated silica, tert-butylcarbamoylquinine CSPs and quinidine-based anion exchangers in analytical and preparative scale [85]. Fenoterol enantiomers were separated after precolumn fluorescence derivatization with naphthylisocyanate on cellulose tris(3,5-dimethylphenylcarbamate)-coated silica gel column

(OD-RH column) in RP mode [86]. More than 200 racemic compounds of pharmaceutical interest were used for the evaluation of three complementary three polysaccharide-based CSPs, *i.e.,* cellulose tris(3-chloro-4-methylphenylcarbamate), amylose tris(2-chloro-5-methylphenylcarbamate) and cellulose tris(3,5-dimethylphenylcarbamate) CSPs in RP mode compatible using mass spectrometry (MS) detection. Chiral separation in RP mode was compared with NP and PO modes [87]. Amylose tris(3,5-dimethylphenylcarbamate) CSP was used for the enantioseparation of racemic benzylmandelate. The retention behavior of the enantiomers were explained by nuclear magnetic resonance (NMR) experiments [88]. The enantiorecognition ability of cellulose tris(4-chloro-3-methylphenylcarbamate) coated CSP (Sepapak-4) was evaluated by the chiral separation of ten basic drugs of different structures and hydrophobicities using PO mobile phases [89]. Enantioseparation of 14 similar chiral solutes (with one or two chiral centers) were examined on amylose tris(3,5-dimethylphenylcarbamate) CSP in NP mode. The nanostructure of the CS´s cavity and interaction types participating in the interaction mechanism were proposed based on the obtained chromatographic data, infrared spectroscopy and molecular dynamics simulations [90]. Franco and Zhang proposed a screening procedure for the development of analytical methods for resolution of enantiomers in a reasonable time frame performed on a relatively small set of polysaccharide-based columns [91,92].

Several papers describe various approaches for preparation/synthesis of newly derivatized polysaccharide-based CSPs with an improved stability towards the mobile phase components. Bae *et al*. prepared new polysaccharide-immobilized CSP by surface-initiated atom transfer radical polymerization; the enantioselectivity was evaluated by injecting ten racemates under NP conditions [93]. The one-pot method was carried out to synthesize the cellulose 3,5-dichlorophenylcarbamates bearing small amounts of 3-(triethoxysilyl)propyl residues and immobilized onto silica gel through polycondensation. The new CSP was tested with eight racemic mixtures using eluents (chlorophorm, THF) which can not be used with conventional coated CSPs [94]. The one-pot method was also applied to the preparation of the cellulose and amylose 3,5-dimethylphenylcarbamates bearing 4-(trimethoxysilyl)phenyl groups and immobilized onto silica gel through polycondensation of the trimethoxysilyl groups. The enantiorecognition abilities of these columns were examined in the mobile phases containing chlorophorm and THF [95]. Other new CSPs were prepared by immobilization of 3,5-dimethylphenylcarbamates of cellulose and amylose onto silica gel using (3-glycidoxyprolyl)triethoxysilane as a linker. In addition, these CSPs were proven to be compatible with mobile phases containing chlorophorm and THF [96]. Two novel coated composite CSPs were prepared using tris(3,5-dimethylphenylcarbamate) of cellulose and amylose by coating the corresponding derivatives onto 3-aminopropyl silica gel separately and then mixing or by coating the mixed derivatives onto silica gel. The enantioselectivities of these novel CSPs were compared with CSPs containing only one derivative by separation of eight racemates under NP conditions [97]. New cellulose derivatives bearing pyridyl and bipyridyl residues CSPs were also synthesized. These CSPs were used in ligand-exchange chromatography (LEC) for the direct separation of amino acids with mobile phase containing a copper salt [98]. The cellulose derivatives with pyridyl 1 and bipyridyl 2 residues at the 2-, 3- and 6-positions of the glucose ring show low chiral recognition ability while the regioselectively substituted derivatives exhibited relatively high chiral recognition ability. The other new amylose derivatives CSPs bearing different groups were prepared and their enantioselectivities were compared with commercially available polysaccharide columns [99,100]. Novel amylose esters (cinnamate derivatives) CSPs were prepared and evaluated for their application in chiral separations; the recognition of the abilities of these CSPs vary significantly depending on the type and position of substituents on the phenyl group [101].

Chiral screening strategies on diverse columns including polysaccharide-based ones (Chiralcel OD-H, OJ-H, Chiralpak IA-3, IC-3) were described using a set of 19 racemates in isocratic and gradient elution modes with mobile phases compatible using MS detection and suitable for preparative chromatography [102].

2.1.3. Macrocyclic antibiotics-based CSPs

Macrocyclic antibiotics-based CSPs represent another powerful group of CSPs with wide application possibilities. They can be used in RP, NP and PO separation modes. The best separation efficiency and selectivity is achieved mainly with PO mobile phases or in RP separation systems.

Chirobiotic T, T2 (both teicoplanin-based) and TAG (teicoplanin aglycone-based) columns were used to separate the enantiomers of five monoterpene-based 2-amino carboxylic acids under RP conditions [103]. Underivatized γ-amino acids were enantioseparated in RP HPLC systems with a Chirobiotic T, T2, TAG and R (ristocetin A-based) columns, mechanism of chiral recognition were discussed [104]. The complementary of new dalbavancin CSP to the teicoplanin CSP

was examined and verified by enantioseparation of 250 structurally different racemates using three mobile phase compositions [105]. A RP18 monolithic column coated with N-(2-hydroxydodecyl)-vancomycin was prepared and successfully applied to the enantioseparation of dansylamino acids [106]. A two-dimensional HPLC method using a C18 column and teicoplanin CSP under RP conditions was applied for the determination of three pairs of amino acids, *i.e.,* tyrosine, phenylalanine, tryptophane, in order to control transformations in the E-beam irradiated foodstuff [107].

2.1.4. Protein-based CSPs

Protein-based CSPs are used less frequently for the separation of enantiomers in HPLC. Their main disadvantage is their limited compatibility with mobile phases containing higher amounts of organic modifier. However, they can serve as a model environment for studies of drug interactions in organisms (human body).

New simplified, efficient and generic protocols for sample screening on CHIRAL-AGP column (utilizes α_1-acid glycoprotein as CS) for liquid chromatoghraphy with MS detection (LC-MS) analyses in RP mode were developed [108]. Chrysanthakopoulos *et al*. studied the retention behavior of 39 structurally diverse drugs on human serum albumin CSPs (HSA CSP) in RP mode for the calculation/simulation of plasma protein binding data [109]. A Chiralpak AGP column was successfully used for the separation of a mixture of racemic pharmaceuticals using mobile phase composed of 1% propane-2-ol in 10 mM ammonium acetate, pH 5, compatible with MS detection [110].

2.1.5. Pirkle-type CSPs

The π-donor or π-acceptor CSPs belong to the oldest applications in chiral HPLC separations. Nevertheless, it is still used in various combinations. Both commercially available and newly π-donor acceptor modified CSPs appear in the literature.

Adsorption of naproxen enantiomers on (*R,R*) Whelk-O1 and (*S,S*) Whelk-O1 CSPs were studied in RP mode; the mechanism of adsorption and separation is also discussed [111,112]. The enantioseparation of vesamicol and six new azaspirovesamicols was accomplished on two Pirkle-type columns, *i.e.,* Reprosil Chiral-NR (π-donor acceptor) and Reprosil Chiral-OH (π-donor acceptor, esp. for aromatic alcohols) and compared with other types of CSPs – teicoplanin aglycone, cellulose and amylose-based CSPs [113]. The inverted chirality columns approach was used for the determination of enantiomeric excess of camptothecin derivative – namitecan in the systems with (*R,R*) Whelk-O1 and (*S,S*) Whelk-O1 CSPs [114]. (*S,S*) ULMO column (based on a 3,5-dinitrobenzoyl derivative of diphenylethylenediamine) were used for the semipreparative enantioseparation of four axially chiral biscarbostyrils (4,4´-bisquinoline-2-ones). For this specific case three different calculation methods of dynamic peak shape were compared [115]. A new Pirkle-type CSP was prepared using Sepharose 4B as a matrix, L-tyrosine as a spacer arm, and the aromatic amino derivative of L-glutamic acid as ligand and applied to resolution of (±)-β-methylphenylethylamine [116].

Two brush-type CSPs of single selector were synthesized by immobilization of ((2*S*,3*S*)-1-(benzyloxy)-4-chloro-1,4-dioxobutane-2,3-diyl)dibenzoate and (1*R*,2*R*)-1,2-diphenyl-2-(3-phenylureido)ethyl 4-isocyanatophenyl urea CSs on aminated silica gel; a combination of these both CSs was also immobilized on aminated silica gel to prepare a mixed CSP. The columns were tested by enantioseparation of various analytes in RP mode [117]. Three novel brush-type CSPs differing in the size of silica particles (4.3 μm, 2.6 μm, 1.9 μm) were prepared by covalent grafting of the π-acidic bis(3,5-dinitrobenzoyl)-derivative of trans-1,2-diaminocyclohexane. The enantioselectivity of these CSPs were tested using different pairs of enantiomers [118].

2.1.6. Crown ether CSPs

As these CSPs can be used for a limited group of enantiomers they did not gain an important position among chiral stationary phases with a wide application field. In addition, crown ether-based CSPs were not employed in many papers dealing with liquid chromatography during this review period.

CSP based on (+)-(18-crown-6)-2,3,11,12-tetracarboxylic acid was applied to the resolution of 1-aryl-1,2,3,4-tetrahydroisoquinolines in PO mode [119]. The same CSP under PO conditions was used to resolve flecainide (antiarrythmic drug) and its analogues [120] and for the separation of native diaminopimelic acid stereoisomers in RP mode [121]. Doubly tethered CSP based on (+)-(18-crown-6)-2,3,11,12-tetracarboxylic acid was used for the enantioseparation of tocainide (antiarrythmic drug) and its analogues in RP HPLC, the influence of mobile phase composition and temperature on enantioseparation was examined [122].

2.1.7. Cyclofructan-based CSPs

Cyclofructan-based chiral selectors were introduced in 2009 [123]. The cyclofructan-based chiral stationary phases (CF CSPs) offer a crown ether core for interaction with analytes. While native CF CSPs have just very

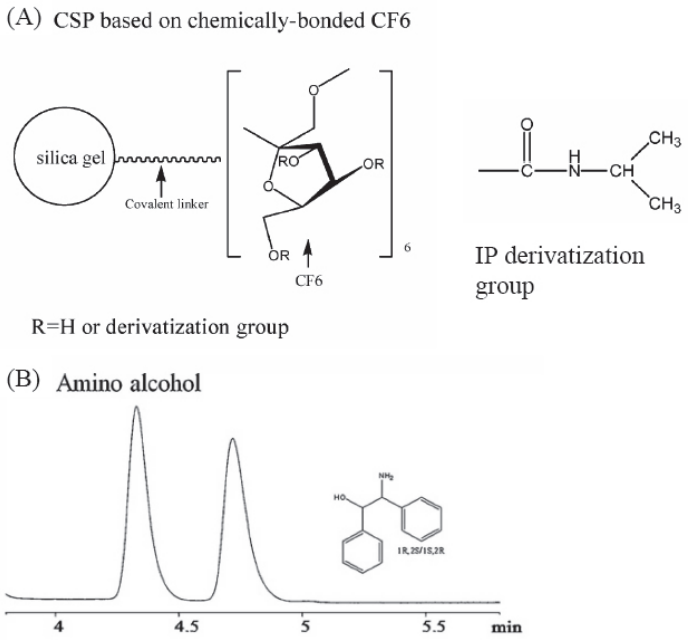

Figure 1. (A) Scheme of chemically bonded derivatized-CF6 CSP and chemical structure of isopropyl (IP) derivatization group. Reprinted with permission from [125], Copyright (2011) American Chemical Society. (B) Chromatogram of enantioseparation of primary alcohol 2-amino-1,2-diphenylethanol. CSP : isopropyl functionalized CF6, mobile phase composed of ACN/MeOH/acetic acid/triethylamine 30/70/0.3/0.2. Reprinted from [129], Copyright (2011), with permission from Elsevier

limited enantioseparation abilities their derivatized analogs were shown to give good resolution for various enantiomers.

The interaction possibilities of *R*-naphthylethyl cyclofructan 6 CSP in NP mode were revealed by linear free energy relationship (LFER) method and compared with those of *R*-naphthylethyl-β-CD CSP; chiral separation of binaphthyl catalysts was examined [124]. *R*-naphthylethyl cyclofructan 6 and dimethylphenyl cyclofructan 7 CSPs were reported to provide enantioselectivity for a broad range of compounds, *e.g.* chiral acids, amines, metal complexes, neutral compounds [125]. Native cyclofructan 6 is suitable for achiral separation of polar compounds in HILIC mode [126]. Isopropyl functionalized cyclofructan 6 CSP (Fig. 1A) demostrate a high efficiency for enantioseparation of compounds possessing primary amino groups (Fig. 1B) [127].

2.1.8 Polymeric CSPs

Polymeric CSPs keep effort to find their position in the enantioselective separation science. In general, results obtained using CSPs based on naturally occurring CSs (or just their modifications) give better results.

New polymeric chiral stationary phases based on the monomers: N-(2-acryloylamino-(1*R*,2*R*)-cyclohexyl) acrylamine (P-CAP CSP), N,N´-[(1*R*,2*R*)-1,2-diphenyl-1,2-ethanediyl]bis-2-propenamide (P-CAP DP CSP) and trans-9,10-dihydro-9,10-ethanoanthracene-(11*S*,12*S*)-11,12-dicarboxylic acid bis-4-vinylphenylamide (DEAVB CSP) were used for the enantioseparation of 17 chiral organic sulfoxides in three separation modes [128], with the best enantioselectivities were obtained under NP conditions. Three new polymeric CSPs were synthesized based on (1*S*,2*S*)-1,2-bis(2,4,6-trimethylphenyl)ethylenediamine, (1*S*,2*S*)-1,2-bis(2-chlorophenyl)ethylenediamine, and (1*S*,2*S*)-1,2-di-1-naphthylethylenediamine *via* a simple free radical initiated polymerization in solution. Their enantioselectivities were evaluated by the separation of various racemates (amines, amides, alcohols, amino acids, ester *etc.*) in NP mode and compared with structurally related commercial P-CAP-DP CSP [129]. Two helical polyisocyanide-based CSPs covalently bonded to silica gel (polyisocyanides are composed of the same L-alanine repeating units, but they are completely different in their helical sense (right- and left-handed helices)) were prepared and chiral separation of 15 structurally different compounds were investigated in NP mode [130].

2.1.9. CSPs for ligand/ion exchange chromatography

LEC represents one of the oldest environments used for the separation of enantiomers. The simplest system can be created using one enantiomer of an amino acid (as chiral ligand) and mostly Cu(II) as a central atom forming the complex with another amino acid as analyte.

The click chemistry was applied to immobilize L-prolinamide derivative onto azide-modified silica gel to obtain a novel CSP for ligand exchange chromatography; the CSP was evaluated by enantioseparation of some amino acids [131]. Proton pump inhibitors, *i.e.,* omeprazole, pantoprazole, lansoprazole, rabeprazole were enantioseparated using ligand exchange CSP prepared by bonding (*R*)-phenylglycinol derivative, sodium N-[(*R*)-2-hydroxy-1-phenylethyl]-N-undecylaminoacetate, to silica gel [132].

LEC is often performed using achiral columns and mobile phases with chiral additives. Ofloxacin enantiomers were enantioseparated in the system with a C18 column and a mobile phase composed of methanol/water containing different concentrations of L-isoleucine and copper sulfate [133] or a C18 column and a mobile phase composed of methanol/water containing L-1 amino acid ionic liquid and copper sulfate [134]. Racemic amino acids (valine, methionine, leucine, phenylalanine and tyrosine) were separated on RP-C8 column with aqueous mobile phase containing N,N-dimethyl-L-phenylalanine and copper [135]. The influence of non-ionic surfactants on the selectivity and retention were also examined [136]. A chiral LEC was applied to the separation of four glutamate analogs (1-aminospiro [2.2]pentyl-1,4-dicarboxylic acids) first on a CSP obtained by dynamic coating of C18 with *S*-trityl-(*R*)-cysteine, and then in chiral mobile phase prepared from O-benzyl-(*S*)-serine [137]. Enantiomer elution order of amino acids in chiral LEC was elucidated by computational studies [138].

Novel anion exchange 1,2,3-triazole-linked CSPs were prepared by click chemistry of 10,11-didehydrocinchona *tert*-butylcarbamates to azido-grafted silica gels. These CSPs were tested under PO and RP conditions with a set of structurally diverse racemates (acids, N-protected amino acids, aromatic and aryloxycarboxylic acids, binaphtholphosphate) [139]. Ion chromatography with cation exchange column employing crown ether and carboxylate and phoshonate cation exchange sites was applied for determination of imidazolium and pyridinium ionic liquid cations [140].

2.1.10. Miscellaneous CSPs

Chiral macrocycles with a hydrogen bond donor/acceptor site in the cavity were synthesized and covalently bonded to silica gel to give five different CSPs. These phases showed excellent abilities to separate various chiral compounds, *e.g.* ketones, esters, carboxylic acids, amines *etc.* [141]. Four novel dendrimer-type CSPs were prepared by immobilizing (1*S*,2*R*)-1,2-diphenyl-2-(3-phenylureido)ethyl 4-isocyanatophenylcarbamate on dendrimers of various generations (Fig. 2), and the chiral separation of structurally diverse analytes were performed in RP and NP modes [142]. Two new quinine-based CSPs, *i.e.,* QN CSP and QN CSP (EC) were developed by the immobilization of quinine on porous silica particles, one CSP was subsequently endcapped with n-hexyl hydrocarbon chains. The enantioselectivity was evaluated by the separation of twenty N-derivatized 2,4-dinitrophenyl α-amino acids in RP mode [143]. Enantioseparation of an amino acid derivative phthalylvaline was achieved on quinine-carbamate based CSP, the effect of mobile phase composition was investigated [144].

3. Electromigration methods

Recent reviews pursuing a survey of enantioseparations performed in various electromigration systems are listed in Table 2.

3.1. Recent enantioselective capillary electrophoresis

While the chromatographic part of this review is simply divided into subchapters according to different structure/chemistry of chiral stationary phases, a similar approach is not possible in the electrophoresis chapter. In this part the sort is based on the subject of the paper reviewed, electromigration methods utilized and only then on the chiral selectors used.

3.1.1. Theory and recognition mechanism

Some physico-chemical studies were carried out to determine the CS-analyte interaction constants and to create mathematical models for the explanation of a separation mechanism and/or prediction of separation behavior and chiral recognition.

The method for the determination of a rate constant of interconversion of enantiomers in chiral and achiral environments of a dynamic enantioseparation system was evaluated in terms of its accuracy, sensitivity and robustness [186]. Two different enantioseparation systems were selected and compared statistically. Clarification of enhanced selectivity in CZE multi-chiral selector systems, namely mixtures of highly sulfated β-cyclodextrins (HS-β-CDs), as compared with single-isomer CD was reported by Dubsky *et al.* [187]. The presumptions resulting from the theoretical

Table 2. Review articles dealing with chiral separations in capillary electrophoresis methods published in the period between January 2008 and May 2011.

Methods	Chiral selector*	Topic; Group of analytes	Ref.
CE, HPLC		developments and applications	[5,31]
CE, HPLC, GC		general strategies, suitable for beginners	[145]
CE, NACE, CEC, chip-CE		chiral separation principles, developments, applications, new chiral selectors	[146]
CZE, NACE, MEKC, MEEKC, CEC		chiral and non-chiral analyses of phytochemical substances	[147]
CE, CCE, CEC		separation principles, chiral recognition mechanisms, applications to drugs	[148]
ligand exchange in CE, HPLC, CEC		essential papers, authors´ own activities	[2]
CE-MS		electrolytes systems for chiral separations	[149]
CE-MS		chiral separations of amino acids	[150]
EKC-MS		various approaches of on-line coupling	[151]
CE-MS		enantiomeric analysis of compounds in different matrices	[152]
MEKC		classical and newly used pseudo-stationary phases	[153]
MEEKC		advances in chiral separations	[154-156]
CE		on-line sample preparation, ultratrace chiral determination of biologically active compounds	[157]
nano-CE, nano-LC		nano scale chiral separations	[158]
CZE, MEKC, CEC		chiral separation of amino acids, pesticides, polyphenols, food compounds	[159]
CE		methodological and instrumental improvements for enhancing sensitivity in chiral analysis	[160]
chip CE		enantioseparations by microchip electrophoresis	[161,162]
NACE		list of chiral separation	[163]
MEKC		innovations of instruments and methodology	[164]
CE, MEKC, MEEKC, CEC, chip CE		enantioseparations of pharmaceuticals, biochemicals, agrochemicals, fine chemicals, specific test compounds, new chiral selectors, separation mechanism	[165]
CE		recent strategies to improve resolution	[166]
MEKC		fundamental characteristics	[167]
CE	CDs	boron cluster species	[168]
LC, CE		fluoroquinolones	[9]
CE, GC, HPLC		commercial organophosphorus pesticides	[8]
CE		active pharmaceutical ingredients	[169]
CE, GC, HPLC, SFC		pyrethroids (synthetic pesticides)	[11]
MEKC		amino acids, several types of biomatrices	[170]
CE		amino acids	[171]
CE, LC		D-isomers of amino acids, biological matrices, various modes of detection	[24]
CE, HPLC, GC		chiral pesticides	[22]
CE, LC		triptamine based drugs	[23]
CE		peptide stereoisomers	[172]
CE		drugs, metabolites, biomarkers in biological samples, new approaches and enantioselective agents, on-line sample pretreatment, detection modes	[173]
CE		environmental pollutants	[174]
CE, LC		andrenergic drugs	[37]
CE, LC		thalidomide and its metabolites	[36]
CE	antibiotics	pharmaceuticals	[175]
CE	crown ethers crown ethers + CDs	chiral and non-chiral applications	[176]
CE	single isomer derivatives of CDs		[177]
CE	antibiotics polysaccharides		[178]
	uncharged CDs	fundamental contributions	[179]

Continued **Table 2.** Review articles dealing with chiral separations in capillary electrophoresis methods published in the period between January 2008 and May 2011.

Methods	Chiral selector*	Topic; Group of analytes	Ref.
	charged CS	major developments	[180]
EKC	polymeric pseudo-stationary phases	chiral and achiral applications	[181]
CE, LC	Penicillin G acylase	stereoselective molecular recognition mechanism	[27]
CE, LC	monosubstituted positively charged CDs	work carried out in authors´ laboratory, amino acids, anionic pharmaceuticals, neutral analytes	[182]
CE	CDs	new derivatives and applications, drug, environmental and food analysis, bioanalysis	[183]
CE, CEC	CDs	recent employment of CDs	[184]
CE	CDs	applicability of CD selectors	[185]

** If the CSs are not stated the review gives an overview of various types.*

multi-CS model were verified experimentally with the enantioseparation of lorazepam in the presence of a commercial mixture of HS-β-CDs and single-isomer HS-β-CD, heptakis(6-O-sulfo)-β-CD. Binding constants of modafinil enantiomers with the sulfated β-CD were determined using the CE technique and three different linear plotting methods[188]. Computational calculations of the complexation energies of inclusion complexes of sulfated β-CD with ofloxacine and ornidazole enantiomers were utilized to elucidate differences between migration times of the both analytes and their enantiomers. The migration order of the enantiomers are reflected in the different complexation energies [189]. Computational modeling based on the calculations of complexation energies of inclusion complexes were carried out to elucidate the migration behavior of the enantiomers of primaquine and quinocide in the presence of α- and β-CD and 18-crown-6-ether as chiral selectors [190]. The epimerization rate constants of amygdalin under basic microemulsion conditions at different epimerization times were determined by the microemulsion electrokinetic chromatography (MEEKC) method [191].

Propranolol was repeatedly used as the test compound for studying the structures of intermolecular selector-analyte complexes. Possible molecular mechanisms of enantioseparation of propranolol in the presence of heptakis(2,3-di-O-methyl-6-O-sulfo)-β-CD (HDMS-β-CD) and heptakis(2,3-di-O-acetyl-6-O-sulfo)-β-CD (HDAS-β-CD) in aqueous and non-aqueous background electrolytes (BGEs) were investigated by CE and rotational frame nuclear Overhauser effect spectroscopy (ROESY) experiments[192]. Major structural differences were found between the propranolol complexes with native β-CD and heptakis(6-O-sulfo)-β-CD by 1D ROESY NMR experiments [193]. The 2D ROESY technique was used for the elucidation of the structures of inclusion complexes of pregabaline derivatives and β-CD [194] and vinca alkaloids with various CDs [195]. High resolution MS and various NMR techniques were utilized to investigate the mechanism of enantioselective recognition of HDAS-β-CD towards propranolol. The enantiomeric nuclear Overhauser effect was observed for the first time. The switch between external complex and inclusion of the propranolol/HDAS-β-CD pair was observed when an aqueous buffer was changed to a non-aqueous methanolic electrolyte [196]. The binding free energies of HP-β-CD with propranolol and its five analogues were calculated by molecular docking. The calculated results were in agreement with experimentally obtained order of *R*/*S* enantiomers [197].

3.1.2. Detection

Detection is an inseparable part of any separation technique. Sensitive detection offering low limits of detection (LOD) and quantification (LOQ) is essential for analytical applications. Therefore, we present the works, in which detection is the main topic in this special chapter.

New on-line coupling of chiral MEKC to atmospheric pressure photoionisation MS (APPI-MS) was reported for the first time. Four structurally similar neutral test solutes (benzoin derivatives) were successfully ionized by APPI-MS [198]. Ligand-exchange capillary electrophoresis (LECE) utilizing 6-mono-deoxy-6-[4-(2-aminoethyl) imidazoyl]-β-CD complexing with copper(II) as chiral selector was hyphenated to electrospray ionisation mass spectrometry (ESI-MS). LECE-ESI-MS gave better values of LOD of tryptophane enantiomers than LECE with ultraviolet (UV) detection [199]. CE-ESI-MS/MS arrangement was used for the determination of D-carnitine as enantiomeric impurity in L-carnitine in pharmaceutical formulations [200] and dietary food supplements [201]. Chiral CE-ESI MS/MS mode was utilized in the enantioseparations of 1,2,3,4-tetrahydroisoquinoline derivatives. To avoid any potential contamination of MS ionisation source with non-volatile chiral selector (sulfated β-CD), a partial filling technique

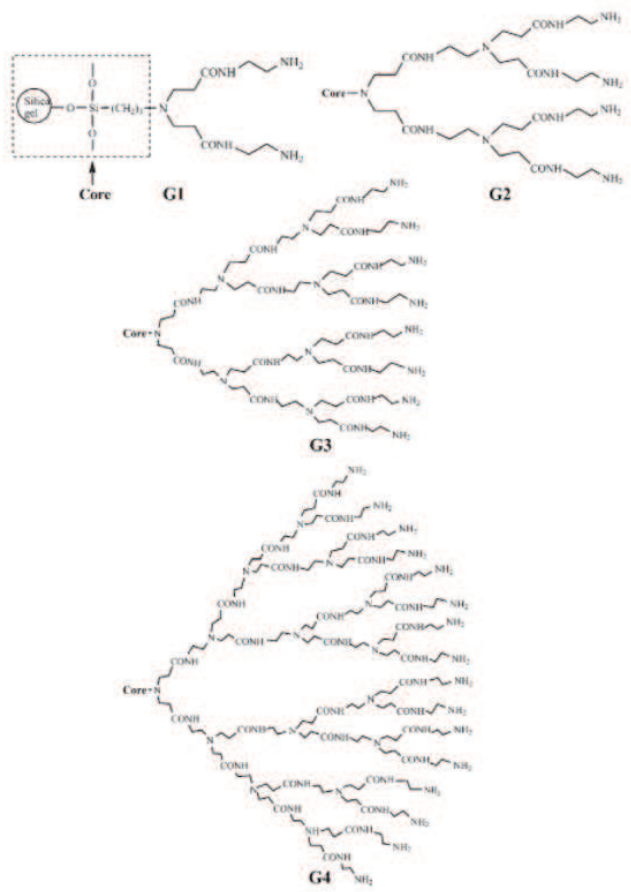

Figure 2. The structure of generation-various dendrimers. G1, G2, G3 and G4 represent one to four-generation dendrimer respectively. Reprinted from [144]. Copyright (2011), with permission from Wiley

was employed [202]. The impact of the BGE composition on the ionization performance in analysis of carvedilol by non-aqueous capillary electrophoresis (NACE) with ESI-MS was investigated under three achiral (ammonium formate, acetate or camphorsulfonate in methanol) and three chiral (addition of HDMS-β-CD, HDAS-β-CD or heptakis(2-O-methyl-3-O-acetyl-6-O-sulfo)-β-CD (HMAS-β-CD)) conditions. The results showed that the chiral selector must be selected not only according to its ability to enantioseparate the compound of interest, but also according to its effect on the ionization efficiency [203]. CE with an end-column amperometric detection was developed for sotalol enantiomers analysis [204]. CE combined with electrochemiluminescence detection was successfully used for enantioseparation of antidepressant trimipramine in aqueous-organic media [205]. A new detection method was introduced for the analysis of the chiral drug, bupropion. The detection was based on the phosphorescence in both the direct mode and the indirect mode. In the indirect mode an analyte acts as an energy donor to the phosphorescent acceptor providing phosphorescence with higher intensity. In this case, biacetyl was utilized as the energy acceptor. LODs of both enantiomers obtained by indirect detection were 40 times lower than those obtained in the direct mode [206]. The detection of non-UV-absorbing α-hydroxy- and amino-substituted alkylcarboxylate enantiomers were achieved by capacitively coupled contactless conductivity detection (C^4D). Derivatization of the analyzed compounds was not necessary when C^4D was used [207]. Two C^4D detectors were utilized in heart-cutting 2D-CE method for chiral separation of native amino acids [208]. Light-emitting diode-induced fluorescence detection (LEDIF) was used for recording D- and L-Asp enantiomers. D- and L-Asp were derivatized with naphthalene-2,3-dicarboxaldehyde to form fluorescent derivatives prior to CE-LEDIF [209].

3.1.3. Sensitivity enhancement by preconcentration

Sensitivity of an analytical method (detection) can be also improved either by derivatization or using a preconcentration step.

Wang *et al*. [210] developed CE method combining a partial filling technique with large volume sample stacking. The method was applied to the enantioseparation of racemic fenoprofen and six 9-fluorenylmethyl chloroformate amino acid derivatives. Under the optimized electrokinetic injection and separation conditions, an almost 1000-fold enhancement in detection sensitivity compared to the normal injection was achieved. Two on-line preconcentration methods: (i) hyphenated MEKC stacking with reverse migrating micelles (SRMM), and (ii) sweeping were used to improve LOD of three triazole fungicides [211]. Poly(ethylene oxide) (PEO) zone was utilized as a concentrating medium during enantiomeric separation of D- and L-aspartic acid by cyclodextin-modified MEKC (CD-MEKC). Migrating sodium dodecylsulfate-analyte (SDS-analyte) complexes were slowed down in the PEO zone and stacked through the viscosity difference between PEO and the sample zone. Approximately 100-fold improvement in the sensitivity of D- and L-aspartic acid detection was achieved [209]. On-line sample preconcentration step, field-amplified sample injection (FASI), substantially improved values of LODs of D,L-tetrahydropalmatine enantiomers and enabled analysis of a real sample [212]. Transient moving chemical reaction boundary (tMCRB) was investigated as the on-line preconcentration possibility for native amino acids in heart-cutting 2D-CE. The first dimension of the heart-cutting 2D-CE provided a non chiral separation and isolation of the fraction of interest and the second dimension rendered chiral separation of the selected amino acid. The LODs were improved by a factor of 10 using the tMCRB focusing step [208].

3.1.4. C(Z)E

In the literature the capillary electrophoresis system with a CS in a BGE is considered either as a CZE with chiral additives or as electrokinetic chromatography (EKC) with chiral pseudostationary phase. We decided to keep the classification used by the authors themselves in their papers and put these works together in one chapter entitled C(Z)E.

3.1.4.1. Cyclodextrins

CD derivatives belong to the most popular group of chiral selectors used in CE. Enantioseparations using the well-established and/or newly designed and prepared derivatives regularly appear in the literature. CDs can be applied in all possible separation modes – CZE, MEKC, MEEKC, CEC.

Several CD derivatives were evaluated for their ability to separate a series of fifteen racemic 4,5-disubstituted imidazole compounds by CE. The mechanism of the chiral recognition was discussed [58]. Hydroxypropyl-γ-CD (HP-γ-CD) was revealed as the most effective chiral selector towards iodiconazole, a new antifungal drug, and its analogues [213]. Sulfobutyl ether-β-CD was utilized for the determination of enantiomeric purity of a new antiarrhytmic agent marked RS86017. The optimized method was validated [214]. Zhu *et al*. separated sibutramine enantiomers by either methyl-β-CD or carboxymethyl-β-CD (CM-β-CD) as chiral selectors [215]. This research group also investigated the reversal of the enantiomer migration order in CE based on separations of sibutramine as a function of the concentration of native β-CD and acetyl-β-CD [216]. 1,2,3,4-tetrahydroisoquinoline derivatives, neurotoxins inducing Parkinsonism, were baseline enantioseparated by CE-ESI-MS/MS with sulfated β-CD as CS. The resolution values were better than those reported previously by a HPLC method [202]. In order to evaluate the enantioselective binding of zoplicone enantiomers to human serum albumin (HSA), the EKC with partial filling of the anionic CM-β-CD as chiral selector was applied. The results suggested that *S*-zopiclone exhibits twice the affinity to HSA than *R*-zopiclone [217]. The selection of 22 neutral and anionic CDs were screened in terms of their ability to effectively separate the enantiomers of five antimalarial drugs [218]. Neutral and anionic CDs were also tested for the enantiomeric separation of benzoxazolinone amino alcohols and their aminoketone precursors [219]. A method for the simultaneous analysis of *R*-(−)-, *S*-(+)-baclofen and an impurity (4*R*,*S*)-4-(4-chlorophenyl)pyrrolidin-2-one utilizing α-CD as CS was established. A PEO-coated capillary was used and an optimized method was validated [220]. The comparison of β-CD, γ-CD, dimethyl-β-CD (DM-β-CD), heptakis(2,3,6-tri-O-methyl)-β-CD (TM-β-CD) and HP-β-CD for their ability to separate fenoterol enantiomers were reported and the obtained results were compared with HPLC experiments [86]. A novel single isomer of positively charge β-cyclodextrin, mono-6-deoxy-6-((2*S*, 3*S*)-(+)-2,3-O-isopropylidene-1,4-tetramethylenediamine)-β-CD was designed and synthesized. The chiral resolution capabilities of a new chiral selector were studied using 10 dansylamino acids as model analytes [221]. Native α-, β-, and γ-CDs and their hydroxypropylated, randomly methylated, carboxymethylated and sulfobutylated derivatives were used for the enantioseparations of three vinca alkaloid enantiomers (vincamine, vinpocetine and vincadiformine). All vinca alkaloids were successfully enantioresolved but with different CDs [195]. HP-β-CD among other tested CDs (γ-CD, β-CD, DM-β-CD)

provided the best resolution of pheniramine enantiomers [222]. The method was subsequently modified using a partial filling approach that resulted in improved resolution [223]. CE method with sulfated β-CD as chiral selector for the separation of enantiomers of ofloxacin and ornidazole was described. The optimized method was validated and applied for the determination of these analytes in a pharmaceutical formulation [189]. Several CD derivatives (single carboxymethyl-α-, β- and γ-CDs or sulfobutyl-β-CD) were examined to find the most selective system for enantioseparations of 19 pairs of cis-β-lactam stereoisomers of pharmacological importance. From the tested chiral selectors the sulfobutyl-β-CD yielded the best results [224]. A new single-isomer cationic β-cyclodextrins, namely mono-6-deoxy-6-pyrrolidine-β-CD chloride (pyCDCl), mono-6-deoxy-6-(N-methyl-pyrrolidine)-β-CD chloride (N-CH_3-pyCDCl), mono-6-deoxy-6-(N-(2-hydroxyethyl)-pyrrolidine)-β-CD chloride (N-EtOH-pyCDCl), mono-6-deoxy-6-(2-hydroxymethyl-pyrrolidine)-β-CD chloride (2-MeOH-pyCDCl) were synthesized (see Fig. 3A) and used as chiral selectors for the enantioseparation of carboxylic and hydroxycarboxylic acids and dansyl-amino acids. The pyCDCl CS exhibited the greatest resolving ability (Fig. 3B) [225]. CE was utilized for the enantioseparation of seven Tic-hydantoin sigma-1 agonists as an alternative technique to HPLC. The enantiomers were fully resolved with HS-β-CD [226]. The enantiomers of pregabalin derivatized by tosyl- and dansyl-chloride were separated using CD modified CE. The best resolution was obtained using 6-monodeoxy-6-mono-(3-hydroxy)-propylamino-β-cyclodextrin hydrochloride for the tysolated derivate and trimethylated α- and β-CDs for dansylated prebalin [194].

3.1.4.2. Oligosaccharides, polysaccharides

Glycogen, a branched polysaccharide, was introduced as a novel chiral selector. The enantioseparation potential of glycogen (an electrically neutral compound) was tested with one acidic and four basic drugs. The enantiomers of citalopram, cetirizine, nefopam and ibuprofen were baseline separated and partial separation of enantiomers of amlodipine was achieved [227]. Chondroitin sulfate A (CSA), a linear ionic polysaccharide, was used as a chiral selector in the enantioseparation of nefopam hydrochloride by affinity electrokinetic chromatography (AEKC). The selector concentration, pH of the BGE, capillary temperature and applied voltage were systematically optimized in order to obtain the optimum separation of the nefopam enantiomers. A statistical analysis approach revealed that the buffer's pH was the most significant parameter controlling the chiral separation. The enantiorecognition mechanism of CSA towards the enantiomers of nefopam was described [228]. Carboxymethylated cyclosophoraose (CM-Cys) was synthesized and employed as a chiral selector in the enantioseparation of flavonoids [229]. α-Cyclosophorooctadecaose (α-C18), produced by *Rhodobacter sphaeroides*, was successfully isolated and used as chiral selector in the enantioseparation of catechin [230] and five flavanones and three flavanone-7-O-glycosides [231]. Maltodextrin was employed as a chiral selector in the separation of the enantiomers of cetirizine and hydroxyzine in spiked human plasma. The effect of zwitterionic property of cetirizine was also investigated and its cationic form was proven to be advantageous for enantioseparation [232].

3.1.4.3. Antibiotics

Antibiotics represent a very popular group of CSs with a high chiral discrimination power. Their disadvantage is they absorp at the wavelengths usually used for detection of analytes.

Two new chiral selectors from the antibiotic family of macrolides were used within the period of interest for the first time. Erythromycin lactobionate, the structure is depicted in Fig. 4, showed an excellent ability to enantioseparate of the enantiomers of N,N-dimethyl-3-(2-methoxyphenoxy)-3-propylamine, propranolol and duloxetine, while just a partial enantioresolution of primaquine, chloroquine and nefopam [233]. Azithromycin, a semi-synthetic macrolide antibiotic derived from erythromycin, was employed for the enantioseparation of five chiral drugs and tryptophane [234]. Chiral separations of racemic fenoprofen and six 9-fluorenylmethylated acetic acids were achieved employing vancomycin as chiral selector [210]. The same CS was used for the enantioseparations of α-hydroxy- and amino-substituted alkyl carboxylate enantiomers [207]. Three vancomycin-type macrocyclic antibiotics, *i.e.,* balhimycin, bromobalhimycin and dechlorobalhimycin, were used for enantioseparation of N-benzolyated amino acids. Enantioseparation of N-benzoylated derivatives of four amino acids (Leu, Ala, Met and Thr) were compared using a CE method, which combined partial filling approach with a dynamic coating technique and the co-electroosmotic flow (co-EOF) electrophoresis method. The enantiorecognition mechanism was investigated [235].

3.1.4.4. Miscellaneous

Bovine serum albumin was added to a buffer solution to achieve the enantioseparation of D,L-tetrahydropalmatine. Partial filling technique was used to decrease the UV absorption of BGE [212]. Chiral

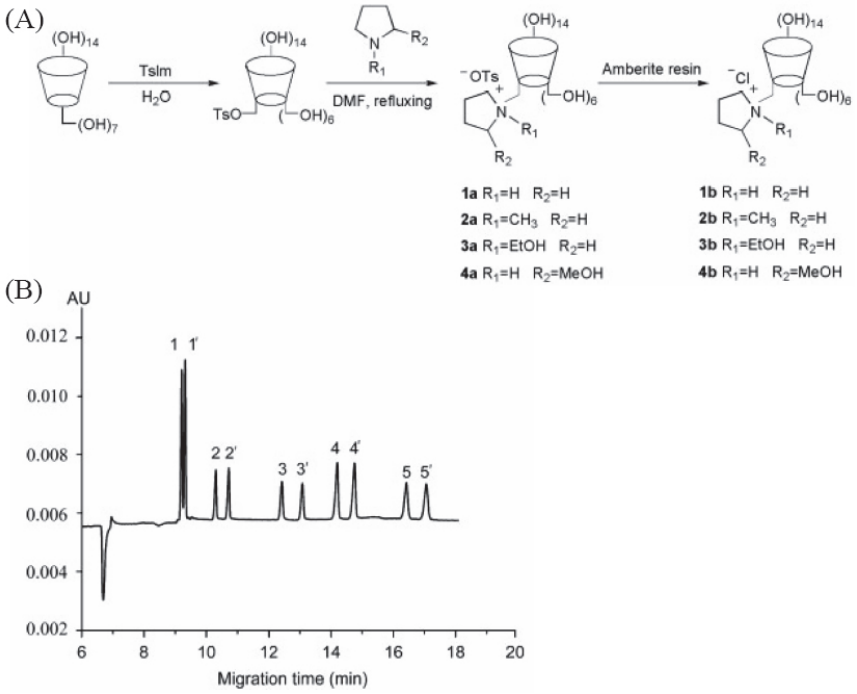

Figure 3. (A) Synthesis of alkyl pyrrolidine substituated single isomer CDs. (B) Enantioseparation of a mixture of five pairs of analytes. 50 mM phosphate buffer, pH 7.0, with 5 mM pyCDCl as chiral selector. (1) dansyl-D,L-serine; (2) 2-(4-hydroxyphenoxy)propionic acid; (3) 2-phenoxypropionic acid; (4) p-hydroxymandelic acid; (5) mandelic acid Reprinted from [225]. Copyright (2011), with permission from Wiley

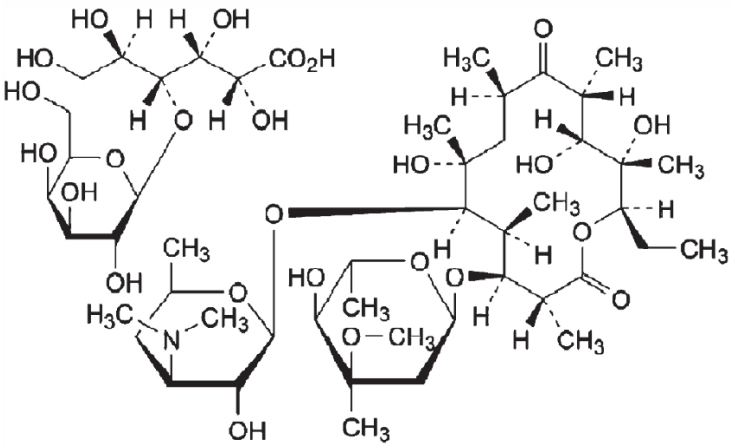

Figure 4. Structure of erythromycin lactobionate, a new antibiotic chiral selector. Reprinted from [233] with kind permission from Springer Science + Business Media.

selector (+)-(18-crown-6)-2,3,11,12-tetracarboxylic acid was employed in the second dimension of heart-cutting 2D-CE to enantioseparate D,L-phenylalanine and D,L-threonine in a mixture of 22 native amino acids [208]. The possibility of using N-blocked bivalent dipeptides, known as chiral mobile phase additives in HPLC, as ion-pairing agents in CE for both non-chiral and chiral separation of amino alcohols was shown [236].

Ionic liquids can be used as BGE additives. However, their exceptional properties become obvious only if they are used solely. The ephedrine-based chiral ionic liquid, (+)-N,N-dimethylephedrinium-

bis(trifluoromethanesulfon)imidate ([DMP]$^+$ [Tf_2N]$^-$), was introduced as chiral selector into non-aqueous separation solution consisting of acetonitrile and methanol. Rabeprazole and omeprazole were enantiosepareted and the effects of the [DMP]$^+$ [Tf_2N]$^-$ concentration, the buffers and the choise of organic solvents were studied. The discussion of separation mechanism was further undertaken [237]. The new fluorescent chiral ionic liquid, L-phenylalanine ethyl ester bis(trifluoromethane) sulfonimide, capable of acting simultaneously as solvent, chiral selector and fluorescent agent in chiral analytical measurements was introduced and properties of the separation system were studied [238].

3.1.4.5. Dual selector systems

If optimization of an enantioseparation system with one chiral selector fails, a dual selector system can be employed. However, in many cases well optimized separation with one CS can yield the same or even better results. Many chiral reagents including cyclodextrins and their derivatives, crown ethers, proteins, chiral surfactants and chiral polymers were used in dual selector systems for the enantioseparation of a series of chiral compounds.

The first investigation of an enantioselectivity of dual selector system, which contained a polysaccharide glycogen, was published. Three dual systems combined glycogen with CSA, β-CD and HP-β-CD were tested. The dual system of glycogen with CSA exhibited good enantiodiscriminative properties towards the tested drugs (duloxetine, cetirizine, citalopram, sulconazole, laudanosine, amlodipine, propranolol, atenolol, nefopam). Enhanced enantioselectivity compared to the single selector systems was observed [239]. A CE assay for the simultaneous determination of charged and uncharged potential impurities (1*S*,2*S*-(+)-norpseudoephedrine, 1*R*,2*S*-(–)-norephedrine, phenylacetone and phenylacetone oxime) of dexamphetamine sulfate including the stereoisomer levoamphetamine was developed and validated. Dual CD system consisting of sulfobutyl ether-β-CD and sulfated β-CD was employed [240]. The simultaneous separation of the stereoisomers of six tetrahydronaphthalenic derivatives (agonists and antagonists for the melatonin binding sites) were successfully achieved using a dual CD system in a capillary dynamically coated with PEO. The HS-β-CD/γ-CD system was proven to be the optimal system for this analysis [241]. Enantioselective abilities of various dual CD selectors (carboxymethyl- and sulfobutyl-β-CDs with neutral β-CDs) towards 19 pairs of cis-β-lactam derivatives were tested. Mixtures of TM-β-CD and the negatively charged sulfobutyl-β-CD were able to separate all the investigated stereoisomeric pairs [224]. HDMS-β-CD with β-CD was used as a dual CS system for the separation of methamphetamine and its related compounds. The main aim of this work was to compare the reproducibility of the analysis obtained in three different capillaries – untreated capillary, poly(vinyl alcohol) (PVA)-coated capillary and a capillary with diol groups. The relative standard deviations of the migration times of analytes were lower for diol- and PVA-coated capillaries (0.1%) than for the untreated one (0.4%) [242]. Single isomer CD and dual CDs systems (phosphated-β-CD with HP-γ-CD) were tested for enantioseparation of tysolated and dansylated pregabalins. The resolution obtained with two enantiomers became better only in a dansyl-pregabalin in acidic environment [194]. An Zn(II)-L-valine complex as chiral selector with the addition of β-CD is another example of a dual CS systems [243]. The presence of CD enhanced enantioselectivity of the LECE system.

3.1.5. LECE

Special separation systems utilizing formation of complexes, in which mostly Zn(II) or Cu(II) serve as central ions and pure enantiomer CS and analyte as ligands, were introduced as early as in 1971 [244] and are still utilized today.The novel chiral selector, Zn(II)-L-prolinamide, was used in a kinetic study of the competitive effect of sodium benzoate on D-amino acid oxidase activity [245]. Aldo-bis-indole derivatives (aldo-BINs) of common monosaccharides were prepared and separated by CE. The enantioseparation of the D,L-pairs of aldo-BINs based on ligand-exchange mechanism was achieved using HP-β-CD as a chiral ligand and borate buffer, where borate anion served as central ion. The usefulness of UV active aldo-BINs for sugar composition analysis was demonstrated [246]. Similarly, the D,L-aldo-naphthylimidazoles (aldo-NAIMs) of various D,L-monosaccharide pairs were prepared and enatioresolved utilizing borate buffer and phosphate buffer with sulfated-α-CD [247]. The separation performance of a new ligand-exchange selector di-L-valinol-copper complex was tested on enantioseparations of D,L-dansyl-amino acids, unmodified amino acids racemates and a β-blocker *R,S*-propranolol by LECE in thermoreversible low molecular weight organogel (LMOG) – trans-(1*S*,2*S*)-1,2-bis-(dodecylamido) cyclohexane. The enantioseparation achieved was proven to be superior to MEKC under similar operating conditions [248]. To separate D,L-isocitric acid enantiomers, D-quinic acid was used as a chiral selector ligand and Mn(II), Fe(III),Co(II), Ni(II), Cu(II), and Zn(II) ions were utilized as the central ions. D,L-isocitric acid was found to be enantioseparable with all the above mentioned metal ions except for Mn(II)

[249]. Different cyclodextrins were employed in chiral LECE because CDs can form inclusion complexes and thus enhance the regiospecificity and stereospecificity. The successful separations of 20 pairs of D,L-amino acids with Zn(II)-L-valine complex in the presence of β-CD were achieved. Furthermore, the kinetics of L-amino acid oxidase enzyme reaction was measured in the proposed dual CS system [243]. Dependence of enantioseparation of tartaric acid on molar ratio of Cu(II)/D-quinic acid was studied. At low (1/1 – 1/3) and high (1/8 – 1/12) molar ratios tartaric acid was enantioresolved, but at medium molar ratios chiral separation was not achieved. Reversed enantiomer migration order at high molar ratios were explained by changes in the coordination structure of Cu(II) ion with D-quinic acid [250]. Sodium arsenyl-(L)-(+) tartrate, a member of tartrate-based transition metal complexes, was introduced as a CS that showed enantioselective associations with many cationic analytes, including primary, secondary, and tertiary amines. Twenty six amine-containing compounds showed enantioselectivity within reasonable analysis time and 13 of them were baseline separated [251].

3.1.6. MEKC

Micellar electrokinetic chromatography (or micellar capillary electrophoresis (MCE)) is a popular technique suitable for separation of uncharged analytes. The enantioselective environment can be formed with chiral micelles, achiral micelles with chiral additives to BGE or using mixed micelles (micelle complexes composed of achiral micelles and CSs).

The CD-MEKC method with a HP-γ-CD chiral selector and SDS micelles was reported for the enantiomeric separation of econazole [252] and three triazol fungicides (hexaconazole, penconazole and myclobutanil) [211]. The same chiral selector and sodium deoxycholate as surfactant were used for enantioseparation of derivatized dipeptides (Tyr-Phe, Tyr-Leu, Ala-Gln). The dipeptides were precolumn derivatized with naphthalene-2,3-dicarboxyaldehyde [253]. A HP-β-CD mediated MEKC was utilized for the separation of Asp enantiomers. The influence of the molar ratio of SDS to HP-β-CD as well as the total concentration of SDS and HP-β-CD on the enantioresolution was investigated [209]. TM-β-CD in the presence of sodium cholate surfactant enabled enantioseparation of the synthetic pyrethroid cis-bifenthrin by CD-MEKC [254]. Enantioseparation of this pyrethroid was reported for the first time. This method can be used for the determination of cis-bifenthrin in commercial insecticides. Chen and Du [255] modified MEKC method by addition of a novel antibiotic CS – clindamycin phosphate. Different types of anionic surfactants, organic additives and BGE compositions were tested. Excellent separation of the enantiomers of nefopam, citalopram, tryptophane, chlorphenamine, propranolol and metoprolol, and partial enantioresolution of tryptophane methyl ester and cetirizine were achieved with SDS in phosphate buffer and propane-2-ol as an organic modifier. Four chiral photoinitiators, hydrobenzoin, benzoin, benzoin methyl ether and benzoin ethyl ether were simultaneously enantioseparated using a mixture of two chiral molecular micelles polysodium N-undecenoxy carbonyl-L-leucinate (poly-L-SUCL) and polysodium N-undecenoyl-L,L-leucylvalinate (poly-L,L-SULV) [198]. The mixed mode separation method combining MEKC with polyelectrolyte multilayer (PEM) coating procedure was used for both chiral and achiral separations. Sodium poly(N-undecanoyl-L-leucylvalinate) (poly-L-SULV) served as both a chiral molecular micelles creator and an adsorbed chiral polymer layer [256]. Two CD-MEKC methods were developed for simultaneous enantiomeric separation of four chiral polycyclic musks (Galaxolide, Tonalide, Traseolide, and Phantolide). The best separation was achieved with SDS micelles in a dual CD system composed of HP-γ-CD and γ-CD [257].

3.1.7. MEEKC

Three different arrangements for enantioselective separation can be used in microemulsion electrokinetic chromatography. A chiral selector can be deposited on the capillary wall, chiral microemulsion can be used or CS can be added to the BGE.

MEEKC carried out in a capillary coated by β-CD enfolded polymer layer provided higher separation efficiency of stereoisomers of sertraline than MEEKC without the presence of a CD polymer coating [258]. The development and validation of a MEEKC method for enantioseparation of phenethylamines was reported. The separation system consisted of sulfated β-CD added to the microemulsion composed of the oil-component ethyl acetate, surfactant sodium dodecylsulfate, cosurfactant 1-butanol, propane-2-ol as the organic modifier and phosphate buffer as the aqueous phase. The results were compared with those obtained by CD-modified CZE [259]. The preparation of chiral microemulsions from eight L- and D-tartrates with different alcohol moieties as chiral oils was described by Hu *et al*. [260]. A water insoluble compound, di-*i*-butyl L-tartrate, was used for the preparation of a stable microemulsion, which was utilized for the enantioseparations of β-blockers. Yu *et al*. utilized MEEKC for the separation and determination of amygdalin and its epimer (neoamygdalin) [191].

Gold nanoparticles modified by thiolated β-CD were revealed as a suitable pseudostationary phase for the

enantioseparation of four dinitrophenyl-labeled amino acid enantiomers (Val, Leu, Glu and Asp) and three pairs of drug enantiomers (chlorpheniramine, zopiclone, carvedilol) [261].

3.1.8. Microchip capillary electrophoresis

Substantially reduced material needs, therefore low cost of analyses, and small sample amounts required for analysis are the main advantage of miniaturized separation techniques.

The MEKC mode of microchip electrophoresis utilizing SDS micelles in borate buffer for quantitative analyses of fluorescein-5-isothiocyanate (FITC) labeled ephedrine and pseudoephedrine in tablet formulations and urine after oral intake of the drugs was reported. The linearity, reproducibility, and applicability of the method were evaluated [262]. Both achiral and chiral separations of proteins and racemic amino acids were studied on a poly(methyl methacrylate) (PMMA) microchip. Immobilization of amino-poly(ethyleneglycol) (PEG–NH_2) onto surface of the microchip reduced irreversible adsorption of proteins on the wall. Chiral separation of tryptophane was achieved after addition of bovine serum albumin to the background solution [263].

A new method was described for 2D separations using a microfluidic chip normally employed for 1D electrophoresis. Gradient elution moving boundary electrophoresis and chiral CZE were combined as the first and the second dimension of the separation process of some amino acids, respectively [264].

3.1.9. NACE

Non-aqueous capillary electrophoresis represents the possibility for changing the interaction mechanism to extend the range of applicability of a given chiral selector because different interaction types prevail in chiral recognition in aqueous *vs*. non-aqueous environments.

Enantioselectivity of single-isomer anionic cyclodextrin HMAS-β-CD towards basic model analytes were tested under various concentrations of HMAS-β-CD and BGE composition in order to propose a generic system for basic drug analysis [265]. Two single-isomer anionic CDs, HMAS-β-CD and HDMS-β-CD, were utilized simultaneously in chiral and achiral separations of fenbendazole and its sulfoxide and sulfone metabolites [266]. Novel NACE method for the enantioseparation of some β-blockers and β-agonists was developed. Di-n-amyl L-tartrate–boric acid complex, *in situ* synthesized by the reaction of di-n-amyl L-tartrate with boric acid in a non-aqueous BGE using methanol as the medium, was tested as the chiral selector. The enantioseparations of all the tested drugs were achieved [267]. Two new antibiotic CSs were tested in NACE mode. Erythromycine lactobionate with mixed buffer solution containing borate buffer and methanol (50/50, *v/v*) was utilized for enantioseparation of N,N-dimethyl-3-(2-methoxyphenoxy)-3-propylamine, propranolol, duloxetine, primaquine, chloroquine and nefopam [233]. Polar organic mixture composed of acetonitrile, methanol, acetic acid and triethylamine (80/20/0.1/0.1, *v/v/v/v*) was employed as BGE for enantioseparation of five chiral drugs and tryptophane with azithromycin as CS [234]. Non-aqueous mode of capillary electrophoresis was also used for enantioseparation of rabeprazole and omeprazole in presence of ephedrine-based ionic liquid $[DMP]^+[Tf_2N]$ [237].

4. Conclusions

The importance of enantioselective separation methods is reflected in the number of publications in the literature. Both liquid chromatography and electromigration techniques have an irreplaceable position in this field. The crucial factor for the creation of a successful enantioselective separation system is the proper choice of a chiral selector or chiral stationary phase. The choice must be based on the structure of the compounds to be analyzed. The separation system must be considered as a whole because the enantiodiscrimination mechanisms can participate in different separation environments with the same CS/CSP. This review is intended to serve as an aid to support the choice of a chiral selector or a chiral stationary phase.

Acknowledgements

Financial supports of the Grant Agency of the Charles Univerisity grant No. 51009, KONTAKTAM2010, project No. LH11018, the Grant Agency of the Academy of Science of the Czech Republic, grant No. IAAX00100903 and the long-term research plan of the Ministry of Education of the Czech Republic, No. MSM 0021620857 are gratefully acknowledged. The authors express their gratitude to R. Gilar for language corrections.

References

[1] B. Natalini et al., Adv. Chromatogr. 49, 71 (2011)
[2] M.G. Schmid, G. Gubitz, Anal. Bioanal. Chem. 400, 2305 (2011)
[3] C.H. Chu, R.H. Liu, Chem. Soc. Rev. 40, 2177 (2011)
[4] H.D. Qiu, X.J. Liang, M. Sun, S.X. Jiang, Anal. Bioanal. Chem. 399, 3307 (2011)
[5] T.J. Ward, K.D. Ward, Anal. Chem. 82, 4712 (2010)
[6] E.A. Christodoulou, Curr. Org. Chem. 14, 2337 (2010)
[7] Y.W. Zhang, S. Yao, H. Zeng, H. Song, Curr. Pharm. Anal. 6, 114 (2010)
[8] L. Li, S.S. Zhou, L.X. Jin, C. Zhang, W.P. Liu, J. Chromatogr. B 878, 1264 (2010)
[9] A.A. Elbashir, B. Saad, H.Y. Aboul-Enein, Curr. Pharm. Anal. 6, 246 (2010)
[10] I. Ilisz, Z. Pataj, A. Aranyi, A. Peter, Mini-Rev. Med. Chem. 10, 287 (2010)
[11] V. Pérez-Fernández, M.A. García, M.L. Marina, J. Chromatogr. A 1217, 968 (2010)
[12] D. Wistuba, J. Chromatogr. A 1217, 941 (2010)
[13] B. Chankvetadze, J. Sep. Sci. 33, 305 (2010)
[14] M. Lammerhofer, J. Chromatogr. A 1217, 814 (2010)
[15] R. Bhushan, R. Kumar, Biomed. Chromatogr. 24, 66 (2010)
[16] N.H. Hashim, S. Shafie, S.J. Khan, Environ. Technol. 31, 1349 (2010)
[17] I. Ilisz, R. Berkecz, A. Péter, J. Chromatogr. A 1216, 1845 (2009)
[18] T. Ikai, Y. Okamoto, Chem. Rev. 109, 6077 (2009)
[19] A.B. Wijeratne, K.A. Schug, J. Sep. Sci. 32, 1537 (2009)
[20] I. Ali, K. Saleem, I. Hussain, V.D. Gaitonde, H.Y. Aboul-Enein, Sep. Purif. Rev. 38, 97 (2009)
[21] F.J.M. de Santana, V. Aparecida, P. Jabor, P.S. Bonato, Bioanalysis 1, 221 (2009)
[22] B.S. Sekhon, J. Pestic. Sci. 34, 1 (2009)
[23] C. Saka, Crit. Rev. Anal. Chem. 39, 32 (2009)
[24] D.L. Kirschner, T.K. Green, J. Sep. Sci. 32, 2305 (2009)
[25] W.B. Holzheuer, M.M. Wong, G.K. Webster, Curr. Pharm. Anal. 5, 346 (2009)
[26] W.B. Holzheuer, M.M. Wong, G.K. Webster, Curr. Pharm. Anal. 5, 10 (2009)
[27] G. Massolini, C. Temporini, E. Calleri, J. Chromatogr. B 875, 20 (2008)
[28] T. Cecchi, Crit. Rev. Anal. Chem. 38, 161 (2008)
[29] A.V. Kostarnoi, G.B. Golubitskii, E.M. Basova, E.V. Budko, V.M. Ivanov, J. Anal. Chem. 63, 516 (2008)
[30] A. Ghassempour, H.Y. Aboul-Enein, J. Chromatogr. A 1191, 182 (2008)
[31] T.J. Ward, B.A. Baker, Anal. Chem. 80, 4363 (2008)
[32] I. D'Acquarica, F. Gasparrini, D. Misiti, M. Pierini, C. Villani, Adv. Chromatogr. 46, 109 (2008)
[33] D. Mangelings, Y.V. Heyden, Adv. Chromatogr. 46, 175 (2008)
[34] J. Haginaka, J. Chromatogr. B 875, 12 (2008)
[35] C. Yamamoto, M. Fujisawa, M. Kamigaito, Y. Okamoto, Chirality 20, 288 (2008)
[36] M.E. Bosch, A.J.R. Sanchez, F.S. Rojas, C.B. Ojeda, J. Pharmaceut. Biomed. 46, 9 (2008)
[37] Z.Z. Wang, O.Y. Jin, W.R.G. Baeyens, J. Chromatogr. B 862, 1 (2008)
[38] T.E. Beesley, LC GC Eur. 24, 270 (2011)
[39] T.D. Lourenco, N.M. Cassiano, Q.B. Cass, Quim. Nova 33, 2155 (2010)
[40] T. Zhang, D. Nguyen, P. Franco, J. Chromatogr. A 1217, 1048 (2010)
[41] K. Liu, D. Zhong, X. Chen, Bioanalysis 1, 561 (2009)
[42] I.R.S. Magalhaes, P.S. Bonato, Curr. Pharm. Anal. 6, 15 (2010)
[43] W. Nowik, M.B.C. de Bellaistre, A. Tchapla, S. Heron, J. Chromatogr. A 1218, 3636 (2011)
[44] G.W. Jin et al., J. Sep. Sci. 33, 564 (2010)
[45] X. Li, Z.M. Zhou, D. Xu, J. Zhang, Talanta 84, 1080 (2011)
[46] X.H. Lai, W.H. Tang, S.C. Ng, J. Chromatogr. A 1218, 3496 (2011)
[47] Z.M. Zhou, X. Li, X.P. Chen, X.Y. Hao, Anal. Chim. Acta 678, 208 (2010)
[48] G.Y. Yu et al., Chromatographia 73, 1049 (2011)
[49] Y. Wang, D.J. Young, T.T.Y. Tan, S. Ng, J. Chromatogr. A 1217, 7878 (2010)
[50] Q. Qin et al., J. Sep. Sci. 33, 2582 (2010)
[51] Z.M. Zhou, X. Li, X.P. Chen, M. Fang, X.A. Dong, Talanta 82, 775 (2010)
[52] Y. Wang, D.J. Young, T.T.Y. Tan, S.C. Ng, J. Chromatogr. A 1217, 5103 (2010)
[53] H.S. Wang, P. Jiang, M. Zhang, X.C. Dong, J. Chromatogr. A 1218, 1310 (2011)
[54] H.S. Wang, D. Xu, P. Jiang, M. Zhang, X.C. Dong, Analyst 135, 1785 (2010)
[55] Y.Q. Lv, D.P. Mei, X.X. Pan, T.W. Tan, J. Chromatogr. B 878, 2461 (2010)
[56] J. Zhao et al., Talanta 83, 286 (2010)
[57] S.K.T. Chelvi, E.L. Yong, Y.H. Gong, J. Sep. Sci. 33, 74 (2010)

[58] Z.S. Breitbach et al., Supramol. Chem. 22, 758 (2010)
[59] C. Lin et al., J. Sep. Sci. 33, 1558 (2010)
[60] Z. Bikadi et al., Chromatographia 71, S21 (2010)
[61] G. Fodor et al., Chromatographia 71, S29 (2010)
[62] C.L. Wang, Z.S. Breitbach, D.W. Armstrong, Sep. Sci. Technol. 45, 447 (2010)
[63] H.P. Nguyen, S.H. Yang, J.G. Wigginton, J.W. Simpkins, K.A. Schug, J. Sep. Sci. 33, 793 (2010)
[64] R. Berta, Z. Szakacs, M. Babjak, M. Gazdag, Chromatographia 71, S35 (2010)
[65] V. Gonzalez-Ruiz, A.I. Olives, M.A. Martin, Anal. Bioanal. Chem. 400, 395 (2011)
[66] D. Guillarme et al., Chirality 22, 320 (2010)
[67] P. Rodriguez-Bonilla, J.M. Lopez-Nicolas, F. Garcia-Carmona, J. Chromatogr. B 878, 1569 (2010)
[68] S.Q. Tong, J.Z. Yan, Y.X. Guan, Y.E. Fu, Y. Ito, J. Chromatogr. A 1217, 3044 (2010)
[69] C. Zhang, W.X. Huang, Z. Chen, A.M. Rustum, J. Chromatogr. A 1217, 4965 (2010)
[70] T. Zhang et al., J. Chromatogr. A 1075, 65 (2005)
[71] H. Kazoka, O. Rotkaja, L. Varaceva, Chromatographia 73, S123 (2011)
[72] P. Peluso et al., Curr. Org. Chem. 15, 1208 (2011)
[73] A.A. Younes, D. Mangelings, Y.V. Heyden, J. Pharmaceut. Biomed. 55, 414 (2011)
[74] E. Stern et al., Chirality 23, 389 (2011)
[75] K.S.S. Dossou, P. Chiap, A.C. Servais, M. Fillet, J. Crommen, J. Sep. Sci. 34, 617 (2011)
[76] C. Zhang et al., Chirality 23, 215 (2011)
[77] C.G. Lv, Z.Q. Zhou, J. Sep. Sci. 34, 363 (2011)
[78] K.G. Gebreyohannes, V.L. McGuffin, J. Liq. Chromatogr. Relat. Technol. 34, 258 (2011)
[79] R.F. Gomes, N.M. Cassiano, J. Pedrazzoli, Q.B. Cass, Chirality 22, 35 (2010)
[80] C.Z. Zheng, D.T. Zhang, Q. Wu, X.F. Lin, Chirality 23, 99 (2011)
[81] Y.P. Zhang et al., J. Chromatogr. B 878, 1285 (2010)
[82] A. Ciogli, W. Bicker, W. Lindner, Chirality 22, 463 (2010)
[83] I. Ilisz et al., J. Chromatogr. A 1217, 2980 (2010)
[84] S. Caccamese, R. Chillemi, J. Chromatogr. A 1217, 1089 (2010)
[85] M. Lammerhofer et al., J. Chromatogr. A 1217, 1033 (2010)
[86] T. Ullrich et al., Biomed. Chromatogr. 24, 1125 (2010)
[87] L. Peng, S. Jayapalan, B. Chankvetadze, T. Farkas, J. Chromatogr. A 1217, 6942 (2010)
[88] V. Friebolin, S. Marten, K. Albert, Magn. Reson. Chem. 48, 111 (2010)
[89] K.S.S. Dossou et al., J. Sep. Sci. 33, 1699 (2010)
[90] R.B. Kasat, E.I. Franses, N.H.L. Wang, Chirality 22, 565 (2010)
[91] P. Franco, T. Zhang, LC GC Eur. 23, 302 (2010)
[92] P. Franco, T. Zhang, LC GC N. Am. 28, 818 (2010)
[93] I.A. Bae, J.H. Park, S.H. Choi, Polym. Int. 60, 833 (2011)
[94] H.T. Qu et al., J. Sep. Sci. 34, 536 (2011)
[95] S.W. Tang, T. Ikai, M. Tsuji, Y. Okamoto, Chirality 22, 165 (2010)
[96] S.W. Tang, T. Ikai, M. Tsuji, Y. Okamoto, J. Sep. Sci. 33, 1255 (2010)
[97] F.Y. Pan, X.F. Li, G.H. Liu, Y.L. Li, S.W. Tang, Chinese J. Anal. Chem. 39, 7 (2011)
[98] Y. Katoh et al., Polym. J. 43, 84 (2011)
[99] J. Shen, T. Ikai, X.D. Shen, Y. Okamoto, Chem. Lett. 39, 442 (2010)
[100] J. Shen, T. Ikai, Y. Okamoto, J. Chromatogr. A 1217, 1041 (2010)
[101] Y. Sugiura, C. Yamamoto, T. Ikai, M. Kamigaito, Y. Okamoto, Polym. J. 42, 31 (2010)
[102] M.K. Mone, K.B. Chandrasekhar, Chromatographia 73, 985 (2011)
[103] L. Sipos et al., J. Chromatogr. A 1217, 6956 (2010)
[104] Z. Pataj et al., Chromatographia 71, S13 (2010)
[105] X.T. Zhang, Y. Bao, K. Huang, K.L. Barnett-Rundlett, D.W. Armstrong, Chirality 22, 495 (2010)
[106] E. Pittler, M.G. Schmid, Biomed. Chromatogr. 24, 1213 (2010)
[107] V. Guillen-Casla, M.E. Leon-Gonzalez, L.V. Perez-Arribas, L.M. Polo-Diez, Anal. Bioanal. Chem. 397, 63 (2010)
[108] T. Michishita, P. Franco, T. Zhang, J. Sep. Sci. 33, 3627 (2010)
[109] M. Chrysanthakopoulos, C. Giaginis, A. Tsantili-Kakoulidou, J. Chromatogr. A 1217, 5761 (2010)
[110] G.B. Cox, N.M. Maier, T. Zhang, P. Franco, LC GC N. Am., 18 (2010)
[111] L. Asnin, K. Horvath, G. Guiochon, J. Chromatogr. A 1217, 1320 (2010)
[112] L. Asnin, F. Gritti, K. Kaczmarski, G. Guiochon, J. Chromatogr. A 1217, 264 (2010)
[113] B. Wenzel, S. Fischer, P. Brust, J. Steinbach, J. Chromatogr. A 1217, 3855 (2010)
[114] E. Badaloni et al., J. Chromatogr. A 1217, 1024 (2010)
[115] G. Uray, S. Jahangir, W.M.F. Fabian, J. Chromatogr. A 1217, 1017 (2010)

[116] H. Yilmaz, G. Topal, R. Cakmak, H. Hosgoren, Chirality 22, 252 (2010)
[117] W.J. Wei, H.W. Deng, W. Chen, Z.W. Bai, S.R. Li, Chirality 22, 604 (2010)
[118] G. Cancelliere et al., J. Chromatogr. A 1217, 990 (2010)
[119] A. Lee, H.J. Choi, K.B. Jin, M.H. Hyun, J. Chromatogr. A 1218, 4071 (2011)
[120] A. Lee, H.J. Choi, M.H. Hyun, Chirality 22, 693 (2010)
[121] G.K. Toth, A. Hetenyi, I. Ilisz, A. Peter, Chirality 23, 133 (2011)
[122] H.J. Kim, H.J. Choi, M.H. Hyun, B. Korean Chem. Soc. 31, 678 (2010)
[123] P. Sun, C. Wang, Z.S. Breitbach, Y. Zhang, D.W. Armstrong, Anal. Chem. 81, 10215 (2009)
[124] K. Kalikova, L. Janeckova, D.W. Armstrong, E. Tesarova, J. Chromatogr. A 1218, 1393 (2011)
[125] P. Sun et al., Analyst 136, 787 (2011)
[126] H.X. Qiu et al., J. Chromatogr. A 1218, 270 (2011)
[127] P. Sun, D.W. Armstrong, J. Chromatogr. A 1217, 4904 (2010)
[128] T.C. Lourenco, D.W. Armstrong, Q.B. Cass, Chromatographia 71, 361 (2010)
[129] T. Payagala, E. Wanigasekara, D.W. Armstrong, Anal. Bioanal. Chem. 399, 2445 (2011)
[130] K. Tamura, T. Miyabe, H. Iida, E. Yashima, Polym. Chem. 2, 91 (2011)
[131] C.M. Fu, H.Y. Shi, Z.W. Li, G.S. Qian, Chinese J. Anal. Chem. 38, 1011 (2010)
[132] J.J. Ha, H.J. Choi, J.S. Jin, E.D. Jeong, M.H. Hyun, J. Chromatogr. A 1217, 6436 (2010)
[133] M.L. Tian, H.S. Row, K.H. Row, Monatsh. Chem. 141, 285 (2010)
[134] W.T. Bi, M.L. Tian, K.H. Row, Analyst 136, 379 (2011)
[135] P. Dimitrova, H.J. Bart, Chem. Biochem. Eng. Q. 24, 75 (2010)
[136] P. Dimitrova, H.J. Bart, Anal. Chim. Acta 663, 109 (2010)
[137] B. Natalini et al., Anal. Bioanal. Chem. 397, 1997 (2010)
[138] B. Natalini et al., J. Chromatogr. A 1217, 7523 (2010)
[139] K.M. Kacprzak, N.M. Maier, W. Lindner, J. Chromatogr. A 1218, 1452 (2011)
[140] M. Molikova, S. Studzinska, P. Kosobucki, P. Jandera, B. Buszewski, J. Liq. Chromatogr. Relat. Technol. 33, 225 (2010)
[141] T. Ema et al., J. Org. Chem. 75, 4492 (2010)
[142] B.J. He, C.Q. Yin, S.R. Li, Z.W. Bai, Chirality 22, 69 (2010)
[143] S. Keunchkarian, J.M. Padro, J. Gotta, A.M. Nardillo, C.B. Castells, J. Chromatogr. A 1218, 3660 (2011)
[144] R. Fegas, A. Bensalem, Z. Bettache, F. Ouahba, M. Righezza, Asian J. Chem. 22, 1582 (2010)
[145] A.M. Stalcup, Annu. Rev. Anal. Chem. 3, 341 (2010)
[146] G. Gubitz, M.G. Schmid, J. Chromatogr. A 1204, 140 (2008)
[147] R. Gotti, J. Pharmaceut. Biomed. 55, 775 (2011)
[148] H.A. Lu, G.N. Chen, Anal. Methods 3, 488 (2011)
[149] P. Pantuckova, P. Gebauer, P. Bocek, L. Krivankova, Electrophoresis 32, 43 (2011)
[150] C. Desiderio, F. Iavarone, D.V. Rossetti, I. Messana, M. Castagnola, J. Sep. Sci. 33, 2385 (2010)
[151] G.W. Somsen, R. Mol, G.J. de Jong, J. Chromatogr. A 1217, 3978 (2010)
[152] C. Simo, V. Garcia-Canas, A. Cifuentes, Electrophoresis 31, 1442 (2010)
[153] S. El Deeb, M. Abu Iriban, R. Gust, Electrophoresis 32, 166 (2011)
[154] R. Ryan, S. Donegan, J. Power, E. McEvoy, K. Altria, Electrophoresis 30, 65 (2009)
[155] R. Ryan, S. Donegan, J. Power, K. Altria, Electrophoresis 31, 755 (2010)
[156] R. Ryan, E. McEvoy, S. Donegan, J. Power, K. Altria, Electrophoresis 32, 184 (2011)
[157] P. Mikus, K. Marakova, Curr. Pharm. Anal. 6, 76 (2010)
[158] I. Ali, Z.A. Al-Othman, K. Saleem, H.Y. Aboul-Enein, Comb. Chem. High Throughput Screen. 13, 562 (2010)
[159] M. Herrero, C. Simo, V. Garcia-Canas, S. Fanali, A. Cifuentes, Electrophoresis 31, 2106 (2010)
[160] L. Sanchez-Hernandez, C. Garcia-Ruiz, M.L. Marina, A.L. Crego, Electrophoresis 31, 28 (2010)
[161] S. Nagl, P. Schulze, M. Ludwig, D. Belder, Electrophoresis 30, 2765 (2009)
[162] S. Nagl et al., Anal. Chem. 83, 3232 (2011)
[163] L. Geiser, J.L. Veuthey, Electrophoresis 30, 36 (2009)
[164] M. Silva, Electrophoresis 30, 50 (2009)
[165] B. Preinerstorfer, M. Lammerhofer, W. Lindner, Electrophoresis 30, 100 (2009)
[166] A. Varenne, S. Descroix, Anal. Chim. Acta 628, 9 (2008)
[167] S. Terabe, Chem. Rec. 8, 291 (2008)
[168] H. Horakova, B. Gruner, R. Vespalec, Chirality 23, 307 (2011)
[169] L. Suntornsuk, Anal. Bioanal. Chem. 398, 29 (2010)
[170] S. Viglio, M. Fumagalli, F. Ferrari, P. Iadarola,

Electrophoresis 31, 93 (2010)
[171] V. Poinsot, P. Gavard, B. Feurer, F. Couderc, Electrophoresis 31, 105 (2010)
[172] G.K.E. Scriba, Electrophoresis 30, S222 (2009)
[173] P. Mikus, K. Marakova, Electrophoresis 30, 2773 (2009)
[174] I. Ali, V.K. Gupta, H.Y. Aboul-Enein, Crit. Rev. Anal. Chem. 38, 132 (2008)
[175] A.F. Prokhorova, E.N. Shapovalova, O.A. Shpigun, J. Pharmaceut. Biomed. 53, 1170 (2010)
[176] A.A. Elbashir, H.Y. Aboul-Enein, Curr. Pharm. Anal. 6, 101 (2010)
[177] V. Cucinotta, A. Contino, A. Giuffrida, G. Maccarrone, M. Messina, J. Chromatogr. A 1217, 953 (2010)
[178] Y.X. Du, B. Chen, Chim. OGGI 28, 37 (2010)
[179] S. Fanali, Electrophoresis 30, S203 (2009)
[180] B. Chankvetadze, Electrophoresis 30, S211 (2009)
[181] C.P. Palmer, Electrophoresis 30, 163 (2009)
[182] W.H. Tang, S.C. Ng, J. Sep. Sci. 31, 3246 (2008)
[183] G.K.E. Scriba, J. Sep. Sci. 31, 1991 (2008)
[184] T. Cserhati, Biomed. Chromatogr. 22, 563 (2008)
[185] Z. Juvancz, R.B. Kendrovics, R. Ivanyi, L. Szente, Electrophoresis 29, 1701 (2008)
[186] J. Svobodova, P. Dubsky, E. Tesarova, B. Gas, Electrophoresis 32, 595 (2011)
[187] P. Dubsky, J. Svobodova, E. Tesarova, B. Gas, Electrophoresis 31, 1435 (2010)
[188] K.M. Al Azzam, B. Saad, H.Y. Aboul-Enein, Electrophoresis 31, 2957 (2010)
[189] K.M. Al Azzam, B. Saad, R. Adnan, H.Y. Aboul-Enein, Anal. Chim. Acta 674, 249 (2010)
[190] A.A. Elbashir, F.E.O. Suliman, B. Saad, H.Y. Aboul-Enein, Biomed. Chromatogr. 24, 393 (2010)
[191] L.S et al., Electrophoresis 32, 218 (2011)
[192] A.C. Servais et al., Electrophoresis 31, 1467 (2010)
[193] A.C. Servais et al., J. Sep. Sci. 33, 1617 (2010)
[194] S. Beni et al., J. Pharmaceut. Biomed. 51, 842 (2010)
[195] T. Sohajda et al., J. Pharmaceut. Biomed. 53, 1258 (2010)
[196] K. Lomsadze, A. Salgado, E. Calvo, J.A. Lopez, B. Chankvetadze, Electrophoresis 32, 1156 (2011)
[197] D.H. Xia, Y.H. Shang, H. Li, Chinese J. Anal. Chem. 39, 414 (2011)
[198] J. He, S.A. Shamsi, Electrophoresis 32, 1164 (2011)
[199] A. Giuffrida, A. Contino, G. Maccarrone, M. Messina, V. Cucinotta, Electrophoresis 32, 1176 (2011)
[200] L. Sanchez-Hernandez, C. Garcia-Ruiz, A.L. Crego, M.L. Marina, J. Pharmaceut. Biomed. 53, 1217 (2010)
[201] L. Sanchez-Hernandez, M. Castro-Puyana, C. Garcia-Ruiz, A.L. Crego, M.L. Marina, Food Chem. 120, 921 (2010)
[202] H. Wu, B.Q. Yuan, Y.M. Liu, J. Chromatogr. A 1218, 3118 (2011)
[203] A.C. Servais et al., Electrophoresis 31, 1157 (2010)
[204] X.P. Wu, X.Y. Chen, M.M. Zheng, Chinese J. Anal. Chem. 38, 1776 (2010)
[205] C.X. Yu, B.Q. Yuan, T.Y. You, Chem. Res. Chinese U. 27, 34 (2011)
[206] M. Castro-Puyana, I. Lammers, J. Buijs, C. Gooijer, F. Ariese, Electrophoresis 31, 3928 (2010)
[207] W. Pormsila, X.Y. Gong, P.C. Hauser, Electrophoresis 31, 2044 (2010)
[208] S. Anouti, O. Vandenabeele-Trambouze, H. Cottet, Electrophoresis 31, 1029 (2010)
[209] K.C. Lin, M.M. Hsieh, C.W. Chang, E.P. Lin, T.H. Wu, Talanta 82, 1912 (2010)
[210] Z.Y. Wang, C. Liu, J.W. Kang, J. Chromatogr. A 1218, 1775 (2011)
[211] W.A.W. Ibrahim, D. Hermawan, M.M. Sanagi, H.Y. Aboul-Enein, Chromatographia 71, 305 (2010)
[212] H.Z. Ye et al., Electrophoresis 31, 2049 (2010)
[213] W.H. Li et al., Chromatographia 73, 1009 (2011)
[214] M.X. Liu, Y. Zheng, Y.B. Ji, C. Zhang, J. Pharmaceut. Biomed. 55, 93 (2011)
[215] H. Zhu et al., B. Korean Chem. Soc. 31, 1496 (2010)
[216] H. Zhu et al., J. Pharmaceut. Biomed. 54, 1007 (2011)
[217] L. Asensi-Bernardi, Y. Martin-Biosca, M.J. Medina-Hernandez, S. Sagrado, J. Chromatogr. A 1218, 3111 (2011)
[218] K. Nemeth et al., J. Pharmaceut. Biomed. 54, 475 (2011)
[219] E. Lipka, M.P. Vaccher, C. Vaccher, J.P. Bonte, Anal. Lett. 43, 2356 (2010)
[220] L. Suntornsuk, S. Ploryngam, J. Pharmaceut. Biomed. 51, 541 (2010)
[221] P. Liu et al., Chirality 22, 914 (2010)
[222] K. Phatthiyaphaibun, W. Som-Aum, M. Srisa-ard, J. Threeprom, J. Anal. Chem. 65, 755 (2010)
[223] K. Phatthiyaphaibun, W. Som-Aum, M. Srisa-ard, J. Threeprom, J. Anal. Chem. 65, 803 (2010)

[224] K. Nemeth et al., J. Pharmaceut. Biomed. 53, 382 (2010)
[225] Y. Xiao et al., J. Sep. Sci. 33, 1797 (2010)
[226] A.C. Cabordery et al., J. Chromatogr. A 1217, 3871 (2010)
[227] J.Q. Chen, Y.X. Du, F.X. Zhu, B. Chen, Electrophoresis 31, 1044 (2010)
[228] F. Yang, Y.X. Du, B. Chen, Q.F. Fan, G.F. Xu, Chromatographia 72, 489 (2010)
[229] Y. Jeon, C. Kwon, E. Cho, S. Jung, Carbohyd. Res. 345, 2408 (2010)
[230] C. Kwon, D. Jeong, S. Jung, B. Korean Chem. Soc. 32, 1361 (2011)
[231] C. Kwon, S. Jung, Carbohyd. Res. 346, 133 (2011)
[232] S. Nojavan, A.R. Fakhari, Electrophoresis 32, 764 (2011)
[233] G.F. Xu, Y.X. Du, B. Chen, J.Q. Chen, Chromatographia 72, 289 (2010)
[234] A.P. Kumar, J.H. Park, J. Chromatogr. A 1218, 1314 (2011)
[235] Z.J. Jiang, Z.H. Yang, R.D. Sussmuth, N.W. Smith, S.T. Lai, J. Chromatogr. A 1217, 1149 (2010)
[236] J. Haglof, C. Pettersson, Electrophoresis 31, 1706 (2010)
[237] Z. Ma, L.J. Zhang, L.N. Lin, P. Ji, X.J. Guo, Biomed. Chromatogr. 24, 1332 (2010)
[238] D.K. Bwambok, S.K. Challa, M. Lowry, I.M. Warner, Anal. Chem. 82, 5028 (2010)
[239] J.Q. Chen, Y.X. Du, F.X. Zhu, B. Chen, J. Chromatogr. A 1217, 7158 (2010)
[240] S. Wongwan, B. Sungthong, G.K.E. Scriba, Electrophoresis 31, 1475 (2010)
[241] E. Lipka, C. Danel, S. Yous, J.P. Bonte, C. Vaccher, Electrophoresis 31, 1529 (2010)
[242] Y. Iwamuro et al., Forensic Toxicol. 28, 19 (2010)
[243] L. Qi, G.L. Yang, H.Z. Zhang, J.A. Qiao, Talanta 81, 1554 (2010)
[244] V.A. Davankov, S.V. Rogozhin, J. Chromatogr. 60, 280 (1971)
[245] H.Z. Zhang, L. Qi, J. Qiao, L.Q. Mao, Anal. Chim. Acta 691, 103 (2011)
[246] C.Y. Kuo, K.S. Liao, Y.C. Liu, W.B. Yang, Molecules 16, 1682 (2011)
[247] C.C. Lin, C.Y. Kuo, K.S. Liao, W.B. Yang, Molecules 16, 652 (2011)
[248] D. Rizkov, S. Mizrahi, S. Cohen, O. Lev, Electrophoresis 31, 3921 (2010)
[249] S. Kodama et al., Electrophoresis 31, 3586 (2010)
[250] S. Kodama et al., Electrophoresis 31, 1051 (2010)
[251] M.Y. Tong, T. Payagala, S. Perera, F.M. MacDonnell, D.W. Armstrong, J. Chromatogr. A 1217, 1139 (2010)
[252] D. Hermawan, W.A.W. Ibrahim, M.M. Sanagi, H.Y. Aboul-Enein, J. Pharmaceut. Biomed. 53, 1244 (2010)
[253] Y. Chen, J.H. Zhang, L. Zhang, G.N. Chen, Electrophoresis 31, 1493 (2010)
[254] V. Perez-Fernandez, M.A. Garcia, M.L. Marina, Electrophoresis 31, 1533 (2010)
[255] B. Chen, Y.X. Du, J. Chromatogr. A 1217, 1806 (2010)
[256] C.A. Luces, I.M. Warner, Electrophoresis 31, 1036 (2010)
[257] A.B. Martinez-Giron, A.L. Crego, M.J. Gonzalez, M.L. Marina, J. Chromatogr. A 1217, 1157 (2010)
[258] H.Y. Cheng, B.K. He, Q.L. Zhang, Y.F. Tu, Anal. Sci. 26, 1087 (2010)
[259] C. Borst, U. Holzgrabe, J. Pharmaceut. Biomed. 53, 1201 (2010)
[260] S.Q. Hu et al., J. Chromatogr. A 1217, 5529 (2010)
[261] L. Yang et al., Electrophoresis 31, 1697 (2010)
[262] D. Belder, K. Tolba, S. Nagl, Electrophoresis 32, 440 (2011)
[263] F. Kitagawa, K. Kubota, K. Sueyoshi, K. Otsuka, J. Pharmaceut. Biomed. 53, 1272 (2010)
[264] D. Ross, J.G. Shackman, J.G. Kralj, J. Atencia, Lab Chip 10, 3139 (2010)
[265] A. Rousseau et al., J. Pharmaceut. Biomed. 54, 154 (2011)
[266] A. Rousseau et al., Electrophoresis 31, 1482 (2010)
[267] L.J. Wang, S.Q. Hu, Q.L. Guo, G.L. Yang, X.G. Chen, J. Chromatogr. A 1218, 1300 (2011)

2. Cíle dizertační práce

Cíle práce byly zaměřené na zlepšení možnosti predikce a identifikace systémových zón a píků v kapilární zónové elektroforéze, které by mohly zlepšit nebo rozšířit uplatnění programu PeakMaster v analytické praxi. Dále pak cíle směřovaly k prohloubení poznatků o chování systémových píků v komplikovanějších systémech, zejména takových, které zatím není možné efektivně vyšetřovat pomocí simulačních programů.

Konkrétní cíle práce byly následující:

- Potvrdit správnost a funkčnost nového nelineárního modelu odvozeného a implementovaného do nové verze programu PeakMaster 5.3 za účelem predikce tvaru systémových píků
  - (i) porovnat výpočty PeakMasteru 5.3 se simulacemi programu Simul 5
  - (ii) vybrat vhodné elektroforetické systémy a srovnat predikce PeakMasteru 5.3 s reálnými experimenty, zejména změnu tvaru a polarity systémových píků v závislosti na složení a velikosti dávkované zóny
- V elektromigračních systémech, kde dochází ke komplexaci složky pufru s komplexačním činidlem:
  - (i) vyšetřit změny základních vlastností pufru v důsledku této komplexace
  - (ii) odhalit a popsat případný dopad těchto změn na elektroforetické výsledky
  - (iii) vyšetřit chování systémových píků v daných systémech a porovnat je s predikcemi lineární teorie elektromigrace

3. Experimentální podmínky

Veškeré elektroforetické experimenty probíhaly na přístrojovém vybavení naší laboratoře, tedy na přístrojích Agilent^{3D}CE nebo CE 7100 (Agilent Technologies, Waldbronn, Německo). Přístroje jsou vybaveny vestavěnými UV/Vis detektory s diodovým polem a vodivostními detektory navrženými v naší laboratoři [61]. Oba typy přístrojů jsou ovládány softwarem ChemStation. Měření pH probíhalo na PHM 240 pH/ion metru firmy Radiometer (Copenhagen, Dánsko).

Používány byly křemenné kapiláry s vnějším polyimidovým potahem. Délky, průměry a promývání kapilár se nevymykaly běžným postupům. Použité chemikálie byly vysoké čistoty, voda byla deionizována systémem UPLTRAPUR od firmy Watrex (Praha, ČR).

Z použitých komerčních softwarů lze jmenovat Origin 8.1 (OriginLab Corporation, Norhampton, USA) a MS Office Excel (Microsoft Corporation, USA) pro vyhodnocování naměřených dat. Dále byly používány simulační programy řady Simul a PeakMaster, vyvinuté v naší laboratoři [47].

Detailní experimentální podmínky jsou uvedeny vždy v příslušné publikaci, a proto zde nejsou detailněji zmiňovány.

4. Výsledky a diskuze

4.1 Předpověď tvarů systémových píků

Lineární teorie elektromigrace (LTE) je velmi dobrou aproximací nelineárních elektromigračních procesů pro mód kapilární zónové elektroforézy. Umožňuje získat hodnoty důležitých parametrů elektroforetických systémů a dokáže obsáhnout a popsat mnoho podstatných rysů daných systémů. Stále se však jedná jen o přibližný popis, který má jistá omezení. Pomocí LTE mohou být například vypočítány amplitudy systémových píků, ale jejich tvar není možné na základě LTE předpovědět. LTE také selhává, pokud má dávkovaná zóna komplikovanější tvar (nejčastěji dávkování dlouhé zóny vzorku). V takovém případě pak nemohou být správně předpovězeny ani tvary píků analytů.

V Publikaci 2 byl formulován zjednodušený nelineární model elektroforézy, který nabízí lepší možnosti než dosavadní LTE, ale stále je ještě řešitelný pomocí maticového zápisu. Kompletní matematické zpracování, založené na Taylorově rozvoji rovnic popisujících elektromigraci a následném zahrnutí konstantního a prvního nelineárního členu elektromigrace a konstantního členu difúze do tohoto zjednodušeného modelu, je popsáno v Publikaci 2. Model je pak řešen pro dvě počáteční podmínky dávkování vzorku – ve tvaru Diracovy funkce a obdélníkového pulsu. Řešením pro první případ je Haarhoff – van der Lindeho (HVL) funkce. Pro druhý více realistický případ bylo použito řešení poprvé odvozené pro chromatografii a v Publikaci 2 označené jako HVLR funkce. HVLR funkce tak umožní přesnější zobrazení tvarů píků, zejména pokud je nadávkována širší zóna vzorku. Nelineární model byl implementován do nové verze programu PeakMaster označené jako PeakMaster 5.3. I tato verze je volně a zdarma dostupná na stránkách naší skupiny [47]. Běžný uživatel pak pocítí změnu oproti předešlým verzím programu PeakMaster v přítomnosti podokna *Amplitudes and Shapes*, kde se po vyplnění konkrétního složení vzorku a šířky dávkované zóny vypočítají parametry pro všechny zóny – jejich složení, vodivostní odezva, lineární mobilita a nově také tzv. nelineární elektromigrační mobilita, $u_{EMD,i}$, která je mírou elektromigrační disperze i-té zóny. Všechny vypočítané parametry jsou následně

převedeny i do grafické podoby a pod tlačítkem *Show/HideGraph* je možné si prohlédnout výsledný elektroferogram pro daný BGE, dané experimentální podmínky, dané složení vzorku a danou šířku dávkované zóny.

Přesnost nového modelu v programu PeakMaster 5.3 byla ověřena srovnáním se simulacemi v programu Simul 5 [14], který řeší dané nelineární rovnice popisující elektromigraci numericky. *Figure 3* v Publikaci 2 dokládá velmi dobrou shodu simulací systémových píků programem PeakMaster 5.3 a Simul 5. Správnost a použitelnost modelu a nové verze PeakMasteru tak byla ověřena. Zatímco simulace v programu Simul 5 jsou časové náročné (řádu hodin i dní) a nabízejí jen grafické zobrazení výsledných profilů, PeakMaster 5.3 je schopen výsledek stejného elektroforetického experimentu předpovědět během několika vteřin na základě výpočtů daných parametrů elektroforetického systému.

V Publikaci 3 byl nový PeakMaster 5.3 otestován srovnáním s experimenty prováděnými na třech různých systémech. V každém systému byly vyšetřovány systémové píky vybuzené čtyřmi různými poruchami (vzorky obsahující +/- 10% jedné nebo druhé složky pufru oproti koncentraci v BGE). Testovány byly následující systémy:

i) TRIS a kyselina benzoová při neutrálním pH. Tento systém má mobility obou systémových píků blízké nule. Systémové píky tak mohou tvořit tzv. cikcak tvar nebo, pokud mají oba stejnou polaritu, mohou v záznamu splynout a budit dojem pouze jednoho systémového píku. (*Figure 1*)

ii) TRIS a kyselina benzoová v kyselé oblasti pH. Jeden ze systémových píků má kvůli již značně nízkému pH poměrně rychlou kationickou mobilitu. Mobilita druhého systémového píku zůstává blízká nule. (*Figure 2*)

iii) TRIS a kyselina ftalová s nízkou pufrační kapacitou. Jeden systémový pík zůstává téměř nulový, druhý je rychlý, anionický. Anionický systémový pík má velkou hodnotu u_{EMD} a má proto silně trojúhelníkovitý tvar. (*Figure 3*)

Ve všech třech případech, i v případě dávkování dlouhých zón (*Figure 5*), byly předpovědi programu PeakMaster 5.3 v naprosté shodě s experimenty.

Nový PeakMaster 5.3 může zlepšit možnosti predikce a identifikace systémových píků v experimentálně získaných elektroferogramech, protože předpovídá nejen pozice systémových píků, ale také jejich polarity a tvary. Systémové píky tak mohou být v záznamech snadněji rozpoznány a méně často tak může dojít k záměně systémových píků s píky analytů. Nově pak může být před samotnou analýzou optimalizováno i složení vzorku právě s ohledem na polaritu a tvary systémových píků, jak je naznačeno na Obrázku 1.

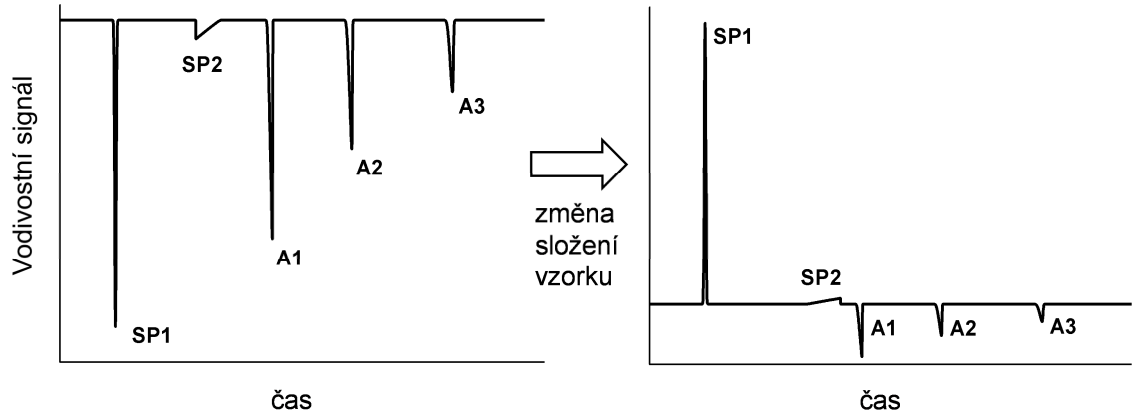

Obrázek 1 *Ilustrace možnosti optimalizace složení vzorku z pohledu vhodné polarity a tvaru systémových píků v programu PeakMaster 5.3; SP - systémový pík, A - analyt*

O výhodách nového PeakMasteru 5.3 vypovídá také Obrázek 2. Stará verze, která systémové píky znázorňuje pouze jako svislé čáry nemůže být schopna dobře popsat situace, kdy se systémové píky překrývají (Obrázek 2A) nebo kde kvůli svému tvaru zasahují do píku analytu (Obrázek 2B).

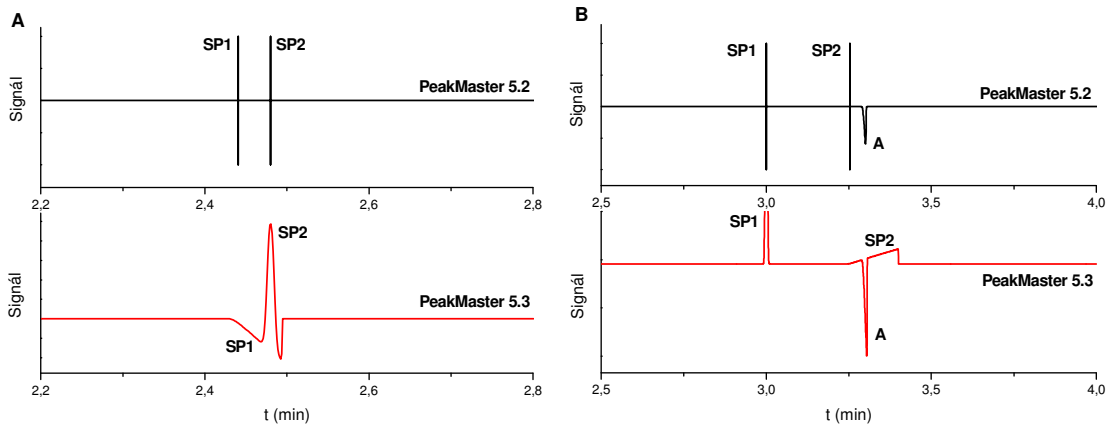

Obrázek 2 *Rozdíl v predikci dvou systémových píků (A) a dvou systémových píků a jednoho píku analytu (B) v programu PeakMaster 5.2 (starší verze) a PeakMaster 5.3 (nová verze); SP – systémový pík, A - analyt*

Implementace nového matematického modelu do programu PeakMaster výrazně posunula možnosti tohoto účinného nástroje pro předpovědi výsledků kapilární zónové elektroforézy.

Publikace 2

A nonlinear electrophoretic model for PeakMaster: I. Mathematical model

*Hruška V.,**Riesová M**., Gaš B.*

Electrophoresis, 2012, 33, 923-930

Vlastimil Hruška*
Martina Riesová
Bohuslav Gaš

Faculty of Science, Department of Physical and Macromolecular Chemistry, Charles University in Prague, Prague, Czech Republic

Received October 19, 2011
Revised November 20, 2011
Accepted November 20, 2011

Research Article

A nonlinear electrophoretic model for PeakMaster: I. Mathematical model

We extended the linearized model of electromigration, which is used by PeakMaster, by calculation of nonlinear dispersion and diffusion of zones. The model results in the continuity equation for the shape function $\varphi(x,t)$ of the zone: $\varphi_t = -(\nu_0 + \nu_{EMD}\varphi)\varphi_x + \delta\varphi_{xx}$ that contains linear (ν_0) and nonlinear migration (ν_{EMD}), diffusion (δ), and subscripts x and t stand for partial derivatives. It is valid for both analyte and system zones, and we present equations how to calculate characteristic zone parameters. We solved the continuity equation by Hopf–Cole transformation and applied it for two different initial conditions—the Dirac function resulting in the Haarhoff-van der Linde (HVL) function and the rectangular pulse function, which resulted in a function that we denote as the HVLR function. The nonlinear model was implemented in PeakMaster 5.3, which uses the HVLR function to predict the electropherogram for a given background electrolyte and a composition of the sample. HVLR function also enables to draw electropherograms with significantly wide injection zones, which was not possible before. The nonlinear model was tested by a comparison with a simulation by Simul 5, which solves the complete nonlinear model of electromigration numerically.

Keywords:
Diffusion / Eigenvalues / Nonlinear electromigration / Simulation / System peak
DOI 10.1002/elps.201100554

1 Introduction

Formulation of basic laws able to describe movement of charged particles in liquid solution under the influence of an outer electric field is not difficult in itself. The basic set of continuity equations was introduced in 1897 by Kohlrausch [1], who derived a certain conservation law, which must be obeyed in electromigration systems and which is now called the Kohlrausch regulating function. Later, additional conservation laws [2–4] were found. Nevertheless, finding conservation function is not a full solution of the continuity equations. Because of the inherent nonlinearity, an exact closed-formula solution of the governing continuity equations is unattainable. A numerical solution, or simulation, is a way how to obtain information about phenomena taking place in electromigration and is used in many instances. For this purpose, several simulation programs are available [5], such as GENTRANS [6, 7], SIMUL5 [8], or SPRESSO [9]. Unfortunately, numerical simulation is often too slow to study phenomena in the realistic physical scale, and, more importantly, the output are just concentration profiles of all constituents so it cannot directly provide parameters of the system such as mobilities or velocity slopes of zones or to find general laws of broader validity.

In capillary zone electrophoresis, the situation is more favorable in a certain sense. Thanks to the experimental setup of zone electrophoresis the governing equations can be linearized and resulting equations are still able to describe many important features. This is because the constituents forming the background electrolyte (BGE) are axially almost uniformly distributed along the separation channel and the analyte constituents are injected as a sample into a certain site of the channel in a concentration that is usually much smaller than that of the BGE. It allows to formulate continuity equations as a perturbation problem. This approach was started in electrophoresis by Poppe et al. [10, 11] who showed that solving the linearized equations leads to the eigenvalue problem for a matrix. In the two papers [12, 13], our group presented a linear mathematical model of capillary zone electrophoresis and introduced PeakMaster, a free software program that implements the linear approach. We introduced a term the system eigenmobility, which is the eigenvalue of the Jacobian matrix **M** of the electromigration system. The system eigenmobility is the mobility of the system zone, which can be formed during electromigration. We showed that the BGE composed

Correspondence: Vlastimil Hruska, Faculty of Science, Department of Physical and Macromolecular Chemistry, Charles University in Prague, Prague, Czech Republic
E-mail: vlastimilhruska@gmail.com
Fax: +420-2-2491-9752

Abbreviations: HVL, Haarhoff-van der Linde; **HVLR**, HVL-like function based on initial rectangular pulse disturbance

*Current address: Agilent Technologies GmbH, Hewlett-Packard-Straße 8, 76337, Waldbronn, Germany

Colour Online: See the article online to view Fig. 3 in colour.

of N constituents has N system eigenmobilities and N corresponding system zones. The spectral decomposition of the matrix **M** implemented in PeakMaster 5.2 enables to calculate the amplitudes of system eigenpeaks [14] when composition of the injected sample is known.

The linear model we introduced together with both versions of PeakMaster, 5.1 and 5.2, attracted the interest of electrophoretists, as we can estimate from the number of downloading of the software from our web page. However, the linear model is only an approximation of the original nonlinear equations and in some cases it has limitations. For example, it allows to calculate the amplitudes of the system peaks but not their shape as appears in detectors. Especially, when the injected profiles of the analytes into the separation channel have a more complex shape, the linear model cannot predict the resulting profiles.

As noticed above, the exact closed-formula solution of the original equations is not known so far. The aim of this paper is to formulate a simplified nonlinear model of electrophoresis, which will be more rigorous and more accurate than the linear model and which will still be solvable in the matrix notation. Such model will be then implemented in the new version of PeakMaster, PeakMaster 5.3. In addition to the previous versions, this will allow to obtain practically important information about peak shapes of both the system peaks and peaks of the analytes in zone electrophoresis in much shorter time when compared to numerical simulation.

2 Theory

2.1 Continuity equations

The electrophoretic model consists of N one-dimensional continuity equations for N constituents, which can be acids, bases, or ampholytes, which can be present either in the sample (analytes) or can be a part of the BGE. Ions H_3O^+ and OH^- do not have to be described by the continuity equations because they are bound by the electroneutrality condition and autoprotolysis of water (ionic product of water) [12]. The continuity equation describes a change of the net concentration c_i of the ith constituent in spatial, x, and time, t, coordinate

$$\frac{\partial c_i}{\partial t} = -\sum_{z=n_i}^{p_i}\left(\frac{\partial J_{i,z}}{\partial x}\right) \tag{1}$$

where $J_{i,z}$ is a mass flux of the ith constituent in its ionic form with charge number z, and n_i and p_i are the most negative and positive ionic forms of the ith constituent, respectively. Unlike the previous model we introduced [12], this one will consider the mass flux composed of both electromigration movement (driven by the gradient of the electric potential Φ) and diffusion (driven by the gradient of concentration)

$$J_{i,z} = -\mathrm{sgn}\,(z)\, c_{i,z} u_{i,z}\frac{\partial \Phi}{\partial x} - D_{i,z}\frac{\partial c_{i,z}}{\partial x} \tag{2}$$

where $c_{i,z}$, $u_{i,z}$, and $D_{i,z}$ stand for the ionic concentration, ionic electrophoretic mobility, and diffusion coefficient of the zth ionic form of the ith constituent, respectively. Note that we use the ionic mobility $u_{i,z}$ defined as an unsigned proportionality constant in the dependence of ionic velocity $v_{i,z}$ on intensity of electric field E: $v_{i,z} = \mathrm{sgn}(z) u_{i,z} E$. Electric potential in Eq. (2). can be ruled out by introducing the current density j

$$j = F\left[\sum_{i=1}^{N}\sum_{z=n_i}^{p_i}(zJ_{i,z}) + J_H - J_{OH}\right] \tag{3}$$

where F is the Faraday constant and subscripts H and OH stand for hydronium H_3O^+ and hydroxide OH^- ions, respectively. Using Eq. (2) in Eq. (3) yields

$$J_{i,z} = -D_{i,z}\frac{\partial c_{i,z}}{\partial x} + \frac{\mathrm{sgn}\,(z)\, c_{i,z} u_{i,z}}{\kappa}\,(j - j_{diff}) \tag{4}$$

where j_{diff} is the diffusion current density (j_{diff}/κ is the diffusion potential) and κ is the electric conductivity

$$j_{diff} = -F\left[\sum_{i=1}^{N}\sum_{z=n_i}^{p_i}\left(zD_{i,z}\frac{\partial c_{i,z}}{\partial x}\right) + D_H\frac{\partial c_H}{\partial x} - D_{OH}\frac{\partial c_{OH}}{\partial x}\right] \tag{5}$$

$$\kappa = F\left[\sum_{i=1}^{N}\sum_{z=n_i}^{p_i}(|z|\, u_{i,z} c_{i,z}) + u_H c_H + u_{OH} c_{OH}\right] \tag{6}$$

Using Eq. (4) the right-hand side of continuity Eq. (1) can be arranged as a sum of two terms

$$\begin{aligned}\frac{\partial c_i}{\partial t} &= -\frac{\partial}{\partial x}\sum_{z=n_i}^{p_i}\left(\frac{j}{\kappa}\mathrm{sgn}\,(z)\, c_{i,z} u_{i,z}\right)\\ &\quad+\frac{\partial}{\partial x}\sum_{z=n_i}^{p_i}\left(D_{i,z}\frac{\partial c_{i,z}}{\partial x} - \frac{j_{diff}}{\kappa}\mathrm{sgn}\,(z)\, c_{i,z} u_{i,z}\right)\\ &= \left(\frac{\partial c_i}{\partial t}\right)_{em} + \left(\frac{\partial c_i}{\partial t}\right)_{diff}\end{aligned} \tag{7}$$

The first one, $(\frac{\partial c_i}{\partial t})_{em}$, will be denoted as the electromigration term, the second one $(\frac{\partial c_i}{\partial t})_{diff}$ as the diffusion term. A final solution of continuity Eq. (7) for $i = 1, \ldots, N$ is fully determined by a set of initial and boundary conditions.

2.2 Linearization and Taylor expansion of continuity equations

Before the sample is injected, the separation space is filled by an undisturbed BGE. The injection of the sample creates disturbances $\tilde{c}_i^{in}(x)$ in axial concentration profiles of all BGE constituents as well it forms profiles of analytes. The electromigration begins by application of the electric field. Mathematical expression of the initial condition is [14]

$$c_i\,(x, t = 0) = C_i + \tilde{c}_i^{in}\,(x) \tag{8}$$

$$\tilde{c}_i^{in}\,(x) = \Delta C_i^{in}\varphi^{in}\,(x) \tag{9}$$

where C_i is a concentration of the constituent in the BGE (for analytes $C_i = 0$), ΔC_i^{in} is the magnitude of the initial disturbance in the ith concentration profile, and $\varphi^{in}(x)$ is a function

describing the shape of the injection zone, which is identical for all constituents. A difference between $c_i(x,t)$ and the referential BGE concentration C_i is a set of small disturbances in concentration profiles forming electrophoretic zones. These differences are denoted as $\tilde{c}_i(x,t)$

$$\tilde{c}_i(x,t) = c_i(x,t) - C_i \tag{10}$$

In our previous paper [12], we showed that the electromigration term $(\frac{\partial c_i}{\partial t})_{em}$ can be rearranged to the matrix form without linearization or any approximations

$$\left(\frac{\partial \vec{\tilde{c}}}{\partial t}\right)_{em} = -\frac{j}{\kappa_{BGE}}\mathbf{M}(\tilde{c}_1, .., \tilde{c}_N) \times \frac{\partial \vec{\tilde{c}}}{\partial x} \tag{11}$$

where $\mathbf{M}(\tilde{c}_1, .., \tilde{c}_N)$ is a nonsymmetrical Jacobian matrix and $\vec{\tilde{c}}$ is a column vector composed of disturbances $\tilde{c}_i$, $i = 1, \ldots, N$, and κ_{BGE} is the conductivity of the BGE. Elements of the matrix have dimension of mobility. The linearization of the matrix $\mathbf{M}$ can be simply done by substituting $\tilde{c}_i = 0$ to the matrix $\mathbf{M}(\tilde{c}_1, .., \tilde{c}_N)$ to obtain a constant matrix $\mathbf{M}(0, .., 0) \equiv \mathbf{M}_0$, that is, the absolute term of Taylor expansion. We call the eigenvalues of the matrix $\mathbf{M}_0$ as eigenmobilities. As we showed in [14], the eigenvectors yield information on composition of both analyte and system zones (also called system eigenzones).

In this paper, we will analyze the electromigration in a more complex way to get more information about nonlinear behavior of all zones in the system. We apply the Taylor expansion on $\mathbf{M}(\tilde{c}_1, .., \tilde{c}_N)$ considering its absolute $\mathbf{M}_0$ and linear $\mathbf{M}_{1,k}$ terms

$$\left(\frac{\partial \vec{\tilde{c}}}{\partial t}\right)_{em} = -\frac{j}{\kappa_{BGE}}\left(\mathbf{M}_0 + \sum_{k=1}^{N}\mathbf{M}_{1,k}\tilde{c}_k\right) \times \frac{\partial \vec{\tilde{c}}}{\partial x} \tag{12}$$

Analogously, we perform the linearization of the diffusion term $(\frac{\partial \vec{\tilde{c}}_i}{\partial t})_{diff}$ where we consider only the absolute member of the Taylor expansion expressed by the diffusion matrix $\mathbf{D}$

$$\left(\frac{\partial \vec{\tilde{c}}}{\partial t}\right)_{diff} = \mathbf{D} \times \frac{\partial^2 \vec{\tilde{c}}}{\partial x^2} \tag{13}$$

Combining Eqs. (12) and (13) the final matrix continuity equation is

$$\frac{\partial \vec{\tilde{c}}}{\partial t} = -\frac{j}{\kappa_{BGE}}\left(\mathbf{M}_0 + \sum_{k=1}^{N}\mathbf{M}_{1,k}\tilde{c}_k\right) \times \frac{\partial \vec{\tilde{c}}}{\partial x} + \mathbf{D} \times \frac{\partial^2 \vec{\tilde{c}}}{\partial x^2} \tag{14}$$

The initial condition for disturbances expressed as a column vector $\vec{\tilde{c}}^{in}$ is

$$\vec{\tilde{c}}^{in} = \begin{pmatrix} c_1^{in} - C_1 \\ \ldots \\ c_N^{in} - C_N \end{pmatrix} \tag{15}$$

and the boundary conditions is

$$\lim_{x \to \pm\infty} \tilde{c}_i = 0 \tag{16}$$

that assumes an infinite separation space and vanishing disturbances in infinity, that is, disturbances cannot be infinitely wide. Eqs. (14), (15), and (16) completely define the simplified nonlinear model of electromigration, which we will analyze further.

2.3 Approximate solution of nonlinear matrix equation

Eigenvalues, $\lambda_{0,i}$, of the matrix $\mathbf{M}_0$ are mobilities of system and analyte zones. The corresponding right column and left row eigenvectors ($\vec{q}_{R,i}$ and $\vec{q}_{L,i}$, respectively) together with initial conditions serve for calculation of concentrations of all constituents in all zones. Eigenvalues and eigenvectors can be arranged into matrices in the following way: (i) The eigenvalues are arranged into a diagonal matrix $\mathbf{\Lambda}_0$ of eigenmobilities, where the *i*th diagonal element contains $\lambda_{0,i}$. (ii) Similarly, all right column eigenvectors form a matrix $\mathbf{Q}_R$ and the left row eigenvectors form a matrix $\mathbf{Q}_L$ where the *i*th vector is in the *i*th column and row, respectively. Matrices $\mathbf{Q}_R$ and $\mathbf{Q}_L$ are mutually inverse and they diagonalize $\mathbf{M}_0$

$$\Lambda_0 = \mathbf{Q}_L \times \mathbf{M}_0 \times \mathbf{Q}_R \tag{17}$$

First, we apply matrix transformation of concentrations $\tilde{c}_i$ to characteristic variables $\tilde{w}_i$, which have meaning of functions representing eigenzones

$$\vec{\tilde{c}} = \mathbf{Q}_R \times \vec{\tilde{w}} \tag{18}$$

To find a solution to the nonlinear matrix Eq. (14) we multiply it from the left and right side by matrices $\mathbf{Q}_L$ and $\mathbf{Q}_R$, respectively. Finally, we substitute $\tilde{c}_k$ by $\tilde{c}_k = \sum_{j=1}^{N}(\mathbf{Q}_R)_{k,j}\tilde{w}_j$ to complete the transformation from $\tilde{c}$ to $\tilde{w}$

$$\frac{\partial \vec{\tilde{w}}}{\partial t} = -\frac{j}{\kappa_{BGE}}\left[\Lambda_0 + \Lambda_1(\vec{\tilde{w}})\right] \times \frac{\partial \vec{\tilde{w}}}{\partial x} + \Delta \times \frac{\partial^2 \vec{\tilde{w}}}{\partial x^2} \tag{19}$$

where

$$(\Lambda_1)_{i,i} = \frac{\partial \lambda_i}{\partial w_i}\tilde{w}_i \tag{20}$$

$$(\Delta)_{i,i} = \delta_i \tag{21}$$

All nondiagonal elements of $\Lambda_1(\vec{\tilde{w}})$ and $\mathbf{\Delta}$ are neglected using a simplifying assumption that all zones are immediately separated from each other and therefore there are no electrophoretic interactions among zones that need to be described by these non-diagonal elements. The *i*th diagonal element of the matrix $\Lambda_1(\vec{\tilde{w}})$ is a product of the characteristic function $\tilde{w}_i$ and the constant $\frac{\partial \lambda_i}{\partial w_i}$, which is a slope of the dependence of eigenmobility on $\tilde{w}_i$. Similarly, diagonal elements of $\mathbf{\Delta}$ provide the diffusion coefficient of the *i*th eigenzone, δ_i. The quantity $\frac{\partial \lambda_i}{\partial w_i}$ is calculated as follows:

$$\frac{\partial \lambda_i}{\partial w_i} = \sum_{k=1}^{N}(\mathbf{Q}_R)_{i,k}(\mathbf{Q}_L \times \mathbf{M}_{1,k} \times \mathbf{Q}_R)_{i,i} \tag{22}$$

For the *i*th zone, Eq. (19) is rewritten with using only the diagonal elements

$$\frac{\partial \tilde{w}_i}{\partial t} = -\frac{j}{\kappa_{BGE}}\left(\lambda_{0,i} + \frac{\partial \lambda_i}{\partial \tilde{w}_i}\tilde{w}_i\right)\frac{\partial \tilde{w}_i}{\partial x} + \delta_i \frac{\partial^2 \tilde{w}_i}{\partial x^2} \tag{23}$$

with initial and boundary conditions

$$\tilde{w}_i^{in} = \sum_{j=1}^{N} (\mathbf{Q}_L)_{i,j}\, \tilde{c}_j^{in} \tag{24}$$

$$\lim_{x \to \pm\infty} \tilde{w}_i = 0 \tag{25}$$

2.4 Solution of separated nonlinear partial differential equation

We will focus on obtaining the shape function $\varphi_i(x, t)$ rather than solving Eq. (23) in concentration domain of $\tilde{w}_i$ or $\tilde{c}_i$. $\varphi_i(x, t)$ is initially equal to $\varphi^{in}(x)$. At $t > 0$, it starts to move by electromigration with its linear mobility $\lambda_{0,i}$ and the shape is gradually dispersed by the nonlinearity and diffusion. In order to solve the system, we express the zone function $\tilde{w}_i$ as a product of its amplitude ΔW_i and the respective *i*th shape function $\varphi_i(x, t)$

$$\tilde{w}_i(x, t) = \Delta W_i \varphi_i(x, t) \tag{26}$$

and we insert it to Eq. (23)

$$\frac{\partial \varphi_i}{\partial t} = -(v_{0,i} + v_{EMD,i}\varphi_i)\frac{\partial \varphi_i}{\partial x} + \delta_i \frac{\partial^2 \varphi_i}{\partial x^2} \tag{27}$$

where $v_{0,i} = \frac{j}{\kappa_{BGE}}\lambda_{0,i}$ is the linear velocity of the *i*th zone and $v_{EMD,i} = \frac{j}{\kappa_{BGE}}\frac{\partial \lambda_i}{\partial \tilde{w}_i}\Delta W_i$ is a nonlinear parameter, which we will call the electromigration velocity. In general, $\varphi^{in}(x)$ have to be a function with unitary height to satisfy that ΔW_i is the initial amplitude (concentration) in the *i*th zone. The electromigration velocity $v_{EMD,i}$ is then a measure of electromigration dispersion of the *i*th zone for given initial conditions or, in reality, for the given composition of the sample zone. Experimentally, $v_{EMD,i}$ is a difference between the velocity at the apex of the *i*th zone and the velocity at its base as long as composition of the maximum remains close to the initial conditions, that is, until it become dispersed. If $v_{EMD,i}$ is divided by the applied intensity of the electric field in BGE, $E_{BGE} = j/\kappa_{BGE}$, we get $u_{EMD,i}$, which is a measure of electromigration dispersion of the *i*th zone independent on the actual electrical conditions and which we will call electromigration mobility.

An actual velocity profile within the zone is given by the product of $v_{EMD,i}$ and $\varphi_i(x,t)$. A special case of $\varphi^{in}(x)$ is the Dirac function, which cannot be normalized to unitary height but only to unitary area because its height is not an independent parameter. This case will be discussed later.

Switching temporarily to new coordinates where we let the system move along the *x*-axis with a linear velocity $v_{0,i}$ enables us to remove the velocity $v_{0,i}$ and to express Eq. (27) as the Burgers' equation

$$\frac{\partial \varphi_i}{\partial t} = -v_{EMD,i}\varphi_i \frac{\partial \varphi_i}{\partial x} + \delta_i \frac{\partial^2 \varphi_i}{\partial x^2} \tag{28}$$

After we derive a final solution, we can return to the original coordinates by a simple back-substitution of x by $x - v_{0,i}t$, while t remains unchanged. The analytical solution of the Burgers' equation can be found by using the Hopf (also known as Hopf–Cole) transformation [15]

$$\varphi_i = \frac{1}{\psi_i}\frac{d}{dx}(\ln \omega_i) \tag{29}$$

$$\psi_i = -\frac{v_{EMD,i}}{2\delta_i} \tag{30}$$

This reduces the nonlinear problem to a simple linear diffusive transport problem

$$\frac{\partial \omega_i}{\partial t} = \delta_i \frac{\partial^2 \omega_i}{\partial x^2} \tag{31}$$

that has the well-known solution

$$\omega_i(x, t) = \frac{1}{2\sqrt{\pi \delta_i t}} \int_{-\infty}^{\infty} \omega_i^{in}(\xi) \exp\left(-\frac{(x-\xi)^2}{4\delta_i t}\right) d\xi \tag{32}$$

where the initial condition ω_i^{in} is obtained as a solution of a differential equation $\frac{d}{dx}[\ln \omega_i^{in}(x)] = \psi_i \varphi^{in}(x)$ resulting from Eq. (29)

$$\omega_i^{in}(x) = \exp\left(\psi_i \int \varphi^{in}(x)\, dx\right) \tag{33}$$

We get the final solution $\varphi_i(x, t)$ by substituting ω_i to Eq. (29). It is important to note that the solution is obtained by a double integration of the initial zone shape function $\varphi^{in}(x)$, therefore, we have to use such initial functions that can be analytically integrated, such as Dirac function or stepwise functions. This will be discussed in next two sections.

2.5 Dirac function as initial shape $\varphi^{in}(x)$

For the purpose of zone electrophoresis and chromatography, the simplest possible initial shape is the Dirac function, which is a function with unitary area and its value equals zero everywhere except one point $x = 0$ where its value is infinity, see Fig. 1. The Dirac function is a crude approximation of a common setup where a width of a sample zone is negligible compared to a traveled distance of zones to a detector. In our model, it gives a solution known as the Haarhoff-van der Linde (HVL) function [16–18]

$$HVL_i(x, t) = A_i \varphi_i = \frac{A_i}{\sqrt{4\pi\delta_i t}}\frac{1}{\psi_i}\frac{\exp\left(-\frac{(x-v_{0,i}t)^2}{4\delta_i t}\right)}{\frac{1}{\exp(\psi_i)-1} + \frac{1}{2} + \frac{1}{2}erf\left(\frac{x-v_{0,i}t}{\sqrt{4\delta_i t}}\right)} \tag{34}$$

where A_i is the area in the spatial domain, which could be either in mol.m^{-2} unit if integrated over the length or in mol if over the volume and $\psi_i = -v_{EMD,i}/2\delta_i$ is the constant from the Hopf transformation representing a magnitude of the nonlinearity. Figure 1 shows an example of the HVL plot. Erny et al. [18] defines HVL as a purely spatial function containing four parameters: a_0 (area), a_1 (original position

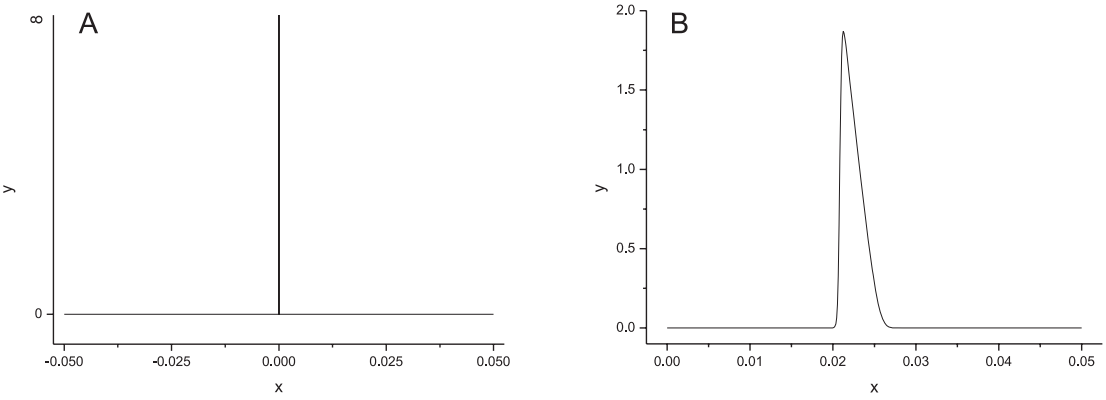

Figure 1. Plot of Dirac and Haarhoff-van der Linde (HVL) function. (A) Dirac function as initial condition with infinite height in its center $x = 0$. (B) Plot of HVL(x,t) function with following parameters: $A = 0.005$ mol.m^{-2}, $v_0 = 1 \times 10^{-4}$ m/s, $\delta = 1 \times 10^{-9}$ m^2/s, $v_{EMD} = -4 \times 10^{-8}$ m/s, and $t = 250$ s. Peak center ($v_0 t$) at 0.025 m.

in the case of a nondispersed peak), a_2 (nondispersed peak width), and a_3 (measure of dispersion). The comparison of the parametric HVL function in Ref. [18] with our solution in both x and t coordinates, Eq. (34), allows to express the parameters a_0–a_3 by real electrophoretic quantities

$$a_0 = A_i, \quad a_1 = v_{0,i}t, \quad a_2 = \sqrt{2\delta_i t}, \quad a_3 = -\frac{v_{EMD,i}}{v_{0,i}} \tag{35}$$

It is obvious that using the Dirac function as the initial condition $\varphi^{in}(x)$ yields the solution expressed as a rather simple formula, Eq. (34). The HVL function has a good capability to parametrically fit most of the nonsymmetrical peaks in chromatography and electrophoresis. For example, it enables to obtain the parameter a_1 (or $v_{0,i}t$), which is much better estimate of the true peak position than the peak maximum or the center of gravity. Its obvious disadvantage is that its height and width are not independent parameters—the initial Dirac function causes an infinite concentration of the peak in $t = 0$, which is decreased in time by overall dispersion. Therefore, we cannot satisfy the condition stated earlier that $\varphi^{in}(x)$ has to have the unitary height. It results in significant overestimation of the nonlinearity and therefore HVL function cannot draw very realistic profile based on real parameters.

2.6 Rectangular pulse function as initial shape $\varphi^{in}(x)$

The rectangular pulse function is a much more realistic initial condition. It is zero everywhere except an interval with a length L between points $x = -L/2$ and $x = L/2$ where its value is 1 as shown in Fig. 2. The initial step-wise function is mathematically represented by two Heaviside functions

$$\varphi^{in}(x) = Heaviside\left(x + \frac{L}{2}\right) - Heaviside\left(x - \frac{L}{2}\right) \tag{36}$$

The Heaviside step function is 0 for $x < 0$, 1/2 for $x = 0$, and 1 for $x > 0$ (in Ref. [19] it is called S_0). The initial rectangular pulse yields a nonlinear solution first derived for chromatography by Houghton [19], which we abbreviate here as the HVLR function

$$HVLR_i(x,t) = C_{0,i}\varphi_i(x,t) = C_{0,i}\frac{R_v}{Q + R_v} \tag{37}$$

$$R_v = erf(a_+) - erf(a_-) \tag{38}$$

$$Q = \exp(E_+)[1 - \mathrm{erf}(b_+)] + \exp(E_-)[1 - \mathrm{erf}(b_-)] \tag{39}$$

$$a_\pm = \frac{x - v_{0,i}t - v_{EMD,i}t \pm \frac{L}{2}}{\sqrt{4\delta_i t}}, \quad b_\pm = \pm\frac{x - v_{0,i}t \pm \frac{L}{2}}{\sqrt{4\delta_i t}} \tag{40}$$

$$E_\pm = \frac{v_{EMD,i}}{2\delta_i}\left(x - v_{0,i}t - \frac{1}{2}v_{EMD,i}t \pm \frac{L}{2}\right) \tag{41}$$

where $C_{0,i}$ is the initial concentration of the rectangular zone for $t = 0$. An example of the HVLR plot is shown in Fig. 2. Since the function is initially rectangular, the relation between concentration $C_{0,i}$ and area A_i is simply

$$A_i = C_{0,i}L \tag{42}$$

Even though HVLR function is given by Eq. (37) and can be in principle evaluated for arbitrary values of its parameters and coordinates (x, t), there are several numerical complications, which have to be addressed during its evaluation. The numerical complications are caused by a finite precision of numbers in computers and most frequently it is a problem connected to the arithmetic overflow of a value (the value magnitude is higher than the maximum what a computer can process) and also insufficient number of digits, which happen when two almost identical numbers are subtracted. Therefore, for the correct evaluation of the HVLR function in PeakMaster 5.3, we developed a numerical scheme that can handle all such problems.

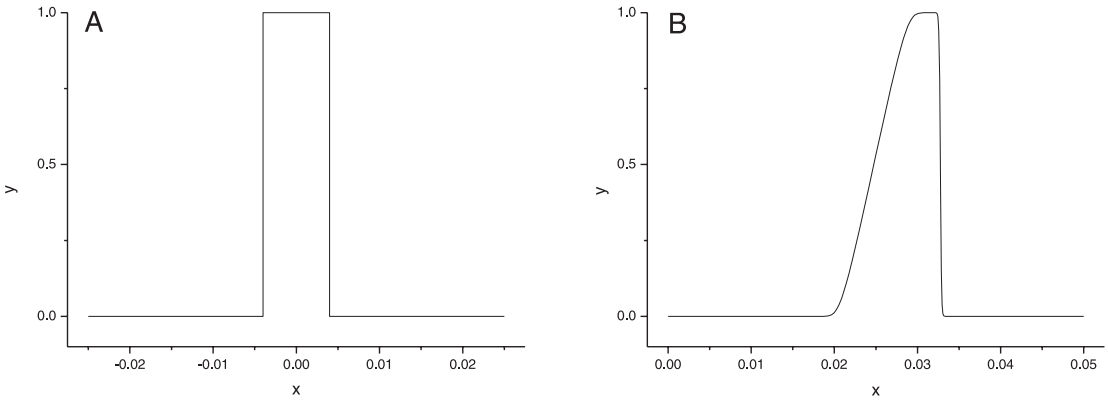

Figure 2. Example of rectangular pulse function and HVLR function. (A) Rectangular pulse as initial condition ($t = 0$) with unitary height ($C_0 = 1$ mM), $L = 0.008$ m, and center in $x = 0$. (B) HVLR(x,t) function with following parameters: $C_0 = 1$ mM, $L = 0.008$ m, $v_0 = 1 \times 10^{-4}$ m/s, $\delta = 1 \times 10^{-9}$ m^2/s, $v_{max} = 3 \times 10^{-5}$ m/s, $t = 250$ s. Peak center ($v_0 t$) at 0.025 m.

3 Discussion

We implemented the model of electromigration based on the Taylor expansion of governing equations where we consider only the constant and the first nonlinear term of electromigration and the constant term of diffusion into the program PeakMaster 5.3. Its user interface is located in the "Amplitude and Shapes" window [14]. Here, the user defines the sample composition and then click on the "Process" button, which calculates various properties of all zones: linear mobilities, composition (i.e., amplitudes, which represent the response for the indirect detection), conductivity response, linear pH disturbance, and the electromigration mobility $u_{EMD} = v_{EMD}/E_{BGE}$, which gives us information about the electromigration dispersion of the zone.

The best way how to test the validity of the model is by means of simulation by Simul 5, which contains the identical model without any approximations [8]. In this paper, we will show such comparison and discuss basic features of the nonlinear model. In the second separate part of the paper [20], we will present verification of PeakMaster 5.3 by experimental data. For the comparison with Simul 5, we utilize a system with the BGE containing 10 mM imidazole and 20 mM acetic acid and the sample composed of 10 mM imidazole and 26 mM acetic acid. The experimental electropherograms of the indirect UV detection at 214 nm were published in Ref. [14]—see Fig. 1, plot "Sample 6." The experimental conditions were as follows: the total capillary length of 0.726 m, the length to the UV detector of 0.641 m, applied voltage –30 000 V, and the mobility of the EOF was approximately -39×10^{-9} m^{2}V^{-1}s^{-1} (the negative mobility of the EOF is due to coating the capillary with Polybrene). The system has two system zones—one with almost zero mobility and one with mobility around 1.4×10^{-9} m^{2}V^{-1}s^{-1}. For simulation purposes, it is sufficient to simulate only 50 mm of the capillary because system mobilities are small compared to the EOF and the EOF itself can be emulated by moving the detector with the mobility of the EOF, which is a useful feature that is enabled in Simul 5. The sample zone width is 1 mm and its diffused edge width is set to 0.025 mm to obtain a rather sharp initial rectangular shape. The voltage is set $0.050/0.726 \times 30\,000$ V = 2066 V to have the same intensity of the electric field as in the experiment. The sample center is at 40 mm and the detector is initially located at 681 mm, which is outside the simulated area. The number of nodes is set to 10 000. When opening the file "Imidazole+Acetate INITIAL.sna" in Simul 5, all the input parameters are set automatically. This file together with all other supplementary files for Simul 5 and PeakMaster 5.3 can by downloaded from our web page www.natur.cuni.cz/gas. Approximately after 390 s of simulation time the detector enters the simulated area and within next 30 s the whole area is recorded by the detector. The final simulation is captured in "Imidazole+Acetate 420s.sna" file. The detector record can be displayed by clicking on Sim/Det button in Simul. Calculation procedure in PeakMaster 5.3 is as follows. In the main window the following parameters should be entered: BGE, Run Parameters, Signal to Indirect UV—Imidazole, range of the x-axis, and switching off the Ionic strength correction mode. In the Amplitude and Shapes window, following parameters should be entered: the sample composition, set the sample width (L) of 1 mm. Also, the PeakMaster's configuration file "Imidazole+Acetate.pmd," which sets all the input data used in the example, can be downloaded from our web page. When pressing the Process button, all parameters are calculated and the plot is drawn.

Experimental UV electropherogram is proportional to the concentration profile of imidazole, which is the UV-absorbing compound in the system, therefore, we used the imidazole profile in Fig. 3 for the calculated and simulated plots. Two blue dotted vertical lines represent the position of system peaks calculated from their linear mobilities. This type of depicting system zones is used in the main window of PeakMaster 5.3—the system peaks are depicted by vertical lines. The black solid curve is generated by the new nonlinear model of electromigration in PeakMaster 5.3 and the red dashed curve is the simulation in Simul 5 (detector profile). The system

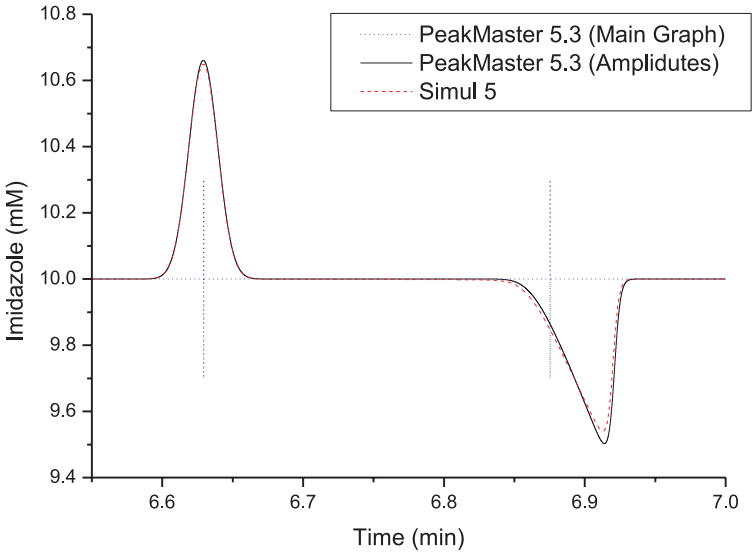

Figure 3. Comparison of PeakMaster 5.3 calculation and Simul 5 simulation of the background electrolytes composed of 10 mM imidazole and 20 mM acetic acid. Blue dotted vertical lines as shown by PeakMaster 5.2 graph in main window symbolize positions of system peaks based on their linear mobility; black solid curve is calculated by nonlinear model of electromigration in PeakMaster 5.3 (in Amplitudes and Shapes window); red dashed curve is simulated in Simul 5 (displayed as detector profile). All curves are profiles of imidazole concentration. Both calculation and simulation were performed without application of ionic strength correction. Calculation and simulation condition are in the text.

peak on the left is practically stationary and both Simul 5 and PeakMaster 5.3 results are practically identical for this peak. The second system peak on the right slowly migrates with cationic mobility of 1.4×10^{-9} $m^2V^{-1}s^{-1}$ and its u_{EMD} is 0.78×10^{-9} $m^2V^{-1}s^{-1}$. Here, the PeakMaster 5.3 and Simul 5 profiles slightly differ. It is the expected consequence of the simplification in the nonlinear model of PeakMaster 5.3, which uses only the first nonlinear term expressed by matrices $\mathbf{M}_{1,k}$ in Eq. (12). But clearly, the accordance is fully sufficient for basic inspection of the shapes of the system peaks. Also, the correspondence of the calculated imidazole profile in Fig. 3 with the experimental curve in Ref. [14] (Fig. 1, Sample 6) is very good.

The system we have chosen is also a good example for discussion what quantity should be used for representation of the electromigration dispersion. The usual practice is to divide the nonlinear parameter by the linear velocity, as is done in Eq. (35) for the parameter $a_3 = -\nu_{EMD}/\nu_0 = -u_{EMD}/\lambda_0$. Parameters a_3 for both system peaks in Fig. 3 are 0.59 and 0.56 for the left and right one, respectively. Obviously, the a_3 overestimates electromigration dispersion of slow zones as they are almost the same but the impact of the nonlinearity is completely different—the left one is symmetrical and the right one is strongly triangulating peak. For more precise assessment of the nonlinearity, we can utilize parameter ψ from Eq. (30), $\psi/E_{BGE} = -u_{EMD}/2\delta$, which considers also differences in diffusion coefficients. Parameters ψ/E_{BGE} for both system peaks in Fig. 3 are -5×10^{-7} V^{-1} and -0.33 V^{-1} for the left and right one, respectively. Obviously, ψ/E_{BGE} clearly predicts the difference in triangulation of both system peaks. It is also worth noting the position of the blue dotted vertical line in Fig. 3 for the right system peak. It marks the position where the peak maximum should be if there were no electromigration dispersion. Therefore, the fitting by nonlinear peak functions is a recommended approach how to determine the proper position of the peak instead of using the peak maximum. As noted earlier for the HVL function, such position is given by the parameter a_1.

4 Concluding remarks

Occurrence of system peaks is an inevitable phenomenon in electrophoresis and chromatography separations. The system peaks can be utilized as a source of information about the system but on the other hand they can negatively influence the separation. PeakMaster 5.3 is a tool for characterization of electrophoretic systems for capillary zone electrophoresis (CZE) separations and it is able to calculate many important parameters of the BGEs and separated analytes. In the version we have presented in this paper, it is now possible not only to calculate positions but also amplitudes and shapes of the system peaks for a given composition of the BGE and sample and a given experimental configuration. We have demonstrated on an example that the comparison of the PeakMaster 5.3 calculation with the simulation in Simul 5 and with the experiment is very good. It must be noticed, however, that there exist highly nonlinear nonconservation systems, such as the oxalic buffer system described in Ref. [12], where the simplified model is not able to describe all features of their behavior. However, such systems are rare, have low buffering capacity, and cannot be used in practice as BGEs.

The support of the Grant Agency of the Czech Republic, Grant No. 203/08/1428, Grant Agency of Charles University, Grant No. 51009, Agilent Technologies Foundation, No. 09EU-648, and the long-term research plan of the Ministry of Education of the Czech Republic (MSM0021620857) is gratefully acknowledged.

The authors declare no conflict of interest.

5 References

[1] Kohlrausch, F., *Ann. Phys. (Leipzig)* 1897, *62*, 209–239.

[2] Dismukes, E. B., Alberty, R. A., *J. Am. Chem. Soc.* 1954, *76*, 191–197.

[3] Jovin, T. M., *Biochemistry* 1973, *12*, 871–879.

[4] Hruška, V., Gaš, B., *Electrophoresis* 2007, *28*, 3–14.

[5] Thormann, W., Mosher, R. A., Breadmore, M. C., *Electrophoresis* 2011, *32*, 532–541.

[6] Mosher, R. A., Dewey, D., Thormann, W., Saville, D. A., Bier, M., *Anal. Chem.* 1989, *61*, 362–366.

[7] Thormann, W., Zhang, C. X., Caslavska, J., Gebauer, P., Mosher, R. A., *Anal. Chem.* 1998, *70*, 549–562.

[8] Hruška, V., Jaroš, M., Gaš, B., *Electrophoresis* 2006, *27*, 984–991.

[9] Bercovici, M., Lele, S. K., Santiago, J. G., *J. Chromatogr. A* 2009, *1216*, 1008–1018.

[10] Poppe, H., *J. Chromatogr.* 1990, *506*, 45–60.

[11] Poppe, H., *Anal Chem* 1992, *64*, 1908–1919.

[12] Štědrý, M., Jaroš, M., Hruška, V., Gaš, B., *Electrophoresis* 2004, *25*, 3071–3079.

[13] Jaroš, M., Hruška, V., Štědrý, M., Zusková, I., Gaš, B., *Electrophoresis* 2004, *25*, 3080–3085.

[14] Hruška, V., Štědrý, M., Včeláková, K., Lokajová, J., Tesařová, E., Jaroš, M., Gaš, B., *Electrophoresis* 2006, *27*, 4610–4617.

[15] Hopf, E., *Commun. Pur. Appl. Math.* 1950, *3*, 201–230.

[16] Haarhoff, P. C., van der Linde, H. J., *Anal. Chem.* 1966, *38*, 573–582.

[17] Erny, G. L., Bergstrom, E. T., Goodall, D. M., *Anal. Chem.* 2001, *73*, 4862–4872.

[18] Erny, G. L., Bergstrom, E. T., Goodall, D. M., Grieb, S., *Anal. Chem.* 2003, *75*, 5197–5206.

[19] Houghton, G., *J. Phys. Chem.-Us* 1963, *67*, 84–88.

[20] Riesová, M., Hruška, V., Gaš, B., *Electrophoresis* 2012, *33*, 933–939.

[21] Horká, M., Šlais, K., *Electrophoresis* 2000, *21*, 2814–2827.

Publikace 3

A nonlinear electrophoretic model for PeakMaster: II. Experimental verification

***Riesová M**., Hruška V.,Gaš B.*

Electrophoresis, 2012, 33, 931-937

Martina Riesová[1]
Vlastimil Hruška[1,2]
Bohuslav Gaš[1]

[1]Faculty of Science, Department of Physical and Macromolecular Chemistry, Charles University in Prague, Prague, Czech Republic
[2]Agilent Technologies GmbH, Waldbronn, Germany

Received October 19, 2011
Revised November 20, 2011
Accepted November 20, 2011

Research Article

A nonlinear electrophoretic model for PeakMaster: II. Experimental verification

We introduce a computer implementation of the mathematical model of capillary zone electrophoresis described in the previous paper in this issue (Hruška et al., *Electrophoresis* 2012, 33), the program PeakMaster 5.3. The computer model calculates eigenmobilities, which are the eigenvalues of the Jacobian matrix of the electromigration system, and which are responsible for the presence of system eigenzones (system zones, system peaks). The model also calculates parameters of the background electrolyte: pH, conductivity, buffer capacity, ionic strength, etc., and parameters of the separated analytes: effective mobility, transfer ratio, molar conductivity detection response, and relative velocity slope. In addition to what was possible in the previous versions of PeakMaster, Version 5.3 can predict the shapes of the system peaks even for a complex injected sample profile, such as a rectangular plug. PeakMaster 5.3 can replace numerical simulation in many practically important configurations and the results are obtained in a very short time (within seconds). We demonstrate that the results obtained in real experiments agree well with those calculated by PeakMaster 5.3.

Keywords:
Eigenmobility / Electromigration dispersion / Simulation / System peak
DOI 10.1002/elps.201100555

1 Introduction

The nonlinearity of the equations that describe the electromigration of ions or charged particles in solutions causes a problem as it is almost impossible to find an analytical solution (in a closed form) for the equations [1]. Instead, a numerical solution can be used to obtain information about the behavior of the system: several simulation programs are available, such as GENTRANS [2, 3], SIMUL5 [4], or SPRESSO [5] that do so. Unfortunately, numerical simulation yields the results only in a numerical or graphical form, so it cannot be used to formulate general laws of broader validity. In our earlier paper [6] we showed that the specific experimental setup of zone electrophoresis allows easy linearization of the laws that describe the electromigration process. The separation channel is filled with a relatively concentrated background electrolyte (BGE) and the sample is introduced into a specific point of the channel with a relatively small amount (concentration), so the concentration of the BGE and its conductivity remain almost unchanged, even in the analyte zones. This enables the linearization of the equations and the formulation of the Jacobian matrix leading to the solution in a particular point—in the point of the BGE. The eigenvalues of the Jacobian matrix correspond to characteristic velocities in the equations (which we call eigenmobilities), and which are the mobilities of both the analytes and the system zones. Further, the spectral decomposition of the Jacobian matrix implemented in PeakMaster 5.2 enables the calculation of the amplitudes of the system eigenzones [6, 7] when the composition of the injected sample is known. The linear model is, of course, only an approximation of the original nonlinear equations and does not allow the description of some of the features of electromigration that are connected with nonlinearity. One of such feature is the distortion of the system zones due to a change in the conductivity in the zone. Since for analyte zones the formula describing their velocity is explicitly known, it is simple to extend the linear model by the nonlinear velocity slope, a quantity that permits the estimation of the extent of electromigration dispersion in the analyte zone. For the calculation of electromigration dispersion in the system zone such an approach is not possible, because the formula for the velocity of the system zones is not known in general.

In the first part of the paper [8] we introduced a simplified nonlinear model of electrophoresis, which is more accurate than the linear model and which is still solvable using matrix notation. The model is implemented in PeakMaster 5.3. In addition to the capabilities of the previous versions of PeakMaster, Version 5.3 can determine the peak shapes of system peaks even for more complex injected sample profiles, such as of a rectangular plug. PeakMaster 5.3 then can

Correspondence: Dr. Martina Riesová, Faculty of Science, Department of Physical and Macromolecular Chemistry, Charles University in Prague, Prague, Czech Republic
E-mail: martina.riesova@natur.cuni.cz
Fax: +420-2-2491-9752

Abbreviations: L_{det}, length to diode array detector; L_{tot}, total capillary length

Colour Online: See the article online to view Figs.1–5 in colour.

replace numerical simulation in many practically important configurations and the results are obtained in much shorter time (within seconds) than by simulation. The first part of our paper showed a very good agreement between the results obtained by PeakMaster Ver. 5.3 and numerical simulation by means of Simul. In the present second part of the paper we demonstrate the agreement between the results obtained in real experiments and those calculated by PeakMaster 5.3.

Table 1. Amplitudes of the system peaks in a BGE composed of 12.5 mM TRIS and 10 mM benzoic acid

Perturbation	A	B	C	D
1st System peak change in concentration of benzoic acid (mM)	0.569	−0.569	0.275	−0.275
2nd System peak change in concentration of benzoic acid (mM)	−0.569	0.569	0.725	−0.725

2 Materials and methods

2.1 Software

The nonlinear PeakMaster 5.3 is a freeware program available at our website (http://www.natur.cuni.cz/gas). It implements the simplified nonlinear model of electrophoresis described in detail in the previous part of the paper [8]. It contains all the features of the previous versions of PeakMaster [9].

The same input parameters are necessary for the analysis of the system as described in the help file accessible from the PeakMaster environment. Also, the basic results of the analysis by PeakMaster 5.3 are obtained in the basic mode by clicking the "Calculate!" button: the pH of the BGE, the effective mobilities of analytes, the transfer ratios for prediction of the signal in indirect photometric detection, the molar

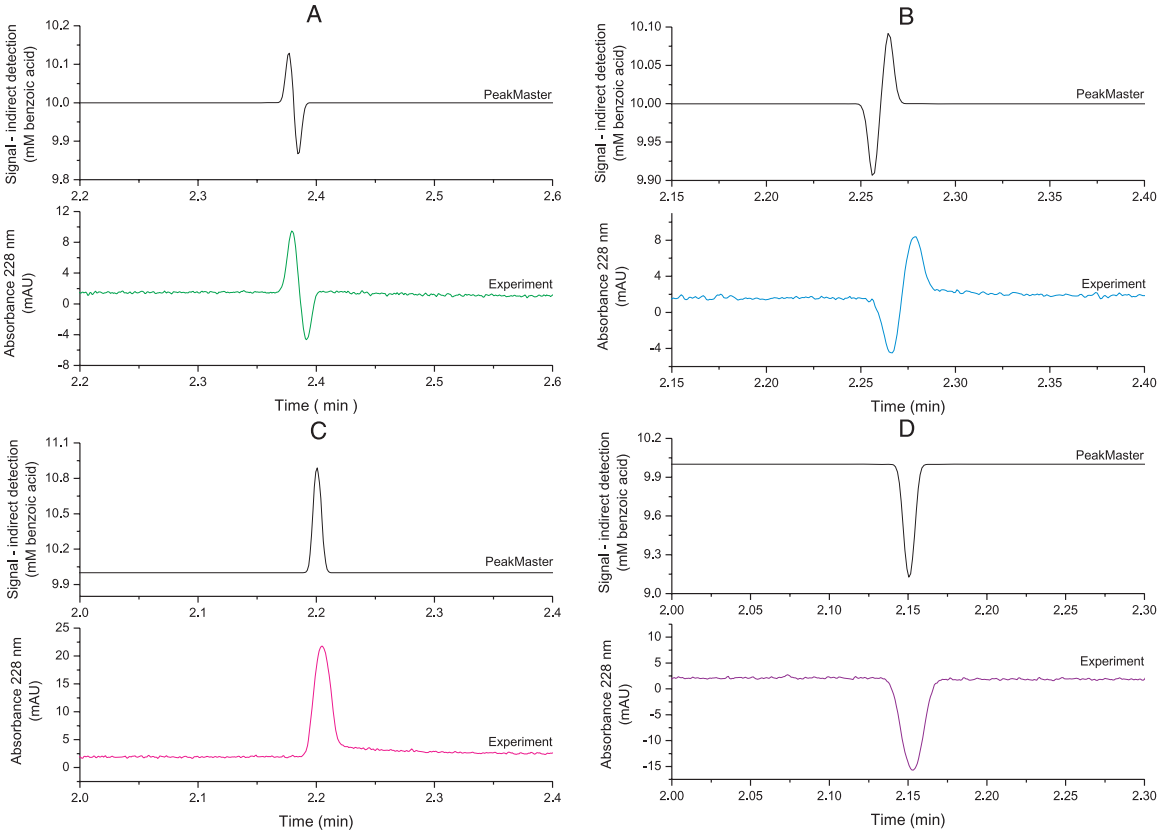

Figure 1. Predicted and experimental electropherograms of system peaks in a BGE composed of 10 mM benzoic acid and 12.5 mM TRIS. Injected samples are as follows: (A) 10 mM benzoic acid, 13.75 mM TRIS (+10% TRIS); (B) 10 mM benzoic acid, 11.25 mM TRIS (−10% TRIS); (C) 11 mM benzoic acid, 12.5 mM TRIS (+10% benzoic acid); (D) 9 mM benzoic acid, 12.5 mM TRIS (−10% benzoic acid). Capillary: $L_{tot} = 49.5$ cm, $L_{det} = 41.0$ cm, id = 50 μm. Injection, 30 mbar × 3 s. Thermostated temperature, 25°C. Voltage, +25 kV. Detection wavelength, 228 nm.

Table 2. Amplitudes of the system peaks and electromigration mobilities in a BGE composed of 7.5 mM TRIS and 10 mM benzoic acid

Perturbation	A	B	C	D
1st System peak change in concentration of benzoic acid (mM)	−0.461	0.461	0.370	−0.370
2nd System peak change in concentration of benzoic acid (mM)	0.461	−0.461	0.630	−0.630
1st System peak u_{EMD} (10^{-9} $m^2V^{-1}s^{-1}$)	−0.935	0.935	0.749	−0.749
2nd System peak u_{EMD} (10^{-9} $m^2V^{-1}s^{-1}$)	0.000	−0.000	0.000	−0.000

conductivity detection response for prediction of the signal in conductivity detection, the relative velocity slope which is a measure of the tendency of the analyte to undergo electromigration dispersion, and the system eigenmobilities.

The nonlinear features are attainable in the "Amplitudes and Shapes" window. First, the user inputs the concentration of all constituents in the injected sample, "c(Sample)", and the length of the injected sample "L (mm)". Then, clicking the "Process!" button reveals many other parameters of the system, including the matrices of amplitudes P [7], the responses in concentration, conductivity, pH, and the parameter $u_{EMD} = v_{EMD}/E$, which we call the dispersion mobility and which is a measure of nonlinearity. The shapes of all peaks, as they appear in various modes of detection, can be displayed by clicking the "Show/Hide Graph" button.

2.2 Chemicals and instrumentation

Chemicals were of analytical reagent grade. Benzoic acid (*p.a.*) and phthalic acid (*p.a.*) were purchased from Fluka (Switzerland), tris(hydroxymethyl)aminomethane (TRIS, >99.9%) was obtained from Sigma-Aldrich (Germany), and a 0.1 M solution of NaOH from Agilent Technologies

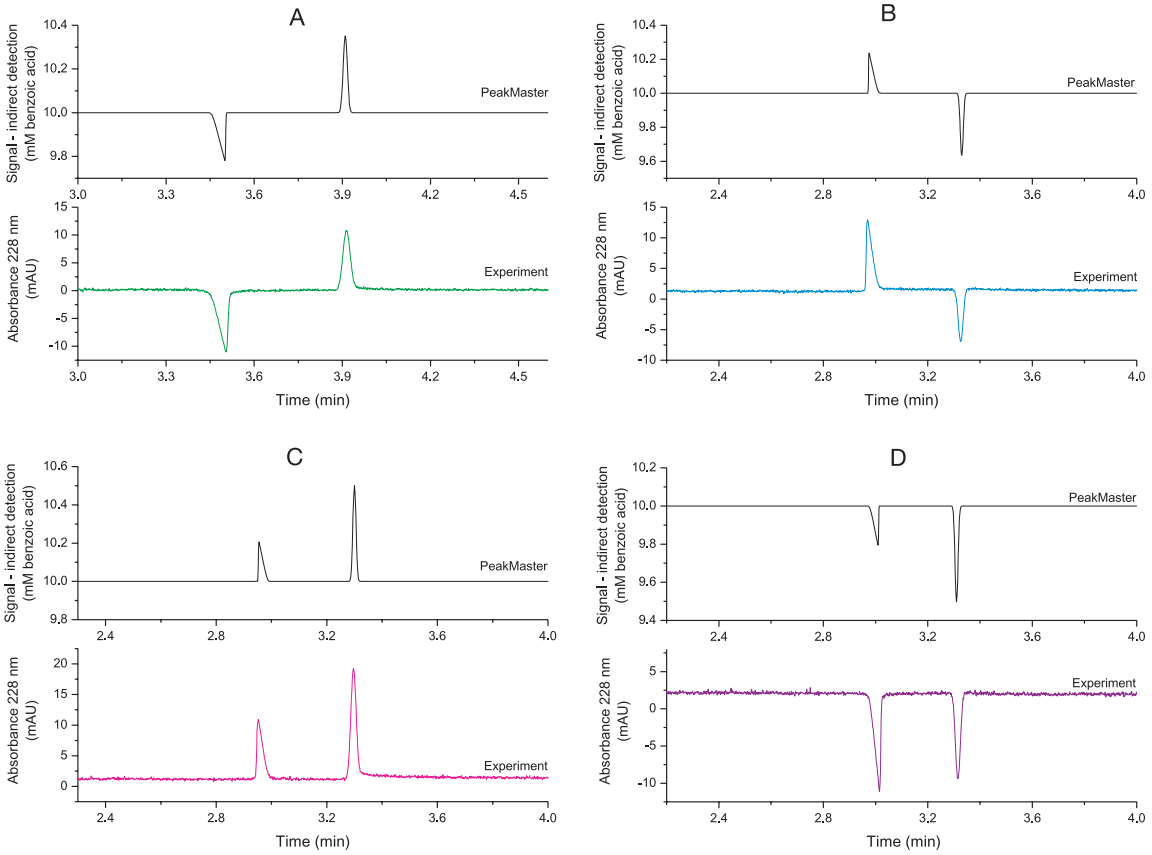

Figure 2. Predicted and experimental electropherograms of system peaks in a BGE composed of 10 mM benzoic acid and 7.5 mM TRIS. Injected samples are as follows: (A) 10 mM benzoic acid, 8.25 mM TRIS (+10% TRIS); (B) 10 mM benzoic acid, 6.75 mM TRIS (−10% TRIS); (C) 11 mM benzoic acid, 7.5 mM TRIS (+10% benzoic acid); (D) 9 mM benzoic acid, 7.5 mM TRIS (−10% benzoic acid). Capillary: L_{tot} = 49.5 cm, L_{det} = 41.0 cm, id = 50 μm. Injection, 30 mbar × 3 s. Thermostated temperature, 25°C. Voltage, +25 kV. Detection wavelength, 228 nm.

Table 3. Amplitudes of the system peaks and electromigration mobilities in a BGE composed of 10 mM TRIS and 5 mM phthalic acid

Perturbation	A	B	C	D
1st System peak change in concentration of phthalic acid (mM)	0.361	−0.361	0.138	−0.138
2nd System peak change in concentration of phthalic acid (mM)	−0.361	0.361	0.362	−0.362
1st System peak u_{EMD} (10^{-9} $m^2V^{-1}s^{-1}$)	−0.000	0.000	−0.000	0.000
2nd System peak u_{EMD} (10^{-9} $m^2V^{-1}s^{-1}$)	23.866	−23.866	−23.890	23.890

(Germany). Water was deionized by the Ultrapur system (Watrex, Czech Republic). pH was measured by means of the PHM 240 instrument (Radiometer, Denmark). All solutions were filtered with a syringe filter, pore size 0.45 μm. Experiments were performed using the HP^{3D}CE capillary electrophoresis system operated with the ChemStation software (Agilent Technologies). Detection was performed with the photometric diode-array detector (DAD) at various detection wavelengths (214, 228, or 230 nm). The driving voltage was 25 kV (cathode was at the detector side). Fused silica capillaries of 50 μm inside diameter (id) and 375 μm outside diameter (od) were provided by Polymicro Technologies (Phoenix, AZ, USA). The total capillary length (L_{tot}) was 49.5 cm, the length to the DAD detector (L_{det}) was 41 cm. A new capillary was preconditioned by rinsing it with deionized water (10 min), 0.1 M NaOH (10 min), and again with deionized water (10 min). Prior to each run, the capillary was flushed with the actual BGE solution for 5 min. The capillary was thermostated at 25°C.

3 Results and discussions

We compared the electropherograms predicted by PeakMaster 5.3 with the experimental electropherograms for several systems. In all cases the BGE was a binary buffer composed of two constituents: Constituent 1 was TRIS, Constituent 2 was either benzoic acid or phthalic acid. Constituent 2 is UV absorbing in order to get a UV signal for the BGE in the DAD. The samples we injected had the same constituents as the BGE but at different concentrations in order to excite, in a controlled way, the system peaks either with positive or negative amplitudes. Four injected sample solutions were made by perturbing the BGE as follows: (A) +10% of Constituent 1, (B) −10% of Constituent 1, (C) +10% of Constituent 2, (D) −10% of Constituent 2. For all four perturbations PeakMaster 5.3 yields all electromigration parameters of the BGE but we will concentrate on the positions and shapes of the system peaks, which are the new features in the nonlinear PeakMaster. At the same time, we performed the corresponding experiments on the HP^{3D}CE capillary electrophoresis system and recorded the electropherograms. Both the electropherograms predicted by PeakMaster 5.3 and the experimental ones are shown together in the figures to facilitate easy comparison. The installation file of PeakMaster 5.3 on our website (http://www.natur.cuni.cz/gas) includes the configuration files for an easy setup of the simulations, described below, that can be opened in the PeakMaster environment.

3.1 The system of TRIS and benzoic acid at neutral pH

The BGE composed of 12.5 mM TRIS and 10 mM benzoic acid has a pH of about 7.5, so its buffering ability is achieved due to the partial protonation of TRIS, the p*K*a of which is 8.076. As both constituents are univalent electrolytes and the pH is almost neutral, both system eigenmobilities are close to zero, 0.000×10^{-9} $m^2V^{-1}s^{-1}$, and -0.032×10^{-9} $m^2V^{-1}s^{-1}$. If we excite both system peaks in one direction, either positive or negative, one would expect at first glance that they should merge together due to their vicinity and form one duplicated peak. However, both system peaks differ somewhat and if we excite one system peak in the positive direction and the second one in the negative direction, the resulting peak may have a zigzag shape. This was confirmed both by the experiments and PeakMaster's predictions. As Constituent 2, benzoic acid, is the UV absorbing constituent, the change of the concentration of benzoic acid in the system peaks determines the resulting amplitude and peak shape. The change in the concentration of benzoic acid in both system peaks, as calculated by PeakMaster 5.3, is given in Table 1. For perturbations (A) and (B), the system peaks have an opposite polarity, which results in a zigzag peak, while for the perturbations (C) and (D) both system peaks have the same polarity, either positive or negative, respectively. Figure 1 shows a direct comparison of PeakMaster's predictions and the experimental records proving that the predicted shape of the system peak reflects reality very well.

3.2 The system of TRIS and benzoic acid at acidic pH

The BGE is composed of 7.5 mM TRIS and 10 mM benzoic acid. Compared to the previous BGE, the concentration of TRIS is less than the concentration of benzoic acid and the pH is about 4.6. The buffering ability of the BGE is due to the partial dissociation of benzoic acid, whose p*K*a is 4.203. The pH is rather acidic which means that one of the system zones will have a relatively high cationic mobility (it will behave as cation). According PeakMaster 5.3, the system eigenmobilities are 4.415×10^{-9} $m^2V^{-1}s^{-1}$ and -0.000×10^{-9} $m^2V^{-1}s^{-1}$. If we excite the system peaks by the same perturbations as in the previous system, the system peaks should behave basically in an analogous pattern. The difference here is that the system peaks will be sufficiently apart and can be observed separately. What is interesting to inspect in this system is the shape of the system peaks and to judge whether the nonlinear feature included in PeakMaster 5.3 allows the prediction of not only the amplitude, but also the correct shape (or electromigration dispersion) of the system peaks. As stated in Part

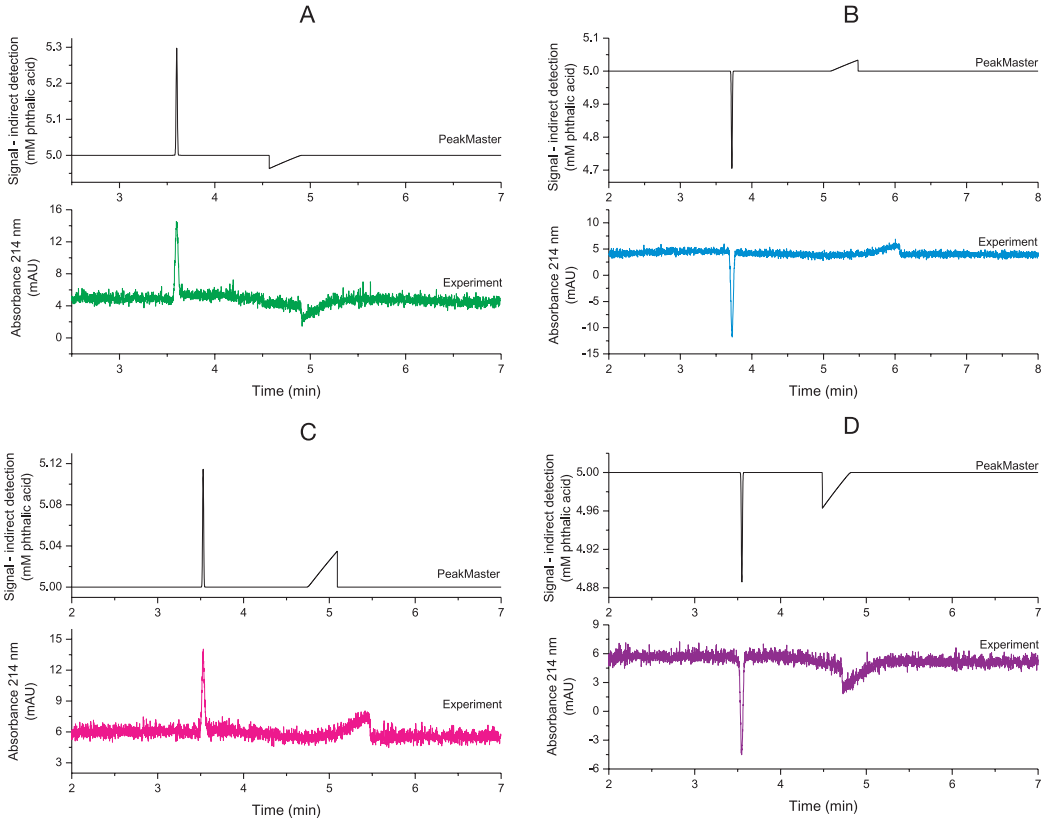

Figure 3. Predicted and experimental electropherograms of system peaks in a BGE composed of 5 mM phthalic acid and 10 mM TRIS. Injected samples are as follows: (A) 5 mM phthalic acid, 11.25 mM TRIS (+10% TRIS); (B) 5 mM phthalic acid, 9 mM TRIS (−10% TRIS); (C) 5.5 mM phthalic acid, 10 mM TRIS (+10% phthalic acid); (D) 4.5 mM phthalic acid, 10 mM TRIS (−10% phthalic acid). Capillary: L_{tot} = 49.5 cm, L_{det} = 41.0 cm, id = 50 μm. Injection, 30 mbar × 3 s. Thermostated temperature, 25°C. Voltage, +25 kV. Detection wavelength, 214 nm.

I of this paper, the quantity responsible for electromigration dispersion of peaks is the dispersion mobility, u_{EMD}, which is the difference between the mobility at the apex of the peak and the mobility at the base of the peak at the beginning of electromigration, before electromigration dispersion will lower the original amplitude of the peak. Both the change in the concentration of benzoic acid, which is a measure of the amplitude of the system peak in the DAD, and u_{EMD}, which provides information about the extent of electromigration dispersion, are given in Table 2. A negative sign of u_{EMD} implies a fronting peak, a positive sign means a tailing peak. All records of the corresponding simulations and experiments shown in Fig. 2 confirm what is predicted above, especially as regards the positions and triangulation of the system peaks.

3.3 The system of TRIS and phthalic acid with low buffer capacity

The BGE composed of 10 mM TRIS and 5 mM phthalic acid has, intentionally, a low buffer capacity. Phthalic acid here is predominantly in the double negative anionic form and TRIS in the single positive cationic form. Such buffer is, in fact, unsuitable for use as a BGE and provides a relatively fast system zone that moves toward the anode. The two system eigenmobilities are 0.001×10^{-9} $m^2V^{-1}s^{-1}$ and -12.122×10^{-9} $m^2V^{-1}s^{-1}$. The system peaks are excited the same way as in the previous systems with benzoic acid, that is, by perturbation of the concentrations of TRIS and phthalic acid in the injected sample. The resulting parameters of the system peaks are given in Table 3.

Obviously, for the second system peak, u_{EMD} has a very high absolute value, 23.866×10^{-9} $m^2V^{-1}s^{-1}$, and, depending on the excitation, it is either positive or negative. This value is even higher than the eigenmobility itself. The velocity of the system zone at points where the concentration is high considerably differs from the velocity at points where the concentration is small. This pushes the crest of the peak to overtake the base of the peak, like a sea wave. Of course, such a breaking wave cannot occur in electrophoresis, because the diffusive flux becomes high in the spots of high concentration gradient and prevents formation of a breaking

wave, but it causes a strong triangulation and the triangle will have a sharp edge. Comparison of the simulations and the experiments is shown in Fig. 3. Although the predicted positions of the system peaks do not fit the experimental ones perfectly (probably due to incorrect input data for phthalic acid), the polarity and shapes of the system peaks are in a good agreement.

3.4 The system of TRIS and benzoic acid with embedded system peaks

This is a rather unusual system, as both peaks have very different shapes and are embedded. It is formed by 15 mM TRIS and 15 mM benzoic acid so, in fact, it is a solution of a salt of a weak acid and a weak base. Such a system has a low buffering capacity and its pH of 6.141 is approximately the average of the p*K*a of benzoic acid, 4.203, and of protonated TRIS, 8.076. The eigenmobilities of the system are 0.889×10^{-9} $m^2V^{-1}s^{-1}$ and -0.000×10^{-9} $m^2V^{-1}s^{-1}$, so both are close to zero. The corresponding amplitudes and dispersion mobilities, u_{EMD}, are given in Table 4.

The first system peak with a positive eigenmobility of 0.889×10^{-9} $m^2V^{-1}s^{-1}$ moves as a cation and has a high negative dispersion mobility, -6.046×10^{-9} $m^2V^{-1}s^{-1}$, which means that it will be strongly fronting. The fronting is so excessive that it is able to overlap the second system peak, which in fact does not move from its originally injected position, so finally both system peaks are embedded together. This may seem like a theoretical construction, but the experiment proves that in reality the peaks look almost exactly as predicted (Fig. 4). The figure also shows the resulting electropherogram as generated by the previous versions of PeakMaster. Here the shapes of the system peaks are not drawn, only their positions are depicted as two vertical lines.

3.5 The system of benzoic acid and TRIS at acidic pH with a long plug of injected sample

The system is the same as in Part 3.2, that is, it is a buffered system composed of 7.5 mM TRIS and 10 mM benzoic acid. Here we have checked whether the Haarhoff-van der Linde-like function based on initial rectangular pulse disturbance

Table 4. Amplitudes of the system peaks and electromigration mobilities in a BGE composed of 15 mM TRIS and 15 mM benzoic acid

Perturbation	A
1st System peak change in concentration of benzoic acid (mM)	−0.999
2nd System peak change in concentration of benzoic acid (mM)	0.999
1st System peak u_{EMD} (10^{-9} $m^2V^{-1}s^{-1}$)	−6.046
2nd System peak u_{EMD} (10^{-9} $m^2V^{-1}s^{-1}$)	0.000

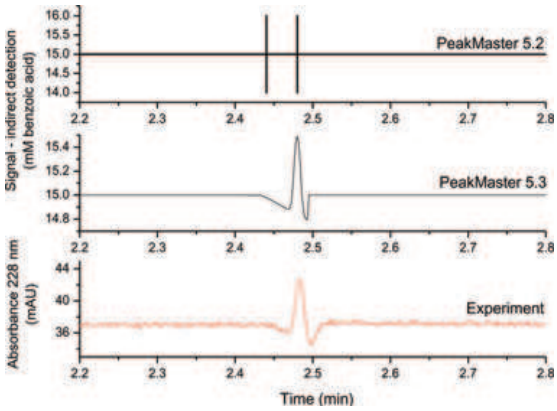

Figure 4. Predicted and experimental electropherograms of system peaks in a BGE composed of 15 mM benzoic acid and 15 mM TRIS. Injected sample are as follows: 15 mM benzoic acid, 17 mM TRIS. Capillary: L_{tot} = 49.5 cm, L_{det} = 41.0 cm, id = 50 μm. Injection, 30 mbar × 3 s. Thermostated temperature, 25°C. Voltage, +25 kV. Detection wavelength, 228 nm.

(HVLR) [8], which is implemented in PeakMaster 5.3, is able to predict correctly the shapes of the system peaks if a sufficiently long plug of the sample is injected. If the injected sample plug is sufficiently long, the resulting peak is no longer Gaussian or triangular in shape, rather it is flat having edges of different steepnesses. The injected sample, 10 mM benzoic acid, 8.25 mM TRIS, had a type (A) perturbation, that is, +10% of TRIS. Injection was done by applying a pressure of 50 mbar for 13 s which, according to Poisseuille's equation, pumped a 10.1 mm long plug into the capillary. The plug is intentionally much longer than is usual in zone electrophoresis, just to verify the ability of the HVLR function to depict the shapes of long plugs. The length of 10.1 mm has to be inserted in the Amplitudes and Shapes window in PeakMaster 5.3 as L (mm). The resulting predicted shape, together with the experimental electropherogram, is shown in Fig. 5. The first negative system peak has a nonsymmetrical trapezoidal shape with a fronting front edge, while the tailing edge is much steeper. This is due to u_{EMD}, which is -0.935×10^{-9} $m^2V^{-1}s^{-1}$ for this peak, see Table 2. The second peak is also trapezoidal, but symmetrical. It does not move and its trapezoidal shape is due to diffusion only, as u_{EMD} is almost zero.

4 Concluding remarks

The Simul 5 software we developed in our laboratory and other dynamical simulation programs are powerful numerical tools for the inspection of the behavior of electromigration systems in general, regardless of the operation mode, be it zone electrophoresis, isotachophoresis, or any other distribution of electrolytes in the separation channel. The price of this achievement, however, is computation time,

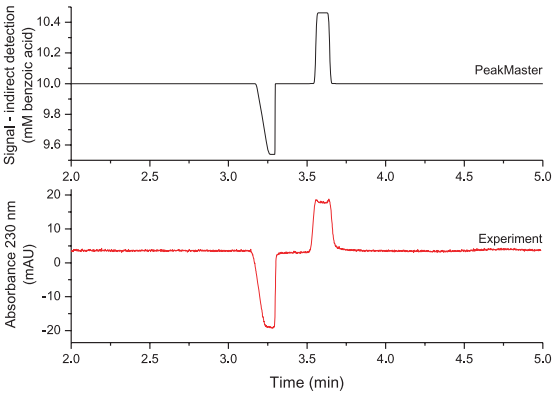

Figure 5. Predicted and experimental electropherograms of long system peaks in a BGE composed of 10 mM benzoic acid and 7.5 mM TRIS. Injected sample are as follows: 10 mM benzoic acid, 8.25 mM TRIS (+10% TRIS). Capillary: L_{tot} = 49.5 cm, L_{det} = 41.0 cm, id = 50 μm. Injection, 50 mbar × 13 s. Thermostated temperature, 25°C. Voltage, +25 kV. Detection wavelength, 230 nm.

which can be in some cases days or even weeks. Of all the possible operation modes, zone electrophoresis offers an easy way to simplify the governing equations and to find their solution. Such simplified, though sufficiently accurate equations are implemented in the PeakMaster software series, which can yield information, in seconds, about many of the features of electrophoresis separations. This helps method development in capillary zone electrophoresis and can significantly reduce the expense and time of experimental work.

The support of the Grant Agency of Charles University, Grant No. 51009, Grant Agency of the Czech Republic, Grant No. 203/08/1428, Agilent Technologies Foundation, No. 09EU-648 and the long-term research plan of the Ministry of Education of the Czech Republic (MSM0021620857), are gratefully acknowledged.

The authors have declared no conflict of interest.

5 References

[1] Gaš, B., *Electrophoresis* 2009, *30*, S7–S15.

[2] Mosher, R. A., Dewey, D., Thormann, W., Saville, D. A., Bier, M., *Anal Chem* 1989, *61*, 362–366.

[3] Thormann, W., Zhang, C. X., Caslavska, J., Gebauer, P., Mosher, R. A., *Anal Chem* 1998, *70*, 549–562.

[4] Hruška, V., Jaroš, M., Gaš, B., *Electrophoresis* 2006, *27*, 984–991.

[5] Bercovici, M., Lele, S. K., Santiago, J. G., *J Chromatogr A* 2009, *1216*, 1008–1018.

[6] Štědrý, M., Jaroš, M., Hruška, V., Gaš, B., *Electrophoresis* 2004, *25*, 3071–3079.

[7] Hruška, V., Štědrý, M., Včeláková, K., Lokajová, J., Tesařová, E., Jaroš, M., Gaš, B., *Electrophoresis* 2006, *27*, 4610–4617.

[8] Hruška, V., Riesová, M., Gaš, B., *Electrophoresis* 2012, *33*, 925–932.

[9] Jaroš, M., Hruška, V., Štědrý, M., Zusková, I., Gaš, B., *Electrophoresis* 2004, *25*, 3080–3085.

4.2 Systémové píky v komplexujících systémech

Přítomnost komplexujícího činidla v základním elektrolytu může nabídnout analytům dodatečné interakce, které pak mohou zvýšit selektivitu daného separačního systému. Nabitá komplexační činidla mohou prostřednictvím interakce s neutrálními analyty tyto analyty „mobilizovat“ a rozšiřují tak použitelnost kapilární elektroforézy i pro nenabité látky. Pokud je použitým komplexačním činidlem chirální selektor, pak může docházet k enantioseparaci chirálních analytů. Komplexující činidla mají tedy jako aditiva do základního elektrolytu široké využití. Zatímco vliv komplexace na chování analytů v takových systémech je poměrně dobře popsán, zejména v oblasti chirálních separací, ucelený popis a možné důsledky komplexace složky základního elektrolytu s přítomným komplexačním činidlem zcela chybí.

Cílem Publikací 4 a 5 bylo zacelit tento nedostatek. Nejprve jsme se zaměřili obecně na roztoky pufrů. Teoreticky i experimentálně jsme vyšetřili případné změny jejich základních vlastností v důsledku komplexace pufrující složky s neutrálním komplexačním činidlem. Velkou pozornost jsme věnovali především změnám pH. Kompletní teoretický popis pufračních systémů, kde probíhá kromě disociace pufrující složky (slabý elektrolyt) současně i komplexace s přítomným neutrální komplexačním činidlem (situace znázorněná na Obrázku 3) není možné řešit analyticky. K výpočtům přesných hodnot základních vlastností komplexujících pufrů je možné využít numerického simulátoru Simul 5 Complex [52], který zahrnuje komplexační model.

$$
\begin{array}{ccc}
 & \overset{K_{HA}}{} & \\
HA + H_2O & \rightleftharpoons & H_3O^+ + A^- \\
+ & & + \\
C & & C \\
K_{XAn} \downarrow\uparrow & & \downarrow\uparrow K_{XAc} \\
HAC + H_2O & \rightleftharpoons & H_3O^+ + AC^- \\
 & \underset{K_{HAC}}{} &
\end{array}
$$

Obrázek 3 *Schéma současně probíhající disociační a komplexační rovnováhy slabého elektrolytu HA s neutrálním komplexačním činidlem C, K_{XAc} a K_{XAn} jsou komplexační konstanty nabité a nenabité formy HA, K_{HA} a K_{HAC} jsou disociační konstanty HA a příslušného komplexu HAC*

Pro získání představy o obecně platných pravidlech změn pH v komplexujících systémech jsme odvodili zjednodušené vztahy pro výpočet koncentrace oxoniových iontů. Z odvozených vztahů platných vždy pro daný typ pufru (kyselý nebo bazický, s vysokým nebo nízkým pH) vyplývá, že poměr komplexačních konstant nabité a nenabité formy pufrující složky s komplexačním činidlem jednoznačně určuje, zda bude pH daného pufru nižší nebo vyšší než pH původního pufrujícího roztoku bez přídavku komplexujícího činidla.

Na dvou modelových systémech jsme ověřili platnost těchto předpokladů. Vyšetřovány byly pufry sestavené (i) z kyseliny benzoové a hydroxidu lithného a (ii) kyseliny *N*-cyklohexyl-2-aminoethansulfonové (CHES) a hydroxidu lithného. Z měření změn pH pufru po přidání neutrálního β-cyklodextrinu (β-CD) vyplývá, že nenabitá forma kyseliny benzoové interaguje s β-CD silněji než nabitá. U CHESu je tomu naopak*. Výsledky těchto závěrů přehledně ilustruje Obrázek 4.

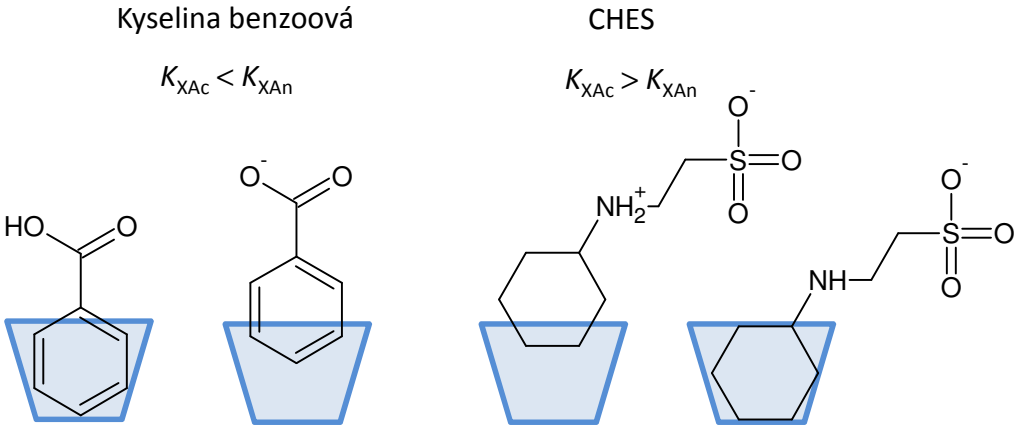

Obrázek 4 *Ilustrace informací získaných o modelových komplexech (kyselina benzoová - β-CD a CHES - β-CD) proměřením změn pH pufrů před a po přídavku β-CD.*

Tyto závěry jsou v souladu literárními údaji i s všeobecným předpokladem, že s hydrofobní kavitou cyklodextrinů budou silněji interagovat hydrofobní molekuly nebo

* Nenabitou formou látky se rozumí stav, kdy je celkový náboj molekuly nulový. V případě CHESu je to tedy stav, kdy je protonizována aminoskupina a zároveň disociována sulfonová skupina.

jejich části resp. nedisociované analyty. Tyto předpoklady a výsledky vyplývající z měření pH byly ověřeny také NMR měřením difúzních koeficientů nabitých a nenabitých forem obou látek v prostředí bez β-CD a s β-CD.

Praktický dopad komplexace složek základního elektrolytu na elektroforetické výsledky je podrobně popsán v druhé části dvoudílné série článků (Publikace 4 a 5). Z výsledků je zřejmé, že stanovování komplexačních konstant pomocí afinitní kapilární elektroforézy je nezbytné provádět v pufrech, které s přítomným komplexačním činidlem neinteragují. Ukázali jsme, že případná (nechtěná, skrytá) interakce složky BGE a komplexačního činidla má zásadní dopad na stanované hodnoty komplexačních konstant a tuto hodnotu závažně zkresluje. Přítomnost komplexačního činidla (třeba za účelem chirální separace) může také výrazně snížit rozlišení separace daných analytů. Tato skutečnost byla demonstrována na sadě aminokyselin, které jsou v pufru bez přídavku komplexujícího činidla dobře separovány (Obrázek 5A). Po přídavku komplexujícího činidla dojde k výraznému zhoršení separace kvůli neočekávané změně pH způsobené komplexací složky BGE s komplexačním činidlem (Obrázek 5B).

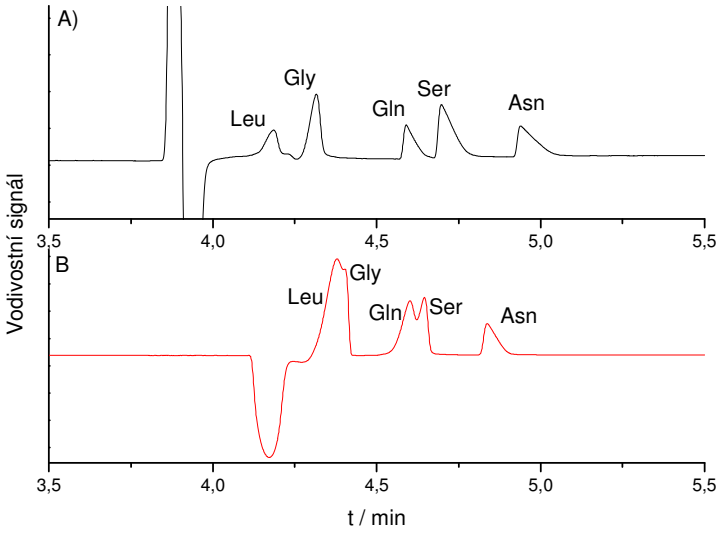

Obrázek 5 *Separace aminokyselin v CHES/LiOH pufru bez přítomnosti β-CD (A) a ve shodném pufru s přídavkem β-CD (B)*

Značnou pozornost jsme věnovali také chování systémových píků v komplexujících systémech. Vznik systémových píků, jejich počet a mobility jsou velmi dobře popsány lineární teorií elektromigrace. Podle této teorie nezpůsobí přídavek neutrální látky do roztoku základního elektrolytu žádnou změnu v existujících systémových zónách[†]. V případě komplexace neutrálního činidla se složkou BGE však byly pozorovány změny v počtu a mobilitách systémových píků. Tento fakt lze vysvětlit vznikem komplexu (v Obrázku 3 komplex HAC), který také podléhá acidobazické rovnováze a je elektroforetickým systémem vnímám jako další složka základního elektrolytu. Způsobuje tak vznik dalšího systémového píku a ovlivňuje (někdy i výrazně) mobility těch stávajících. Tyto „nepředvídatelné" systémové píky lze pak snadno zaměnit za píky analytů nebo mohou píky analytů překrývat a znehodnotit. Elektroforetické výsledky v komplexujících systémech, včetně systémových píků, je v současné době možné pouze numericky simulovat programem Simul 5 Complex [52]. Vypočítat přímo mobility systémových zón zatím možné není[‡]. V Publikaci 5 bylo chování systémových píků v komplexujících systémech opět demonstrováno na modelovém sytému kyselina benzoová/LiOH + β-CD. Prokázali jsme, že i malý přídavek neutrálního komplexačního činidla může zásadně ovlivnit pozice již existujících systémových píků (*Figure 4A* v Publikaci 5). Na rozdíl od uvedeného sytému, kde má vznikající systémový pík velmi nízkou mobilitu, systémový pík, který vzniká po přídavku β-CD do systému CHES/LiOH, má již podstatně větší mobilitu (Obrázek 6) a je pravděpodobné, že může „překážet" píkům analytů v reálných separačních systémech.

[†] Uvažuje se, že neutrální složka vyvolá přítomnost systémového píku s nulovou mobilitou a nulovou amplitudou a neovlivní mobility ani amplitudy již existujících systémových píků

[‡] V současné době v naší skupině pracujeme na linearizaci modelu, který by zahrnoval i komplexační rovnováhy. Hotový model, implementovaný v programu PeakMaster, pak bude cenným nástrojem při systematickém vyšetřování systémových píků v komplexujících systémech

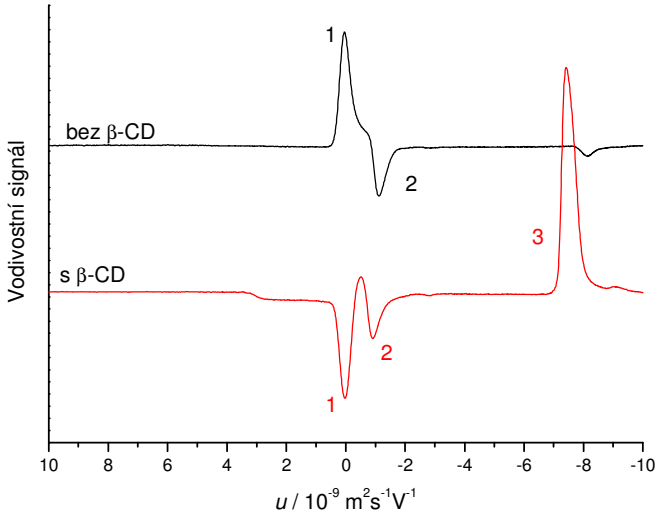

Obrázek 6 *Změna počtu systémových píků v důsledku komplexace složky BGE s neutrální komplexačním činidlem (β-CD) v CHES/LiOH pufru*

Přítomnost komplexačního činidla může výrazně ovlivnit vlastnosti pufru. Tyto změny jsou málokdy očekávány, zejména v případě neutrálního komplexačního činidla. Je-li komplexující pufr použit jako základní elektrolyt v kapilární elektroforéze, může zásadně ovlivnit a zkreslit elektroforetické výsledky. Kontrolování hodnoty pH po přídavku komplexačního činidla do BGE může být jednoduchým testem k odhalení nechtěné komplexace a spolehlivou prevencí špatných interpretací elektroforetických výsledků.

Publikace 4

Complexation of buffer constituents with neutral complexation agents: Part I. Impact on common buffer properties

***M. Riesová**, J. Svobodová, Z. Tošner, M. Beneš, E. Tesařová, B. Gaš*

Analytical Chemistry

Complexation of buffer constituents with neutral complexation agents: Part I. Impact on common buffer properties

Journal:	*Analytical Chemistry*
Manuscript ID:	ac-2013-013804.R1
Manuscript Type:	Article
Date Submitted by the Author:	n/a
Complete List of Authors:	Riesova, Martina; Charles University, Faculty of Science, Department of Physical Chemistry Svobodova, Jana; Charles University in Prague, Department of Physical and Macromolecular Chemistry Tosner, Zdenek; Charles University in Prague, Dept. of Organic Chemistry Benes, Martin; Charles University, Faculty of Science, Department of Physical Chemistry Tesarova, Eva; Charles University, Faculty of Science, Department of Physical Chemistry Gas, Bohuslav; Charles University, Faculty of Science, Department of Physical Chemistry

Complexation of buffer constituents with neutral complexation agents: Part I. Impact on common buffer properties

Martina Riesová[1], Jana Svobodová[1], Zdeněk Tošner[2], Martin Beneš[1], Eva Tesařová[1], Bohuslav Gaš[1]*

[1]Charles University in Prague, Faculty of Science, Department of Physical and Macromolecular Chemistry, Prague, Czech Republic

[2]Charles University in Prague, Faculty of Science, Department of Organic Chemistry, Prague, Czech Republic

* Corresponding Author

E-mail: svobod.j@seznam.cz

Phone: +420-2-2195-1399

Fax: +420-2-2491-9752

complexation constants, NMR, affinity capillary electrophoresis, buffer, simulations

ABSTRACT

The complexation of buffer constituents with the complexation agent present in the solution can very significantly influence the buffer properties, such as pH, ionic strength or conductivity. These parameters are often crucial for selection of the separation conditions in capillary electrophoresis or HPLC and can significantly affect results of separation, particularly for capillary electrophoresis as shown in Part II of this papers series. In this paper the impact of complexation of buffer constituents with a neutral complexation agent is demonstrated theoretically as well as experimentally for the model buffer system composed of benzoic acid/ LiOH or common buffers (*e.g.* CHES/ LiOH, TAPS/ LiOH, Tricine/ LiOH, MOPS/ LiOH, MES/ LiOH, and acetic acid/ LiOH). Cyclodextrins as common chiral selectors were used as model complexation agents. We were not only able to demonstrate substantial changes of pH, but also to predict the general complexation characteristics of selected compounds. Due to the zwitterion character of the common buffer constituents their charged forms complex stronger with cyclodextrins than the neutral ones do. This was fully proven by NMR measurements. Additionally complexation constants of both forms of selected compounds were determined by NMR and affinity capillary electrophoresis with a very good agreement of obtained values. These data were advantageously used for the theoretical descriptions of variations in pH, depending on the composition and concentration of the buffer. Theoretical predictions were shown to be a useful tool for deriving some general rules and laws for complexing systems.

INTRODUCTION

Guest-host interactions have a significant impact in many biological processes, and they are also substantial for a number of separation techniques. The additional interaction of an analyte

can improve results of separation or enable separation of chiral compounds, if a chiral selector is used as a complexation agent. Simultaneously, this kind of interaction was shown to influence the physicochemical properties of the complexed compounds, particularly acid-base behavior, which can result in shifts of its pK_A. The pK_A shifts for various compounds complexing with cyclodextrins (CDs)[1-3], cucurbiturils[4,5] or even micelles or compartmentalized lipids[6] were observed by different techniques particularly fluorescence[1,5], potentiometry[6-8], induced circular dichroism[9], electrophoresis [2,10-12] and NMR[3]. Such pK_A shifts can have a crucial impact on the selection of optimum separation conditions, as was shown for chiral separation in capillary electrophoresis (CE) by Rizzi *et al.*[12] and Hammitzsch-Wiedmann *et al.*[11].

The extent of pK_A shift of an analyte depends on the ratio of the complexation constants of both dissociated and non-dissociated forms of the analyte with a complexation agent. Thus, a pH potentiometric titration of the desired compound was used to determine the complexation constants by Gelb *et al.*.[8,13] Nowadays this method has been replaced by more accurate techniques, such as NMR and electrophoretic techniques. In NMR, concentration of the complexation agent is varied, while chemical shift, relaxation rates or diffusion coefficients are most frequently measured as a response.[14,15] An advantage of NMR is that it can be used to estimate the stoichiometry of the resulting complex or to obtain the additional information on the structure of the complex. In electrophoresis, affinity capillary electrophoresis (ACE) is the most common setup[16-20], in which mobility of an analyte is determined against the concentration of a complexation agent added into the background electrolyte (BGE). ACE-like separation is also frequently used for practical purposes in analytical chemistry. Despite the fact that electrophoretic separation is a complicated nonlinear process, it is very well described theoretically and it generally results in being the common physicochemical property of the buffer

(*i.e.* BGE) that determines the separation efficiency in CE. Some computer programs exist that enable to predict the parameters of the used BGE and/or simulate the separation process. Out of these, Simul[21-24] and PeakMaster[25-27] have been developed in our laboratory and their latest versions were designed to account for complexation in CE.

Clearly, the complexation of the analyte and complexation agent is widely studied. On the other hand, other consequences, such as the impact of the complexation of buffer constituents on the properties of the buffer, are discussed only rarely and in special cases.[28,29] In the present study, we show, both theoretically and experimentally, that an addition of any (even neutral) complexation agent into a BGE might significantly influence buffer properties, *e.g.*, pH, ionic strength or conductivity. We simultaneously demonstrate that changes in pH can reveal some fundamental characteristics of complexation. For example it follows that complexation of common buffer constituents such as CHES, MES, MOPS with common neutral CDs is much stronger if they are present in the charged form than in the neutral one. These findings are in direct consequence with the zwitterion character of these compounds and are additionally proved by independent NMR measurements. The obtained complexation characteristics were used as input data for Simul 5 Complex software to calculate and demonstrate the fundamental buffer properties in the dependence on the concentration of the neutral complexation agent (β-cyclodextrin) complexing with present buffer constituents. Practical impacts of this study, such as a shift of complexation constant, system peaks occurrences or even deterioration of separation, are consequently discussed in Part II of this series of papers.[30]

THEORY

If a weak electrolyte forms the complex with a neutral complexation agent, simultaneous dissociation and complexation equilibria have to be considered, as shown, *e.g.*, for weak acid HA in Scheme 1.

Scheme 1. Reaction scheme for simultaneous dissociation and complexation of a complexation agent and a weak electrolyte compound. C and HA represent the complexation agent and the weak electrolyte, respectively.

$$\begin{array}{ccc} & \xrightarrow{K_{HA}} & \\ HA + H_2O & \rightleftharpoons & H_3O^+ + A^- \\ + & & + \\ C & & C \\ K_{XAn} \downarrow\uparrow & & \downarrow\uparrow K_{XAc} \\ HAC + H_2O & \rightleftharpoons & H_3O^+ + AC^- \\ & \xrightarrow{K_{HAC}} & \end{array}$$

Each equilibrium is characterized by its individual complexation constant (K_{XAn}, K_{XAc} for the neutral or the charged form of the analyte, respectively) or dissociation constant (K_{HA}, K_{HAC})

$$K_{XAn} = \frac{[HAC]}{[HA][C]} \quad (1)$$

$$K_{XAc} = \frac{[AC^-]}{[A^-][C]} \quad (2)$$

$$K_{HA} = \frac{[H_3O^+][A^-]}{[HA]} \quad (3)$$

$$K_{HAC} = \frac{[H_3O^+][AC^-]}{[HAC]} = K_{HA} \cdot \frac{K_{XAc}}{K_{XAn}} \quad (4)$$

where [ ] stands for the equilibrium concentration of individual compounds. We use concentrations rather than activities and thus apparent rather than true thermodynamic equilibrium constants for simplicity without a loss of validity of the theory. However, the resulting values of apparent complexation constants can be corrected for actual ionic strength, as shown in our previous publication.[31]

Simultaneously, total (analytical) concentrations of the analyte and the complexation agent correspond to the sum of equilibrium concentrations of individual forms

$$c_{\mathrm{HA}} = [\mathrm{HA}] + [\mathrm{A}^-] + [\mathrm{AC}^-] + [\mathrm{HAC}] \quad (5)$$

$$c_{\mathrm{C}} = [\mathrm{C}] + [\mathrm{AC}^-] + [\mathrm{HAC}] \quad (6)$$

The complete set of these equations together with the electroneutrality condition, conductivity equation and the expression for ionic product of water (K_w) can be solved numerically using our simulation tool Simul 5 Complex[22-24] with the implemented complexation mode. Simul 5 also enables to apply ionic strength correction based on the Debye-Hückel equation with the linear term. Thus, the precise values of the pH, ionic strength and conductivity can be obtained by the software.

The pH is a fundamental property of the separation buffer solution. For this reason we also derived simplified analytical expressions for the pH of the interacting buffer. However, these equations are limited to buffers consisting of a weak acid or conjugate weak acid and a strong base at an acidic (eq 7) or alkaline (eq 8) pH region, respectively, where concentrations of hydroxide or hydroxonium ions can be neglected. Further, a sufficient excess of the amount of complexation agent is required, so the equilibrium concentration of the complexation agent can be approximated by its analytical (total) concentration.

$$[\mathrm{H_3O^+}] = \frac{-\left(K_{\mathrm{HA}} \cdot Z_A + [\mathrm{B^+}]\right) + \sqrt{\left(K_{\mathrm{HA}} \cdot Z_A - [\mathrm{B^+}]\right)^2 + 4 \cdot K_{\mathrm{HA}} \cdot c_{\mathrm{HA}} \cdot Z_A}}{2} \quad (7)$$

$$[\mathrm{H_3O^+}] = \\ = \frac{-\left(K_{\mathrm{HA}} \cdot \left([\mathrm{B^+}] - c_{\mathrm{HA}}\right) \cdot Z_A - K_w\right) + \sqrt{\left(K_{\mathrm{HA}} \cdot \left([\mathrm{B^+}] - c_{HA}\right) \cdot Z_A - K_w\right)^2 + 4 \cdot K_{\mathrm{HA}} \cdot K_w \cdot [\mathrm{B^+}] \cdot Z_A}}{2 \cdot [\mathrm{B^+}]} \quad (8)$$

where

$$Z_A = \frac{1 + K_{\mathrm{XAc}} \cdot c_{\mathrm{C}}}{1 + K_{\mathrm{XAn}} \cdot c_{\mathrm{C}}} \quad (9)$$

and $[\mathrm{B^+}]$ is the analytical concentration of the strong base utilized for buffer preparation. Analogous equations can be derived also for other buffer types, see Supporting Information S1. These equations (eqs 7, 8) are simple enough to make some general conclusions about behavior of such systems. The illustrative dependence of pH on the concentration of cyclodextrin and the buffer concentration plotted according to the eq 7 is shown in Supporting Information in Figure S1-1.

By comparison of these equations with those valid for systems without complexation, one can see that the complexation introduces the complexation induced pK_{A} shift of the weak acid by the factor of Z_A as shown already by Yoshida *et al.*[3] Thus the system behaves as if a weak acid with its apparent dissociation constant equal to $K_{\mathrm{HA}}^{app} = K_{\mathrm{HA}} Z_A$ was present and the complexation induced pK_{A} shift can be expressed as $\Delta pK_{\mathrm{HA}} = pK_{\mathrm{HA}}^{app} - pK_{\mathrm{HA}} = pZ_A$. Whether the complexation induced pK_{A} shift is negative or positive depends only on the ratio of complexation constants as resulted from eq 9. We especially emphasize that the dissociation constant of the weak acid in its complexed form (K_{HAC}) is not needed to calculate the pZ_A value, which is a consequence of eq 4. In our particular case of a buffer composed of a weak acid or conjugate

weak acid and a strong base, the acid becomes weaker ($pZ_A > 0$) as the complexation of the neutral form of the acid is preferred over the complexation of its charged form ($K_{\mathrm{XAn}} > K_{\mathrm{XAc}}$). This indeed results in a shift in pH of the buffer, which increases as the neutral form of the weak acid complexes stronger with the complexation agent than the charged one does and *vice versa*.

Notice that the complexation induced pK_{A} shift is changing gradually with increasing complexation agent concentration. At sufficiently high agent concentration (so that $\min\{K_{\mathrm{XAc}} \cdot c_{\mathrm{C}}; K_{\mathrm{XAn}} \cdot c_{\mathrm{C}}\} >> 1$) it effectively reaches its limit when $K_{\mathrm{HA}}^{app} = K_{\mathrm{HAC}}$ (see eq 4).

Therefore, at a high concentration of the complexation agent the pH converges to a certain value, which is the function of only the dissociation and complexation constants of weak acid and the initial concentration of buffer constituents. In other words a different buffer composed of a fully complexed weak electrolyte constituent with the shifted value of its dissociation constant (see eq 4) is formed. This indicates that one might estimate some fundamental complexation characteristics even from the very simple pH measurements.

MATERIALS AND METHODS

Chemicals. All chemicals were of analytical grade purity. Lithium hydroxide monohydrate, benzoic acid, [Tris(hydroxymethyl)methyl]glycine (Tricine) and acetic acid were purchased from Fluka (Steinheim, Germany). Formic acid was the product of Lachema (Brno, Czech Republic). 2-(*N*-morpholino)ethanesulfonic acid (MES), 3-morpholinopropane-1-sulfonic acid (MOPS), *N*-cyclohexyl-2-aminoethanesulfonic acid (CHES), 3-[[1,3-dihydroxy-2-(hydroxymethyl)propan-2-yl]amino]propane-1-sulfonic acid (TAPS), ethanolamine, sodium hydrogenphosphate and sodium dihydrogenphosphate were obtained from Sigma Aldrich (Steinheim, Germany). Neutral cyclodextrins (2-hydroxypropyl)-β-cyclodextrin (HP-β-CD) of 0.8 molar substitution and

average M_r = 1460, heptakis(2,6-di-O-methyl)-β-cyclodextrin (DM-β-CD), β-cyclodextrin (β-CD) and native α-CD all from Sigma Aldrich (Steinheim, Germany) were used as complexation agents. Water for solution preparation was deionised by the Watrex Ultrapur system (Prague, Czech Republic). Deuterated water (99.8% D) was obtained from Chemotrade, Leipzig, Germany.

Instrumentation. CE experiments were carried out by using the Agilent HP^{3D}CE capillary electrophoresis instrument operated by ChemStation software from Agilent Technologies (Waldbronn, Germany). Detection was performed with the built-in diode array detector (DAD) and the contactless conductivity detector (CCD) of our construction[32]. Uncoated fused silica capillaries with i.d. of 50 μm and o.d. of 375 μm (Polymicro Technologies, Phoenix, AZ, USA) were utilized for all electrophoretic experiments. CE measurements were performed at temperature 25°C, samples were injected hydrodynamically at 30 mbar × 3 s. New capillary was flushed with deionised water for 20 min and conditioned with actual running buffer prior to each run. All running buffers were filtrated with Minisart syringe filters (Sartorius Stedim Biotech, Goettingen, Germany), pore size 0.45 μm.

All the ^{1}H NMR data were recorded on Bruker Avance III 600 MHz spectrometer at 25ºC (temperature controlled by the manufacturer system) equipped with the cryogenically cooled TCI probe. Chemical shift was referenced according to the residual water signal set to the value of 4.700 ppm. The accuracy of the shift values was estimated to ±0.001 ppm from repeated experiments. Measurements of translational diffusion coefficients were performed with the double stimulated echo experiment with bipolar pulse field gradients described by Jerschow *et al.*.[33] This pulse sequence is optimized to suppress flow and convection artifacts as well as eddy current effects. The use of bipolar gradients removes the possible modulation of the intensity

decay curves by a chemical exchange occurring between the sites with different chemical shifts.[34] The gradients were 1 ms long with 16 different linearly spaced amplitudes spanning the range 1–59 G cm^{-1}, the diffusion time was 0.8 s, and 16 scans were acquired to complete the phase cycle. The calibration was done using a standard sample of 1% H_2O in D_2O (doped with $GdCl_3$) for which the value of the HDO diffusion coefficient at 25ºC is 1.9×10^{-9} m^2s^{-1}.[35] All data processing and fitting of the diffusion coefficients has been done using the spectrometer software (Topspin 2.1, Bruker) with the precision of the results estimated to 2%.

The PHM240 pH/ion meter (Radiometer, Copenhagen, Denmark) calibrated with standard IUPAC buffers, pH 1.679, pH 7.000, pH 10.012 and pH 12.450 (Radiometer Analytical, Lyon, France) was used for pH measurements.

CE measurements. A model buffer system was composed of benzoic acid (24 mM) as a weak electrolyte and lithium hydroxide (9.9 mM) as a corresponding strong base, pH 4.01. The complexation parameters of benzoic acid with β-CD were determined using ACE method. The complexation constant of the dissociated (charged) form, K_{XAc}, of benzoic acid was determined in the buffer at pH where it is fully dissociated, *i.e.*, Tricine/ LiOH buffer (19.41 mM/ 10 mM), pH = 8.13. The complexation constant of the non-dissociated (neutral) form of benzoic acid, K_{XAn}, was determined in acetic acid/ LiOH buffer (61 mM/ 9.9 mM), pH = 3.98. Ionic strength (IS) was always 10 mM. β-CD was dissolved directly in the running buffer, concentration range 0 to 10 mM. The corresponding sets of ACE measurements were performed also for CHES and Tricine compounds complexing with β-CD. The complexation constants of the charged form of CHES and Tricine were determined at pH where these compounds have deprotonized their amino groups and fully dissociated acidic groups, in Tricine/ LiOH buffer (4.0 mM/ 8.0 mM), pH = 11.57, IS = 7.96 mM, and acetic/ LiOH buffer (4.0 mM/ 8.0 mM), pH = 11.42, IS = 7.96

mM, respectively. The complexation constant of the neutral (zwitterionic) forms, K_{XAn}, were obtained in ethanolamine/ Tricine buffer (22 mM/ 8.1 mM), pH = 9.86, IS = 7.99 mM and phosphate/ LiOH buffer (8 mM/ 14.5mM), pH = 7.68, IS = 7.67 mM for CHES and Tricine, respectively. An additional set of measurements for the determination of the complexation constant of fully charged form of CHES was performed in Tricine/ LiOH buffer (35 mM/ 11 mM) pH = 12.17, IS = 34.0 mM. β-CD was dissolved directly in the running buffer, its concentration varied in the range of 0 – 10 mM.

NMR measurements. For NMR measurements the studied compounds (CHES, Tricine, MES, MOPS) were dissolved in deuterated water (99.8% D, Chemotrade, Leipzig) at the concentration of 2 mM. At these conditions these compounds are neutral. The samples of the charged forms were prepared by addition of NaOH. The pH was selected by means of PeakMaster 5.3 to achieve fully charged forms of all compounds. pH* measured by a classical glass pH electrode was 12.06. To achieve a neutral form of benzoic acid 8 mM HCl was added to its 2 mM solution. The host β-CD molecule was dissolved at various concentrations ranging from 0 to 10 mM in the final solutions of CHES and Tricine. The complexation constants were calculated from the dependence of the analyte diffusion coefficient on β-CD concentration. In the case of benzoic acid, MES and MOPS the diffusion coefficients were measured in cyclodextrin free solution and at 10 mM concentration of the host β-CD molecule.

Measurements of pH. All pH measurements were carried out using a combined pH electrode at ambient temperature (24 – 25°C). The pH measurements of buffers with and without complexation agents were conducted in short time intervals to eliminate changes of temperature or other external effects. CDs were always dissolved directly in the measured buffer and, if necessary, further diluted with the same buffer solution. The concentrations of β-CD in the

model system (24 mM benzoic acid/ 9.9 mM LiOH buffer) were 0; 0.1; 0.2; 0.5; 1; 2; 5; 8; 10 and 12 mM. All tested buffers were composed of 10.0 mM weak acid (acetic acid, formic acid, Tricine, TAPS, MOPS, MES or CHES), 5.0 mM LiOH and 10.0 ± 0.5 mM neutral CDs (α-CD, β-CD, DM-β-CD or HP-β-CD). The pH of the CHES buffer was measured in dependence on its concentration, concentration range 0.01 mM to 80 mM. β-CD was always dissolved directly in the buffer at concentration 10 mM. All measurements were performed in triplicates.

Software. Our simulation program Simul 5 Complex[22-24] with the implemented complete mathematical model of electromigration for separation systems with complexation agents was utilized to calculate buffer properties. The computer program PeakMaster 5.3[25,26] was used to optimize the composition of buffers for ACE and NMR measurements. The Simul 5 and PeakMaster software are available as freeware on our website.[36] The program Origin 8.1 (OriginLab Corporation, Northampton, MA, USA) and Microsoft Office Excel 2010 were used for data evaluation.

RESULTS AND DISCUSSION

The theoretical predictions were demonstrated experimentally on the model system: benzoic acid/ LiOH (24 mM/ 9.9 mM) buffer (pH = 4.01, IS = 10 mM) and a neutral β-CD. The pH of this buffer was measured at various concentrations of β-CD. The resulting dependence of the pH shift on the concentration of cyclodextrin (c_{CD}) is shown in Figure 1A. Clearly, pH increases significantly with the increasing concentration of the complexation agent. At 10 mM concentration of β-CD the pH shift was about 0.3 pH units. The increase of pH in this separation system should result from the higher complexation constant of the neutral (non-dissociated) form

of benzoic acid in comparison to the charged (dissociated) form as discussed in the section Theory.

To confirm this assumption, the complexation constants of the charged (dissociated) and neutral (non-dissociated) forms of benzoic acid were determined by ACE, where the dependence of the mobility of benzoic acid on the concentration of the complexation agent was measured at high pH (benzoic acid is fully charged) and low pH (where benzoic acid is only partially dissociated) regions. Obtained dependences were fitted by appropriate theoretical functions, see Supporting Information S2, eq S2-1 and eq S2-2, respectively. The dissociation constant of the resulting complex was calculated by eq 4. The determined complexation parameters of benzoic acid - β-CD complex for the actual ionic strength of 10 mM are $K_{XAn} = 460 \pm 20\ M^{-1}$; $K_{XAc} = 29 \pm 1\ M^{-1}$ (the error is presented as standard error of non-linear fitting); $K_{HAC} = 4.780 \times 10^{-6}$ M. The value of the dissociation constant of benzoic acid at this ionic strength is $K_{HA} = 7.638 \times 10^{-5}$ M. Clearly, the complexation constant of the neutral (non-dissociated) form is indeed more than 10 times higher than that of the charged (dissociated) one, which matches well with the significant positive pH shift.

Determined complexation parameters can be easily used as input data for simulations by Simul 5 Complex and calculations by means of eq 7 to propose the general behavior of this separation system even at those conditions, which are not obtainable experimentally due to the low solubility of β-CD. At first, the pH predicted by Simul 5 Complex was compared with the experimental data to confirm the correctness of the established model, see Figure 1A. Here a very good agreement of theoretical and experimental values was observed. Thus, the values of the pH, conductivity and ionic strength were calculated by Simul 5 for theoretical cyclodextrin concentration range of 0 − 1000 mM, see Figure 1B. All the calculated properties change

significantly with increasing concentration of β-CD, and pH clearly limits to the value of 5.17 as predicted by the theory (eq 7). This value corresponds to the pH of the buffer composed of resulting benzoic acid − β-CD complex, with dissociation constant K_{HAC} = 4.780×10^{-6} M, calculated by eq 4.

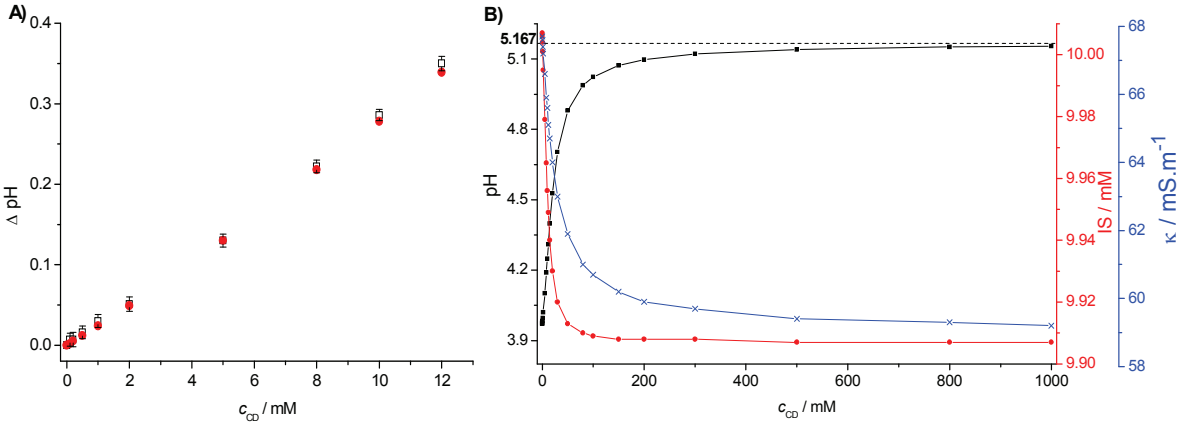

Figure 1. A) Comparison of dependences of Δ pH of 24 mM benzoic acid/ 9.9 mM LiOH buffer on β-CD concentration (c_{CD}) obtained from experiments (black transparent squares) and calculated by Simul 5 Complex (red solid circles). B) Dependence of pH (left axis, black squares), ionic strength (right axis, red circles) and conductivity (second right axis, blue crosses) of 24 mM benzoic acid/ 9.9 mM LiOH buffer on β-CD concentration calculated by Simul 5 Complex. Dashed line and highlighted value represent limiting values of pH calculated by eq 7.

Next, the pH shifts when adding the complexation agent were observed in commonly used buffers composed of weak acids (10 mM Tricine (pK_A = 8.15); 10 mM MES (pK_A = 6.09); 10 mM MOPS (pK_A = 7.20); 10 mM TAPS (pK_A = 8.30), 10 mM CHES (pK_A = 9.55); 10 mM acetic acid (pK_A = 4.76); 10 mM formic acid (pK_A = 3.75)) and a strong base 5 mM LiOH. pH

was measured in the pure buffer and at a 10 mM concentration of several neutral CDs. The resulting pH shifts are shown in Figure 2. Clearly, the biggest pH changes among common buffers tested were observed in the case of the CHES buffer for all cyclodextrins studied. Significant shifts were also found out for MOPS, MES buffers and for the acetic buffer after the addition of α-CD. The pH shifts in the other buffers were less pronounced.

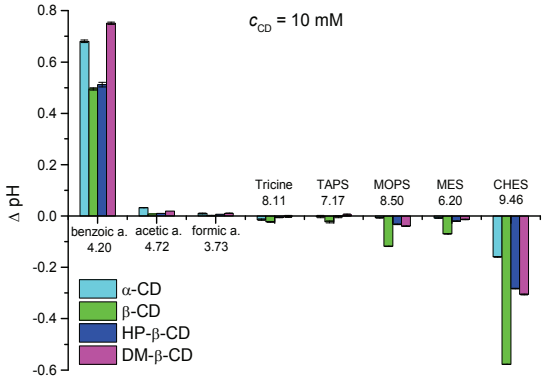

Figure 2. Shifts in pH (Δ pH) after addition of 10 ± 0.5 mM α-CD (cyan), β-CD (green), HP-β-CD (blue) or DM-β-CD (magenta) in six commonly used buffers and the model system (benzoate buffer). Groups of columns are marked by the name of the buffering compound and pH value of the original buffer (without addition of CD). Error bars represent standard deviation of the measured value.

The pH shifts, shown in Figure 2, point to an interesting consequence. While in the model system consisting of benzoic acid and LiOH, pH significantly increased with concentration of β-CD, in the case of common buffer constituents CHES, MES, MOPS, TAPS and Tricine, pH decreased when adding CDs. The increase of the pH of the benzoic acid buffer stems from the higher complexation constant of the neutral (non-dissociated) form than the charged

(dissociated) one, as discussed above. To the contrary, the decrease of the pH of common buffers in Figure 2 has to result from a higher value of the complexation constant of the charged form of the buffering constituent in comparison to the neutral one. This is the direct consequence of the zwitterionic character of these buffering compounds. CHES, MES, MOPS and TAPS are amino alkanesulfonic acids, and tricine is an amino alkanecarboxylic acid, so their buffering properties are based on the amonnium/amine dissociation equilibrium. It means that the molecule behaves as "neutral" at a low pH, where amino groups are protonated and sulfo (carboxyl) groups are dissociated. Consequently, protonation of the amino group hinders the inclusion of the molecule into the cavity and results in weaker complexation. In the "charged" state of these compounds only the sulfo (carboxyl) group is dissociated, which enables deeper inclusion and stronger complexation of the compound.

To confirm these findings we employed NMR measurements of translational diffusion coefficients of the buffer constituents. In the first run we compared those properties for the free analytes and in solutions with excess of β-CD, both in conditions with different pH: (i) in the alkaline solution of 8 mM NaOH where the buffering compounds are charged and (ii) in water where the electrolytes were virtually in the neutral form, in the case of benzoic acid in 8 mM HCl solution. The buffering compounds benzoic acid, CHES, MES, MOPS, and Tricine were always in 2 mM concentration and the complexation agent was at 10 mM concentration. The resulting NMR derived absolute values of translational diffusion coefficients, as summarized in Table 1, fully confirmed our hypothesis. The observed diffusion characteristics of the β-CD remained constant in all samples (D=2.4±0.1 $\times 10^{-10}$ m^2s^{-1} which compares well with 2.9×10^{-10} m^2s^{-1} determined in H_2O[37]) and it seems quite safe to assume that the complex behaves in the same way. It then becomes possible to estimate a fraction of the analyte bound in the complex, as

the apparent diffusion constant is a weighted average of the free and the bound form. The charged forms of (CHES, MOPS, MES and Tricine) always showed a higher degree of complexation after adding the β-CD compared to the neutral ones in contrast to benzoic acid, where the results were exactly opposite. The most profound effects of the cyclodextrin complexation of buffer constituents in common buffers were observed for CHES and benzoic acid, where also the pH shifts were the most significant, as the phenyl and cyclohexyl moieties include in the cyclodextrin cavity. The translational diffusion coefficient of the charged CHES molecule was very close to the value of β-CD, suggesting a tight complex. The same holds for the neutral form of benzoic acid. That is why we studied also the spatial proximity of the hydrogens of the two analytes to β-CD by means of the nuclear Overhauser effect in rotating frame (ROE) combined with selective excitation (excitation sculpting experiment[38]). Clear contacts were observed between the cyclohexyl and phenyl moieties and the 3 and 5 hydrogens from the inside of the β-CD cavity confirming their deep inclusion (for further details see Supporting Information S3).

The complexation is much weaker in the case of the MES and MOPS compounds. This is in agreement with the worse inclusion of morpholine moiety into the cyclodextrin cavity due to the presence of oxygen atom, which makes the morholine moiety less hydrophobic in comparison with cyclohexyl or phenyl groups[39]. Very weak complexation was observed also for Tricine whose polar character does not allow deep inclusion into the cavity.

Table 1. Diffusion coefficients of charged (C^-) and neutral (N) forms of buffer constituents in cyclodextrin free solution (D_A) and at a 10 mM concentration of β-CD (D_C); ratio $\frac{D_A - D_C}{D_A - D_{ACD}}100$ corresponds to the fraction of the complexed analyte, where D_{ACD} is the diffusion coefficient of the complex, which was approximated by the diffusion coefficient of free CD $D_{ACD} = 2.4 10^{-10}$ $m^2 s^{-1}$

	benzoic acid		CHES		MOPS		MES		Tricine	
	N	C^-	N	C^-	N	C^-	N	C^-	N	C^-
D_A / 10^{-10} $m^2 s^{-1}$	7.20	6.57	5.21	4.83	5.42	5.17	6.13	5.45	5.26	5.14
D_C / 10^{-10} $m^2 s^{-1}$	3.23	5.77	4.74	2.76	5.42	4.48	6.08	4.67	5.09	4.81
$\frac{D_A - D_C}{D_A - D_{ACD}}100$	83%	19%	17%	85%	0%	25%	1%	26%	6%	12%

Determination of the complexation constants of CHES with β-CD both by NMR and ACE techniques. For a mutual comparison with benzoic acid we observed the complexation constants of CHES and Tricine, the most and least complexing buffer constituents, respectively, with β-CD both by NMR and ACE techniques. Both the diffusion coefficients derived from the NMR measurements and the effective mobilities of CHES resulting from ACE were measured as a function of cyclodextrin concentration.

The ACE measurements were performed at pH 11.57 and 9.86 in order to determine the complexation constant of the charged and neutral form of CHES, respectively. Unfortunately the dissociation of β-CD at high a pH (the pK_A of cyclodextrin is about 12.20) brings additional complexity to the system. At the high pH a part of cyclodextrin becomes negatively charged. Complexation of the charged form of cyclodextrin with CHES is assumed to be negligible due to

electrostatic repulsion, therefore the concentration of β-CD must be corrected to obtain the concentration of the neutral form of β-CD in the buffer. This correction was done by PeakMaster 5.3 software, which allows the calculation of the concentrations of the individual dissociation forms of each buffer constituent. Such corrected concentrations of the non-dissociated (neutral) form of cyclodextrin were used for data evaluation in the ACE measurements. The plausibility of corrections was proved by ACE measurements at higher pH of 12.17, where β-CD is dissociated to different extent. The appropriate fitting functions for data evaluation are described in the Supporting Information S2. The measurements at different pH values provided the same values of the complexation constant in the range of experimental error.

In the NMR study the diffusion coefficients of CHES were measured for dependence on the concentration of cyclodextrin. The complexation constant of the charged form of CHES was measured in the 2 mM solution of CHES with 8 mM NaOH added and that of the neutral form was measured in a 2 mM deutered water solution of CHES. Analogous corrections due to the dissociation of β-CD were performed as in the ACE measurements. However, *pK*a of β-CD in D_2O is much higher, 13.66, so this correction was much smaller.[40]

Both NMR and ACE techniques provided similar values of complexation constants. The complexation constant of the charged form of CHES with β-CD determined by ACE and NMR were 440 ± 30 M^{-1} and 360 ± 30 M^{-1} (the error is presented as standard error of non-linear fitting), respectively. Unfortunately, the complexation constant of the neutral form of CHES could not be determined with a sufficient precision by any method, as its value is certainly very small. For the purpose of simulations the complexation constant of the neutral form was estimated as 30 M^{-1}. For more details regarding the determination of the complexation constants by ACE and NMR see Supporting Information S2. Clearly, the complexation constants are in the

same range as those of benzoic acid, but there are opposite as regards to the complexation of the charged and neutral form. This fully agrees with the similar value of the pH shift of these two compounds only in opposite direction (ΔpH (CHES) = □0.58, ΔpH (benzoic acid) = 0.50), see Figure 2.

The same sets of NMR and ACE measurements were performed for the Tricine compound. However, both techniques showed that the complexation of Tricine and β-CD is negligible, and the values of complexation constants cannot be evaluated. This result is in agreement with the very small pH deviations observed for the Tricine buffer (ΔpH (Tricine) = - 0.02).

Impact of buffer concentration on pH shifts. Determined values of complexation constants can be again used as input parameters for calculations in the Simul 5 Complex to predict the general properties of the buffer systems. This was already shown for the dependence of pH, IS and conductivity on the concentration of the complexation agent in the model benzoic acid buffer, see Figure 1B. The complexation constants determined for interaction of CHES with β-CD were used to calculate how the pH is influenced when the 10 mM solution of β-CD is added to the CHES/ LiOH buffer (ratio of CHES and LiOH concentration was kept constant 2:1) of different concentrations. For comparison, we also calculated the pH of the cyclodextrin free CHES/ LiOH buffer at gradually increasing concentration. Both dependences are shown in Figure 3. In the same figure we also show experimentally measured values of pH. A very good agreement of the experimental and calculated values is clear.[†]

It is worth noting that at a high concentration of the buffer, the pH difference between the pure buffer and the buffer containing 10mM β-CD diminishes and limits to zero, while at a low

[†]Such measurements are not obtainable in a benzoic acid buffer due to its low solubility, for this reason a CHES buffer was used for this demonstration.

concentration the pH difference was almost 1 pH unit. This is expectable because at a high concentration of the buffer the concentration of CD is insufficient to complex a significant part of CHES, and pH cannot be significantly influenced.

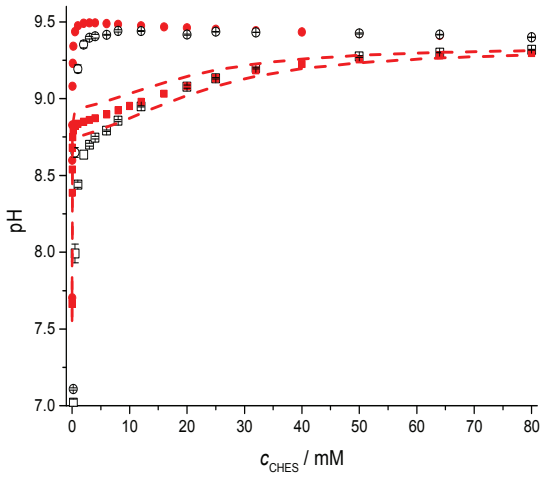

Figure 3. Dependence of pH on concentration of CHES buffer, the ratio of CHES and LiOH was kept constant at 2:1. Circles and squares symbols represent data for the cyclodextrin free solution and at a 10 mM concentration of β-CD, respectively. Solid red symbols are simulated data (K_{XAc}=440 M^{-1}, K_{XAn}=30 M^{-1}), transparent black symbols are experimental data. Red dashed lines represent the confidence interval taking into account the error of estimate of the determination of complexation constants: the upper curve (K_{XAc}=410 M^{-1}, K_{XAn}=70 M^{-1}) and the lower curve (K_{XAc}=470 M^{-1}, K_{XAn}=1 10^{-3} M^{-1}).

In summary, the complexation of buffer constituents with the complexation agent added to the buffer can significantly influence its pH and other important properties such as IS or conductivity. The pH of the complexing buffer depends not only on the concentration of complexation agent but also on the type of buffer and concentration of buffer constituents.

CONCLUDING REMARKS

Complexation of buffer constituents with a complexation agent present in the buffer, even if the complexation agent is neutral, can severely influence the buffer properties. This results to a shift in pH, ionic strength and conductivity, which can significantly affect the CE or HPLC separations when such buffers are used as background electrolytes or present in mobile phases. This is demonstrated for CE in Part II of this series of papers. Herein, we propose a theory of this phenomenon and show that is in good agreement with experimental results.

We revealed that some common chemicals used for preparation of buffers, such as CHES, MES and MOPS form complexes with β-cyclodextrin. The complexation is much stronger with the charged forms of the buffer constituents when compared to their neutral forms due to their characteristic zwitterion behavior. This fact was further proved by NMR measurements. We determined the complexation constants of β-cyclodextrin with both the charged and neutral form of benzoic acid and CHES, which were consequently used as input data for simulations. Simulation program Simul 5 Complex was shown to be a precise tool for the prediction of behavior of complexing buffer systems. Clearly, but against the contemporary usual practice, the pH of the buffer should always be controlled after the addition of the complexation agent (even a neutral chiral selector) to reveal a possible complexation with the constituents of the buffer.

ASSOCIATED CONTENT

Supporting Information. Additional information as noted in text. This material is available free of charge via the Internet at http://pubs.acs.org.

ACKNOWLEDGMENT

The support of the Grant Agency of the Czech Republic, Grant No.13-01440S, Grant Agency of Charles University, Grant No. 323611 and Grant No. 570213, and the long-term research plan of the Ministry of Education of the Czech Republic (MSM0021620857), are gratefully acknowledged.

ABBREVIATIONS

ACE, affinity capillary electrophoresis, BGE, background electrolyte, CCD, contactless conductivity detector, CD, cyclodextrin, CE, capillary electrophoresis, CHES, *N*-cyclohexyl-2-aminoethanesulfonic acid, DAD, diode array detector, DM-β-CD, heptakis(2,6-di-*O*-methyl)-β-cyclodextrin, HP-β-CD, (2-hydroxypropyl)-β-cyclodextrin, IS, ionic strength, MES, 2-(*N*-morpholino)ethanesulfonic acid, MOPS, 3-morpholinopropane-1-sulfonic acid, TAPS, 3-[[1,3-dihydroxy-2-(hydroxymethyl)propan-2-yl]amino]propane-1-sulfonic acid, Tricine, [Tris(hydroxymethyl)methyl]glycine

REFERENCES

(1) Singh, M.K.; Pal, H.; Ainavarapu, R.K.; Sapre, A.V. *J. Phys. Chem. A* **2004**, *108*, 1465-1474.

(2) Lelievre, F.; Gareil, P.; Jardy, A. *Anal. Chem.* **1997**, *69*, 385-392.

(3) Yoshida, N.;.Seiyama, A.; Fujimoto, M. *J. Phys. Chem.* **1990**, *94*, 4254-4259.

(4) Marquez, C.; Nau, W.M. *Angew. Chem., Int. Ed.* **2001**, *40*, 3155-3160.

(5) Mohanty, J.;.Bhasikuttan, A.C.; Nau, W.M.; Pal, H. *J. Phys. Chem. B* **2006**, *110*, 5132-5138.

(6) Eftink, M.R.;.Andy, M.L.; Bystrom, K.; Perlmutter, H.D.; Kristol, D.S. *J. Am. Chem. Soc.* **1989**, *111*, 6765-6772.

(7) Gelb, R.I.;.Schwartz, L.M.; Cardelino, B.; Fuhrman, H.S.; Johnson, R.F.; Laufer, D.A. *J. Am. Chem. Soc.* **1981**, *103*, 1750-1757.

(8) Gelb, R.I.; Schwartz, L.M.; Johnson, R.F.; Laufer, D.A. *J. Am. Chem. Soc.* **1979**, *101*, 1869-1874.

(9) Zhang, X.Y.; Gramlich, G.; Wang, X.J.; Nau, W.M. *J. Am. Chem. Soc.* **2002**, *124*, 254-263.

(10) Righetti, P.G.;Ettori, C.; Chafey, P; Wahrmann, J.P. *Electrophoresis* **1990**, *11*, 1-4.

(11) Hammitzsch-Wiedemann, M.; Scriba, G.K.E. *Electrophoresis* **2007**, *28*, 2619-2628.

(12) Rizzi, A.M.; Kremser, L. *Electrophoresis* **1999**, *20*, 2715-2722.

(13) Schwartz, L.M.; Gelb, R.I. *Anal. Chem.* **1978**, *50*, 1571-1576.

(14) Fielding, L. *Prog. Nucl. Magn. Reson. Spectrosc.* **2007**, *51*, 219-242.

(15) Fielding, L. *Tetrahedron* **2000**, *56*, 6151-6170.

(16) Dvorak, M.; Svobodova, J.; Benes, M.; Gas, B. *Electrophoresis* **2013**, *34*, 761-767.

(17) Uselova-Vcelakova, K.; Zuskova, I.; Gas, B. *Electrophoresis* **2007**, *28*, 2145-2152.

(18) Rundlett, K.L.; Armstrong, D.W. *Electrophoresis* **2001**, *22*, 1419-1427.

(19) Jiang, C.X.; Armstrong, D.W. *Electrophoresis* **2010**, *31*, 17-27.

(20) Busch, M.H.A.; Carels, L.B.; Boelens, H.F. M.; Kraak, J.C.; Poppe, H. *J. Chromatogr., A* **1997**, *777*, 311-328.

(21) Hruska, V.; Jaros, M.; Gas, B. *Electrophoresis* **2006**, *27*, 984-991.

(22) Svobodova, J.; Benes, M.; Dubsky, P.; Vigh, G.; Gas, B. *Electrophoresis* **2012**, *33*, 3012-3020.

(23) Svobodova, J.;Benes, M.; Hruska, V.; Uselova, K.; Gas, B. *Electrophoresis* **2012**, *33*, 948-957.

(24) Hruska, V.; Benes, M.; Svobodova, J.; Zuskova, I.; Gas, B. *Electrophoresis* **2012**, *33*, 938-947.

(25) Hruska, V.;Svobodova, J.; Benes, M.; Gas, B. *J. Chromatogr., A* **2012**, *1267*, 102-108.

(26) Benes, M.; Svobodova, J.; Hruska, V.; Dvorak, M.; Zuskova, I.; Gas, B. *J. Chromatogr., A***2012**, *1267*, 109-115.

(27) Gas, B.;Jaros, M.; Hruska, V.; Zuskova, I.; Stedry, M. *LC·GC Eur.* **2005**, *18*, 282-+

(28) Fang, L.; Yin, X. B.; Wang, E. *Anal. Lett.* **2007,***40*, 3457-3471.

(29) Chen, Y. R.; Ju, D. D.; Her, G. R. *J. High Resolut. Chromatogr.* **2000,***23*, 409-412.

(30) Benes, M.; Riesova, M.; Svobodova, J.; Tesarova, E.; Dubsky, P.; Gas, B., Part II of this series of papers, submitted to *Anal. Chem.*

(31) Benes, M.;Zuskova, I.; Svobodova, J.; Gas, B. *Electrophoresis* **2012**, *33*, 1032-1039.

(32) Gas, B.; Zuska, J.; Coufal, P.; van de Goor, T. *Electrophoresis* **2002**, *23*, 3520-3527.

(33) Jerschow, A.; Muller, N. *J. Magn. Reson.* **1997**, *125*, 372-375

(34) Johnson, C. S. *Prog. Nucl. Magn. Reson. Spectrosc.* **1999**, *34*, 203-256.

(35) Longsworth, L.G. *J. Phys. Chem.* **1960**, *64*, 1914-1917.

(36) echmet.natur.cuni.cz

(37) Pavlov, G.M.; Korneeva, E.V.; Smolina, N.A.; Schubert, U.S. *Eur. Biophys. J.* **2010**, *39*, 371-379.

(38) Stonehouse, J.; Adell, P.; Keeler, J.; Shaka, A.J. *J. Am. Chem. Soc* **1994**, 116, 6037

(39) Meo, P.I.;D´Anna, F.; Riela, S.;Gryttaduria, M.; Noto, M. *Org. Biomol Chem.* **2003**, 1, 1584-1590.

(40) Maeztu, R.; Tardajos, G.; Gonzalez-Gaitano, G. *J. Inclusion Phenom. Macrocyclic Chem.* **2011**, *69*, 361-367.

For TOC only:

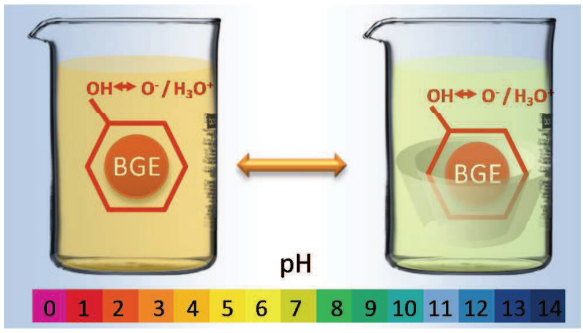

Publikace 5

Complexation of buffer constituents with neutral complexation agents: Part II. Practical impact in capillary zone electrophoresis

*M. Beneš, **M. Riesová**, J. Svobodová**,** E. Tesařová,P. Dubský, B. Gaš*

Analytical Chemistry

Complexation of buffer constituents with neutral complexation agents: Part II. Practical impact in capillary zone electrophoresis

Journal:	*Analytical Chemistry*
Manuscript ID:	ac-2013-01381d.R1
Manuscript Type:	Article
Date Submitted by the Author:	n/a
Complete List of Authors:	Benes, Martin; Charles University, Faculty of Science, Department of Physical Chemistry Riesova, Martina; PrF UK, Prague, Svobodova, Jana; Charles University in Prague, Department of Physical and Macromolecular Chemistry Tesarova, Eva; Faculty of Science, Dept. of Physical & Macromolecular Chem. Dubsky, Pavel; Charles University, Faculty of Science, Department of Physical Chemistry Gas, Bohuslav; Charles University, Faculty of Science, Department of Physical Chemistry

Complexation of buffer constituents with neutral complexation agents: Part II. Practical impact in capillary zone electrophoresis

Martin Beneš, Martina Riesová, Jana Svobodová, Eva Tesařová, Pavel Dubský, Bohuslav Gaš*

Charles University in Prague, Faculty of Science, Department of Physical and Macromolecular Chemistry, Prague, Czech Republic

* Corresponding Author

E-mail: svobod.j@seznam.cz

Phone: +420-2-2195-1399

Fax: +420-2-2491-9752

complexation constant, affinity capillary electrophoresis, buffer, simulations, neutral cyclodextrins

ABSTRACT

This paper elucidates the practical impact of the complexation of buffer constituents with complexation agents on electrophoretic results, namely complexation constant determination,

system peak development and proper separation of analytes. Several common buffers, which were selected based on the pH study in Part I of this paper series (*e.g.* CHES, MES, MOPS, Tricine), were used to demonstrate behavior of such complex separation systems. We show that the value of a complexation constant determined in the interacting buffers environment depends not only on the analyte and complexation agent but it is also substantially affected by the type and concentration of buffer constituents. As the result, the complexation parameters determined in the interacting buffers cannot be regarded as thermodynamic ones and may provide misleading information about the strength of complexation of the compound of interest. We also demonstrate that the development of system peaks in interacting buffer systems significantly differs from the behavior known for non-complexing systems, as the mobility of system peaks depends on the concentration and type of neutral complexation agent. Finally, we show that the use of interacting buffers can totally ruin the results of electrophoretic separation because the buffer properties change as the consequence of the buffer constituents' complexation. As a general conclusion, the interaction of buffer constituents with the complexation agent should always be considered in any method development procedures.

INTRODUCTION

Capillary electrophoresis (CE) is a widely employed separation technique. It offers many useful modifications that make use of the presence of complexation agents in background electrolyte (BGE). This so called pseudostationary phase brings beneficial interaction possibilities, which are traditionally utilized to increase separation efficiency, to achieve enantioseparation or to change the migration order of analytes. Additionally, the fact that

interactions between analytes and complexation agents are reflected in changes of electrophoretic behavior of the respective compounds can be advantageously used to determine complexation constants or for other studies of non-covalent binding in chemistry or biology.

Utilization of complexation agents, most frequently chiral selectors, has widely expanded within the last two decades.[1] For this reason, several attempts were made to describe electrophoretic separation with complexation agents theoretically, and, based on the theory, propose optimization approaches, which would help to save separation time and costs. In 1992 Wren and Rowe[2] presented a theoretical model of the separation of fully charged analytes with neutral chiral selectors. This model was later extended by Rawjee and Vigh[3,4] for weak electrolyte analytes. Based on these theoretical models several objective functions (*e.g.* selectivity, difference in mobilities or resolution) were used for optimizing the separation conditions. However, the authors admitted that for a correct and complete description of such complex separation systems a numerical simulation would be necessary.[5 - 11] In 2012 Hruska *et al.*[12] and Breadmore *et al.*[13] presented a complete theoretical model of electromigration for separation systems with complexation agents. These models were successfully implemented into new versions of simulation programs Simul 5 Complex[14] and GENTRANS, respectively. Simul 5 Complex was shown to provide deep insight into electrophoretic separation in systems with complexation agents and can be used to explain different unexpected phenomena. We used Simul 5 Complex to explain the development of electromigration dispersion (EMD), [15,16] which is responsible for the deterioration of the analyte peaks' shape. The results showed that EMD can be directly related to complexation. An alternative to numerical simulation is the linearized theory of electromigration, which was introduced by Poppe[17] and was extensively developed in our group[18] and implemented in the PeakMaster software[19]. The most important outcome of this

theory is the fundamental understanding of the development of so called system peaks. The system peaks appear as perturbations in the BGE concentration profile travelling through the system independently of the very presence of any analyte. Currently the PeakMaster software was extended for complexing systems with neutral complexation agents complexing with one fully charged analyte[20]. Both software programs are freeware and can be downloaded from our webpage[14].

The complexation of analyte(s) with complexation agent(s) is described in detail in the literature nowadays. However, possible changes of the BGE properties due to the complexation of buffer constituents with the complexation agent are mentioned rarely. Rawjee *et al.*[21] utilized the complexation of buffer constituent with complexation agents to affect the electrophoretic mobility of the co-ion in order to minimize electromigration dispersion of the analyte. Chen *et al.*[22] observed system peaks originating from the interaction of neutral α-, β- and γ-cyclodextrins with *N*-cyclohexyl-2-aminoethanesulfonic acid (CHES) buffer during the cyclodextrin (CD) assisted separation of underivatized gangliosides. Fang *et al.*[23] noticed the induction of an additional peak registered by electrochemiluminescence detection when sulfated β-cyclodextrin and acetonitrile were simultaneously present in BGE. They attributed the presence of the induced peak to the physical interaction between CD and acetonitrile. Potential changes of the basic buffer properties, such as pH or ionic strength that can appear after the addition of a neutral complexation agent are considered rarely. Just a few authors proposed to control the pH of the buffer after the addition of a ligand.[24] The theoretical description of the interaction of buffer constituents with a complexation agent as regards to the fundamental properties of the buffer was proposed in Part I of this series of papers.[25]

Complexation constants and the mobilities of complexes of various compounds as determined by CE can be further used as input data for prediction models or simulation programs. The overview of existing methods and their limitations can be found in several review papers.[26 - 28] The most commonly used technique is affinity capillary electrophoresis (ACE), where the effective mobility of the injected analyte is determined depending on the concentration of the complexation agent dissolved directly in the running buffer. Complexation parameters are evaluated by the fitting of the obtained dependence with an appropriate fitting function. This method relies on constant and precise experimental conditions, and suitable corrections for ionic strength (IS), viscosity or temperature have to be applied to obtain thermodynamic complexation constants as shown in our previous paper.[29]

The aim of this work is to demonstrate, by means of simulations and experiments, the practical impact of the interaction of buffer constituents with the complexation agent on the electrophoretic separation and determination of complexation constants by CE. Several interacting buffers were selected based on the results shown in Part I of this series of papers.[25] The influence of the interaction is demonstrated to determine the complexation constants of fully charged as well as neutral analytes by ACE. The dependence of the resulting value of the complexation constant on the type and concentration of the running buffer is revealed. We also demonstrate the effect of interaction of BGE constituents on the development of system peaks, which clearly differs from their behavior as explained by the linearized theory of electromigration[18] for non-complexing systems. Finally, the influence of the complexation on the results of electrophoretic separation is discussed.

MATERIALS AND METHODS

Chemicals. All chemicals were of analytical grade purity. Lithium hydroxide monohydrate, benzoic acid, [Tris(hydroxymethyl)methyl]glycine (Tricine) and acetic acid were purchased from Fluka (Steinheim, Germany). Hydrochloric acid and maleic acid were products of Lachema (Brno, Czech Republic). 2-(*N*-morpholino)ethanesulfonic acid (MES), 3-morpholinopropane-1-sulfonic acid (MOPS), *N*-cyclohexyl-2-aminoethanesulfonic acid (CHES), 3-[[1,3-dihydroxy-2-(hydroxymethyl)propan-2-yl]amino]propane-1-sulfonic acid (TAPS) and Tri(hydroxymethyl)aminomethane (Tris), ethanolamine, sodium hydrogenphosphate, sodium dihydrogenphosphate, ammonium hydroxide solution, (*R*)-(-)-2-fluoro-α-methyl-4-biphenylacetic acid (*R*-flurbiprofen, *R*-FLU), dimethylsulfoxide (DMSO), glycine, L-leucine, L-glutamine, L-serin, and L-asparagine were obtained from Sigma Aldrich (Steinheim, Germany). Neutral cyclodextrins (2-hydroxypropyl)-β-cyclodextrin (HP-β-CD) of 0.8 molar substitution and average M_r = 1460, heptakis(2,6-di-*O*-methyl)-β-cyclodextrin (DM-β-CD), β-cyclodextrin (β-CD) and native α-cyclodextrin all from Sigma Aldrich (Steinheim, Germany), were used as complexation agents. Water for solution preparation was deionised by the WatrexUltrapur system (Prague, Czech Republic).

Instrumentation. All experiments were performed using Agilent $3D^{CE}$ capillary electrophoresis equipment operated under ChemStation software (Agilent Technologies, Waldbronn, Germany) control. Fused silica capillaries (50 μm i.d., 375 μm o.d.) were provided by Polymicro Technologies (Phoenix, AZ, USA). The experiments were performed in a bare fused silica capillary with a total length and effective length to the detector (diode array detector (DAD)/ contactless conductivity detector (CCD)) of approximately 50.0 cm and 41.5/34.5 cm, respectively. The PHM 220 instrument (Radiometer, Copenhagen, Denmark) calibrated with

standard IUPAC buffers, pH 1.679, pH 7.000, pH 10.012 and pH 12.450 (Lyon, France) was used for pH measurements.

Experimental conditions. Running voltage and parameters of the capillaries were chosen to keep the electric current low (the current was always lower than 33 μA), and thus to avoid the effects of excessive Joule heating. New capillaries were flushed with deionised water for 20 min and 3 min with actual BGE before each experiment. The operating temperature was always 25 °C. All running buffers were filtrated with Minisart syringe filters (Sartorius Stedim Biotech, Goettingen, Germany), pore size 0.45 μm. Every measurement was repeated four times. All analyte or system peaks were fitted by Haarhoff-van der Linde (HVL) function[30, 31] to eliminate the effect of electromigration dispersion on migration time.

Determining complexation constants in interacting buffers by ACE. The composition and parameters of the running BGE used for ACE measurements of the fully charged form of *R*-FLU are summarized in Table 1. Complexation constant of the neutral form of *R*-FLU was determined in 61.0 mM acetic acid/ 9.9 mM LiOH and 24.9 mM benzoic acid/ 9.9 mM LiOH buffer, both pH 3.98 and IS = 10 mM. The chiral selector β-CD, concentration range 0 mM to 10 mM, was dissolved directly in the running buffers. The injected sample was 0.3 mM *R*-FLU and 0.15 mM DMSO, which served as the electroosmotic flow (EOF) marker, and both were dissolved directly in the running buffer. For determination of the mobility of β-CD interacting with buffer constituents, β-CD was injected as the sample at concentration 0.3 mM, 0.15 mM DMSO again as EOF marker. Detection was performed with the DAD at the wavelength of 214 nm. The samples were injected hydrodynamically for 100 mbar×s. The total capillary length (L_{tot}) and the length to DAD (L_{DAD}) were 49.75 cm and 41.25 cm, respectively. The applied voltage was 20 kV (cathode at the detector side).

Impact of buffer complexation on development of system peaks. The BGE of the model system contained 5.0 mM benzoic acid, 2.5 mM LiOH, IS 2.57 mM; pH 4.20. HP-β-CD was dissolved directly in the running buffer in a concentration range of 0 – 40 mM. Samples contained neither analyte nor an EOF marker; only disturbed BGE was injected to generate system peaks. Compositions of the disturbances at the particular HP-β-CD concentration are summarized in Table 2. Composition of the sample injected into the buffer without HP-β-CD was designed by PeakMaster 5.3 in order to obtain convenient shapes, polarities and amplitudes of system peaks. As the complexation model is not included in PeakMaster 5.3, disturbances of BGEs containing HP-β-CD were optimized experimentally to keep similar shapes and polarity of system peaks. The driving voltage was 20 kV (cathode at the detector site). The L_{tot} and the L_{DAD} were 48.7 cm and 40.2 cm, respectively. Indirect UV detection of system zones was performed by DAD at the wavelength 200 nm. System peak investigation was performed in the same common buffers (10 mM weak acid - MES, MOPS, CHES, Tricine, acetate and 5 mM LiOH) as in the pH measurements in Part I of this series of papers. The concentration of various neutral cyclodextrins in BGEs used for electrophoretic measurements was approximately 5 mM. All samples were composed of 11.0 mM weak acid (*i.e.* + 10% of buffering compound against the BGE composition) and 5.0 mM LiOH. This sample composition was designed by PeakMaster 5.3 software to induce system zones with suitable shapes and amplitudes. The samples were injected hydrodynamically for 90 mbar×s. Conductivity detection was performed because of the absence of UV absorbing chromophore in the majority of the tested buffers. The L_{tot} of the capillaries and the length to CCD (L_{CCD}) were always 49.8 cm and 35.0 cm, respectively. Driving voltages were 25 kV for the acetate buffer, 20 kV for the Tricine buffer and 10 kV for the MOPS, MES and CHES buffers, always with the cathode at the detector side.

Table 1. Composition, concentrations of the constituents (*c*), pH and ionic strength (IS) of the running buffers for determining the complexation constants of *R*-FLU. D: diluted buffer.

Buffer constituents	CHES / LiOH	D: CHES / LiOH	MOPS / LiOH	D: MOPS / LiOH	MES / LiOH	D: MES / LiOH
c / mM	50/25.76	10/5.15	50/25.76	10/5.15	50/25.76	10/5.15
IS / mM	25.76	5.15	25.76	5.15	25.76	5.15
pH	9.51	9.54	7.16	7.19	6.06	6.09
Buffer constituents	Tricine / LiOH	D: Tricine / LiOH	phosphoric acid / NaOH	maleic acid / LiOH	NH_3 / HCl	ethanolamine / HCl
c / mM	50/25.76	10/5.15	11/18	12/19	36/25.76	50/25.76
IS / mM	25.76	5.15	25.0	26.0	25.76	25.76
pH	8.11	8.14	7.27	6.18	8.91	9.53

Table 2. Composition of the samples/disturbances studied in electrophoretic experiments. Model system composition: 5.0 mM benzoic acid, 2.5 mM LiOH and 0 – 40 mM HP-β-CD.

BGE	Sample/disturbance composition		
$\frac{c_{\text{HP-β-CD}}}{\text{mM}}$	$\frac{c_{\text{benzoic acid}}}{\text{mM}}$	$\frac{c_{\text{LiOH}}}{\text{mM}}$	$\frac{c_{\text{HP-β-CD}}}{\text{mM}}$
0.0	4.0	0.0	0.0
5.0	2.5	0.0	6.0
10	0.0	0.0	11
20	0.0	0.0	21
30	0.0	0.0	31
40	0.0	0.0	41

Influence of interaction of buffer constituents on result of electrophoretic separation. A set of amino acids was separated in 10 mM ethanolamine/ 5 mM HCl and 10 mM CHES/ 5 mM LiOH buffers, both pH 9.41 and IS 5 mM. The experiments were performed either in a pure buffer or at a 10 mM concentration of β-CD, which was dissolved directly in the buffer. The sample was composed of a mixture of 5 amino acids (1 mM Leu, 1 mM Gly, 1 mM Gln, 1 mM Asn, 1 mM Ser). The samples were injected hydrodynamically for 90 mbar×s. The L_{tot} of the capillary and L_{CCD} were always 49.3 cm and 34.5 cm, respectively. Applied voltage was 8 kV, with the cathode at the detector side.

Software. Our simulation program Simul 5 Complex[16] with an implemented complete mathematical model of electromigration for the separation systems with complexation agents was utilized for simulations of experimental electropherograms and for determining background electrolyte properties. The computer program PeakMaster[19] was used to optimize the composition of BGEs. The new version of this software, PeakMaster 5.3[32,33], which is able to predict shapes and amplitudes of system peaks, was employed to design suitable disturbance in order to induce system peaks with convenient polarity and amplitude. The Simul 5 Complex and PeakMaster 5.3 software are available as freeware at our website.[14] The program Origin 8.1 (OriginLab Corporation, Northampton, MA, USA) and Microsoft Office Excel 2003 were used for data evaluation.

RESULTS AND DISCUSSION

As shown in Part I[25] of this series of papers an interaction of buffer constituents with the complexation agent seriously influences buffer properties. However, the complexation of buffer constituents might have other practical consequences *e.g.* they might play a role in the

determination of physical-chemical parameters of compounds, if incorrectly considered, or have a significant impact on electrophoretic separations in general. In this paper we will focus on three major points:

1. Determination of complexation constants in interacting buffers by ACE;
2. Impact of buffer complexation on the development of system peaks;
3. Influence of the interaction of buffer constituents on the results of electrophoretic separation.

Based on the pH and NMR study presented in Part I of this series we selected suitable buffers to demonstrate the influence of the interaction of buffer constituents with the complexation agent. The MES/ LiOH, MOPS/ LiOH and CHES/ LiOH buffers were used as the interacting buffer systems, while Tricine/ LiOH was suggested as a non-interacting one.

1. Determination of complexation constants in interacting buffers

System of fully charged analyte and neutral complexation agent. At first we focused on the determination of the complexation constants of a fully charged analyte and a neutral complexation agent. The typical setup for determining the complexation constants by ACE is that the complexation agent is dissolved directly in the BGE and the analyte is injected as the sample. The effective mobility of an analyte is measured depending on the concentration of the complexation agent and the resulting data are fitted by the following function

$$u_{\mathrm{A}}^{\mathrm{eff}} = \frac{u_{\mathrm{A}} + u_{\mathrm{AC}} K_{\mathrm{XAc}}[\mathrm{C}]}{1 + K_{\mathrm{XAc}}[\mathrm{C}]} \qquad (1)$$

where K_{XAc} is the complexation constant of the charged analyte, u_{A}, and u_{AC} are the mobilities of the free analyte and the complex, respectively. [C] is the equilibrium concentration of the

complexation agent. The equilibrium concentration can be substituted by an analytical one, if the exact position that the analyte peak would have at virtually infinite dilution is known. This position can be determined by fitting the analyte peak with the HVL function.[30,31] However, if a buffer constituent interacts with the complexation agent, part of the complexation agent`s concentration is "consumed" by this interaction and its equilibrium concentration definitely differs from the analytical one even at the infinite dilution of the analyte. The situation is even more complicated because the buffering constituent is present in both dissociated and non-dissociated forms, which interact with the complexation agent to different extents.[34] Thus, not only is the effective concentration of complexation agent influenced by the presence of the interacting buffer but the pH, ionic strength and conductivity of the buffer are mutually affected by the presence of the complexation agent, particularly so depending on its actual concentration as shown in the first part of this series.

The complexation constant of *R*-FLU with β-CD was determined in different buffers: MES/ LiOH, MOPS/ LiOH, CHES/ LiOH, Tricine/ LiOH, maleic acid/ LiOH, phosphoric acid/ NaOH, ammonium/HCl, and ethanolamine/HCl demonstrate the influence of the interaction of buffer constituents with the complexation agent. The exact composition and parameters of the buffers are summarized in Table 1, and the pH of the buffers was chosen to ensure the complete dissociation of *R*-FLU (pK_A = 4.16). The obtained values of the complexation constants were corrected for ionic strength as proposed in our previous paper[29] and are depicted in Figure 1. Clearly, the complexation constants obtained in ethanolamine, ammonium, maleic, phosphoric, and Tricine buffers are the same about 4800 M^{-1} in the range of experimental error. This result confirms that the interaction of these buffers with β-CD is either the same or most likely negligible. However, complexation constants determined in MES (3500 M^{-1}), MOPS (2800 M^{-1})

and CHES (270 M^{-1}) buffers are significantly lower. Thus, these complexation constants can be regarded as apparent only and valid for this particular separation system including the same concentration of the buffer. These apparent complexation constants are always lower than the true thermodynamic values as an analytical instead of a free concentration of the complexation agent is used for fitting.

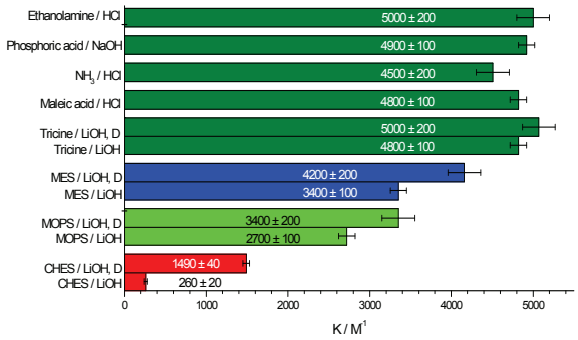

Figure 1. Complexation constants of *R*-FLU with β-CD determined in various buffers. Errors are expressed as standard deviations. Exact compositions and experimental conditions of used buffers are summarized in Table 1. D: diluted buffer.

To demonstrate the strength of the interaction of the buffering compounds, we injected the β-CD as a sample to the pure buffer. The stronger the interaction the higher the effective mobility of β-CD was expected. Effective mobilities of β-CD in CHES, MOPS and MES buffers corrected for ionic strength are summarized in Table 3. The mobility of β-CD in the Tricine buffer was close to zero. It is clear that the highest mobility of β-CD, and consequently the strongest interaction was observed in the CHES buffer followed by the MOPS and MES buffers. This finding fully agrees with the differences in values of complexation constants and the results of the NMR study, see Part I.

Table 3. Effective mobilities of neutral β-CD corrected for ionic strength and determined in various buffers. Composition of buffers: 50 mM CHES, MOPS, MES and 25.76 mM LiOH, ionic strength 25.76 mM; D: diluted buffers: 10 mM CHES, MOPS, MES and 5.15 mM LiOH, ionic strength 5.15 mM.

Buffer	CHES	D: CHES	MOPS	D: MOPS	MES	D: MES
u_{CD}^{eff} / 10^{-9} $m^2V^{-1}s^{-1}$	–13.4 ± 0.1	–10.4 ± 0.2	–9.1 ± 0.1	–4.1 ± 0.1	–7.5 ± 0.1	–1.8 ± 0.2

As the next step we repeated the ACE measurements in five times diluted MES, MOPS, CHES and Tricine separation buffers. It is obvious from Figure 1 that the complexation constant of Tricine did not change with the concentration of the buffer, while in the case of MES, MOPS and CHES buffers the complexation constants increased significantly with buffer dilution. Simultaneously, we observed a decrease of mobilities of β-CD, see Table 3. It means that the complexation constants determined in the interacting buffers do not depend only on the type of analyte and complexation agent but also on the type and concentration of the buffer used.

In order to confirm our finding that the interaction of buffer constituents is the major reason of the discrepancy of the complexation constants values we mimicked the ACE measurements in the CHES buffer by using our simulation program Simul 5 Complex. The complexation constant and mobilities of the complex of *R*-FLU with β-CD determined in the Tricine buffer and the complexation parameters of CHES with β-CD determined by ACE in Part I of this series of papers were used as the necessary input parameters. The comparison of experimental and simulated data for CHES and Tricine buffers is shown in Figure 2. Very good agreement of the

experimental and simulated curves was obtained that proves that interaction of the buffer with the complexation agent is the only reason for the deviation of the data.

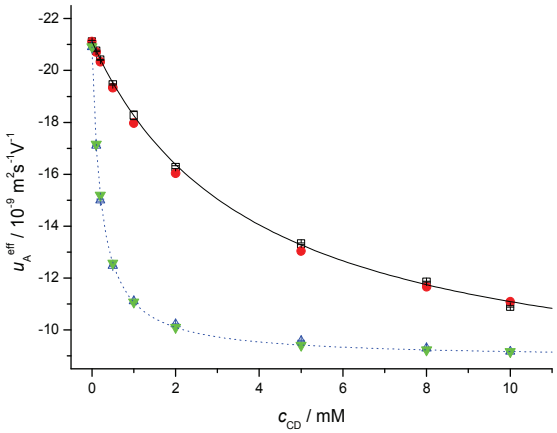

Figure 2. Dependence of effective mobility of *R*-FLU on concentration of β-CD. Red circles and black transparent squares are experimental and simulated data in 50 mM CHES/ 25.76 mM LiOH buffer, respectively. Blue upward triangles and green downward triangles are experimental and simulated data for 50 mM Tricine/ 25.76 mM LiOH buffer, respectively. Black solid and blue dotted lines are the fitted curves by eq 1. Errors are expressed as standard deviations.

Weak electrolyte analyte and neutral complexation agent. An even more complicated situation arises in the case of determining the complexation constants of weak electrolyte analytes, where both complexation constants of a neutral and charged form of the analyte are desired. The complexation constant of the neutral form is observed at pH, where the analyte is only partially dissociated. The resulting dependence of the effective mobility of the weak electrolyte analyte on the concentration of the complexation agent can be fitted by the following equation to obtain complexation parameters

$$u_{\mathrm{A}}^{\mathrm{eff}} = u_{\mathrm{A}} \frac{1 + \frac{u_{\mathrm{AC}}}{u_{\mathrm{A}}} K_{\mathrm{XAc}}[\mathrm{C}]}{1 + K_{\mathrm{XAc}}[\mathrm{C}] + \frac{[\mathrm{H_3O^+}]}{K_{\mathrm{HA}}}(1 + K_{\mathrm{XAn}}[\mathrm{C}])} \quad (2)$$

where K_{XAn} is the complexation constant of the neutral form of analyte, K_{HA} is the dissociation constant of the analyte. It is important to note that this method relies on the constant separation conditions, especially on constant pH value. However, as shown in Part I of this series of papers the pH of the interacting buffer changes significantly with the concentration of the complexation agent. It means that the method for determining complexation constants may completely malfunction in interacting buffers. To confirm this statement we performed two sets of ACE experiments with *R*-FLU complexing with β-CD in an acetic acid/ LiOH buffer and in a benzoic acid/ LiOH buffer, both pH 3.98 and IS 10 mM. At the given pH *R*-FLU is only partially dissociated (pK_{A} = 4.16). As shown in Part I of this series of papers, while the acetic acid buffer does not interact substantially with β-CD, benzoic acid complexes quite strongly. (The pH changes are depicted in Figure 1 of Part I of this series of papers). Obtained dependencies of the effective mobility of *R*-FLU on the concentration of β-CD fitted by eq 2 are shown in Figure 3. The mobility of the free analyte, complex and complexation constant of the fully charged form of *R*-FLU were obtained by separate measurement in the Tricine/ LiOH buffer of the same ionic strength and were used as fixed input parameters. In the acetic buffer, the quality of the fit was good (reduced χ^2 = 44; R^2 = 0.9936) and the resulting complexation constant was 11 100 ± 200 M^{-1}, however in the benzoic buffer the data did not follow the expected hyperbolic trend and could not be fitted by eq 2 with sufficient precision (reduced χ^2 = 490, R^2 = 0.9574), see Figure 3.

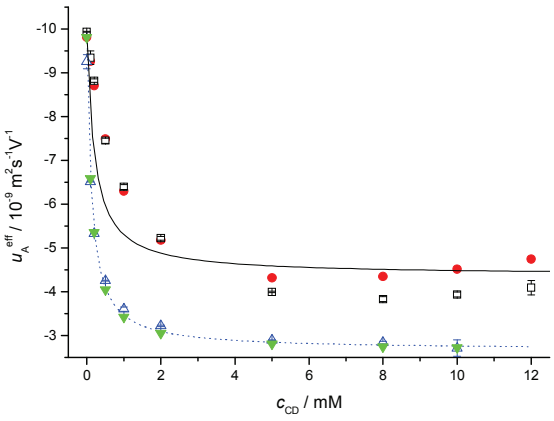

Figure 3. Dependence of effective mobility of *R*-FLU on concentration of β-CD. Red circles and black transparent squares are experimental and simulated data, respectively in a 24 mM benzoic acid/ 9.9 mM LiOH buffer. Blue upward triangles and green downward triangles are experimental and simulated data, respectively for a 61 mM acetic acid/ 9.9 mM LiOH buffer, both pH 3.98 and IS 10 mM. Black solid and blue dotted lines are the fitted curves by eq 2. Errors are expressed as standard deviations.

Both complexation constants of dissociated and non-dissociated forms of benzoic acid, which were determined in Part I of this series of papers, were used as input data for Simul 5 Complex now. The comparison of the simulated and experimental dependencies is shown in Figure 3. Clearly, the data agree well. Both experimental and theoretical dependencies obtained in the benzoic acid buffer show interesting trends at a concentration of β-CD higher than 8 mM, and the mobility of *R*-FLU increases with the increasing concentration of β-CD. This is highly surprising because the increase of the concentration of the neutral complexation agent should always suppress the mobility of analytes. However, in this particular case the increase of mobility of the weak acid (*R*-FLU) is caused by the increase of pH, which is the consequence of the interaction of the buffering constituent with β-CD and that yields to the increase of

dissociation of the weak acid *R*-FLU. At a certain concentration where the analyte is almost saturated by CD, as its concentration is small and its complexation constant high, its mobility almost reaches the limiting value (mobility of complex) and does not decrease steeply anymore. However, at this point the pH changes are still significant because the concentration of the buffer is rather high and a much higher amount of the complexation agent is needed to saturate the buffering compound. Thus, the effect of increasing pH on the mobility of the analyte prevails over the effect of the complexation of the analyte itself.

In conclusion the complexation constants in interacting buffers determined by ACE may be incorrect and provide confusing information about the strength of the interaction of analytes with complexation agents. Moreover, at first sight, unexpected behavior, such as herein demonstrated in an increase in mobility with the increasing concentration of the neutral CD, may appear with analytes that are weak acids or bases. Thus, the potential complexation of the buffer constituents with the complexation agent should be examined independently prior to ACE measurements.

2. *Impact of buffer complexation on the development of system peaks*

The development of system peaks in electrophoretic separation systems is well described by the linear theory of electromigration[26], and their behavior can be easily predicted using the simulation programs. However, the occurrence of system peaks in the interacting buffer systems has not been sufficiently described by now, although we presented that it might differ from expected trends. Thus, we shall demonstrate here the behavior of system peaks in interacting electrolytes, in a model system of a buffer composed of benzoic acid, which was shown to interact strongly with various cyclodextrins, and also in the common separation buffers. The changes of system zones mobilities for the benzoic acid buffer after the addition

of complexation agent HP-β-CD were examined both experimentally and by simulations using the Simul 5 Complex program. The HP-β-CD was selected for this demonstration because of its higher solubility in aqueous environments in comparison to β-CD. The necessary input data for simulations were determined by independent ACE measurements, and the resulting complexation constants and mobilities of complexes are K_{XAc}= 22.3 ± 0.5 M^{-1}, K_{XAn}= 330 ± 30 M^{-1}, u_{AC} = –9.9 ± 0.5 10^{-9} $m^2s^{-1}V^{-1}$. Experimental and simulated electropherograms for a 5.0 mM benzoic acid/ 2.5 mM LiOH buffer with 0 – 40 mM HP-β-CD are shown in Figure 4A and Figure 4B, respectively. All detector records were recalculated for the mobility scale (x-axis) to illustrate changes in system peaks' mobility in a more transparent way. The buffering system without any complexation agent forms two system peaks as results from the linear theory of electromigration. According to calculations in PeakMaster, one of those system peaks has zero mobility and the second one is a cationic system peak with mobility u = 17.3×10^{-9} $m^2s^{-1}V^{-1}$. The experimental results were in a perfect agreement with the simulated ones in regard to positions, amplitudes and shapes of the system zones, see Figure 4, (curve marked as 0 mM). The other electropherograms in Figure 4 show behavior of system peaks at the indicated complexation agent concentration. The addition of HP-β-CD (5 mM) into the 5.0 mM benzoic acid/ 2.5 mM LiOH buffer caused substantial slowdown of the cationic system peak and gave rise to a new slow anionic system peak. The third system peak kept nearly zero mobility.

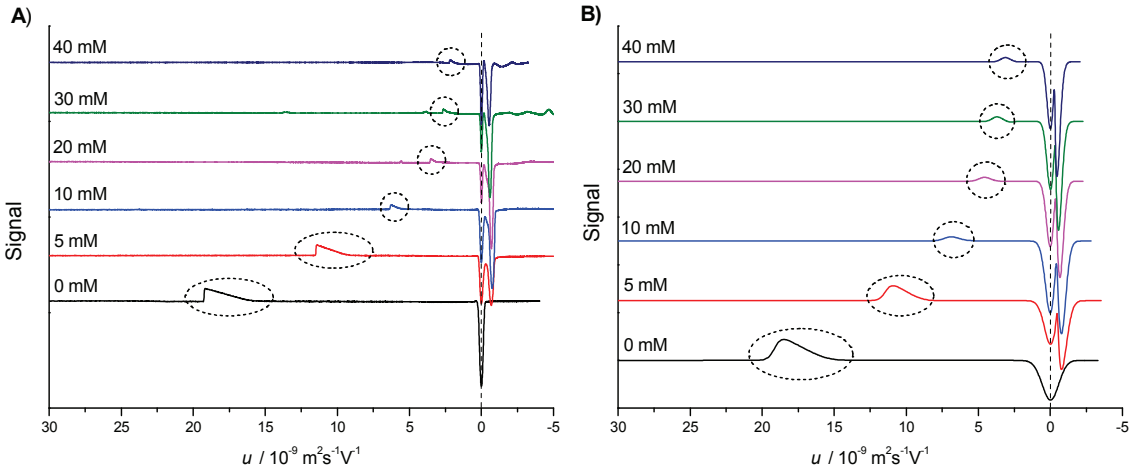

Figure 4. A) Experimental electropherograms recalculated to mobility scale showing changes in mobility and number of system peaks in BGEs with complex-forming ligand; BGE: 5.0 mM benzoic acid, 2.5 mM LiOH and various concentrations of HP-β-CD. Samples: disturbed BGE, compositions summarized in Table 2. Indirect UV detection was performed at a detection wavelength of 200 nm. The curves are marked by concentrations of HP-β-CD in BGE. Cationic system peaks are labeled by dashed circles. B) Simulated electropherograms transformed to mobility scale; conditions for simulations were set according to corresponding real experiments. Curves are marked by concentrations of HP-β-CD in the BGE. Cationic system peaks are labeled by dashed circles.

Dependence of the mobility of experimental and simulated cationic system peaks on HP-β-CD concentration is depicted in Figure 5. Both dependencies agree very well. Such development of system peaks is not predictable using the classical linear theory of electromigration for non-complexing systems. The addition of a neutral non-interacting compound into BGE should definitely result in the formation of a system peak with zero mobility and should not influence the mobility of other system peaks. Complete linear theory of electromigration for complexing

systems was not presented so far. Thus, simulations can be used as the only tool for prediction and explanation of system peaks in such systems.

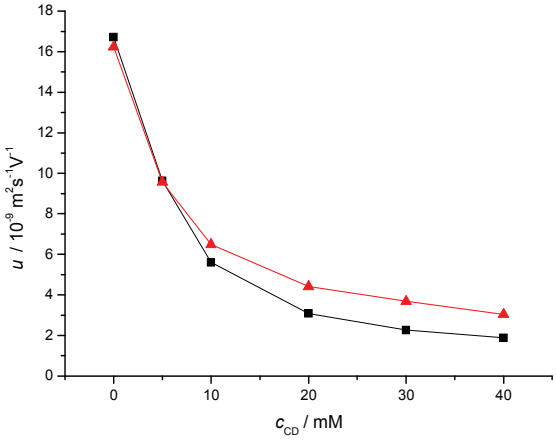

Figure 5. Dependences of the mobilities of cationic system peaks on concentration of HP-β-CD in BGE composed of 5.0 mM benzoic acid and 2.5 mM LiOH calculated from experimental (black squares) and simulated (red triangles) electropherograms.

The development of system peaks was examined also in commonly used buffer systems that were selected based on the results of the pH study. Considering these results (see Figure 2 of Part I of this series of papers) the most significant changes of the system peaks' behavior were expected in the CHES/ LiOH buffer because the addition of all the tested CDs caused a considerable shift of pH in this buffer. Figure 6 shows experimental electrophoregrams obtained after the addition of the neutral CDs to this buffer. Clearly, the addition of all CDs induced an additional system peak. HP-β-CD gave rise to a system peak, which was broadened, and therefore it was difficult to determine its mobility. The presence of α-CD and DM-β-CD in BGEs led to an anionic system peak with a mobility about -3×10^{-9} $m^2s^{-1}V^{-1}$ and -4×10^{-9} $m^2s^{-1}V^{-1}$, respectively. The strongest effect was observed again with β-CD. The addition of β-CD in BGE resulted in the development of an anionic system peak with rather high mobility, about -8×10^{-9}

$m^2s^{-1}V^{-1}$. As the result, the CHES buffer could not be recommended for electrophoretic experiments if a neutral CD is employed because the originating system peak can migrate in the same region as analytes, interact with them and distort them. In addition the pH changes observed are so significant that they can seriously affect the separation results. The development of additional system peaks and changes in system peaks mobility could be observed also in other common buffers. A system peak investigation with other tested buffers, where interactions with various CDs are most probably weak in comparison to CHES buffer, was carried out as well. The detail results can be found in Supporting Information.

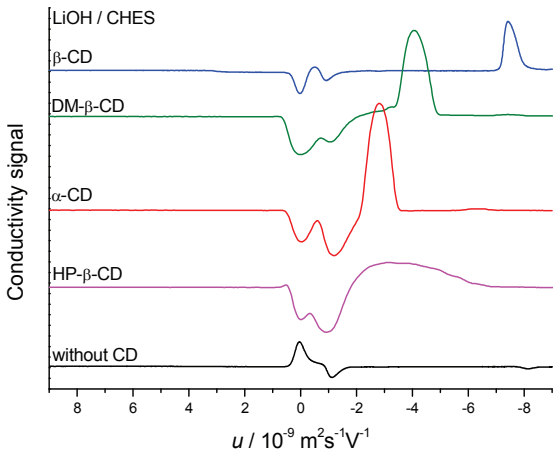

Figure 6. Experimental electropherograms for CHES/ LiOH buffer with various CDs. Concentrations of α-CD, β-CD, DM-β-CD and HP-β-CD in 10.0 mM CHES/ 5.0 mM LiOH buffer were 5.20, 4.54, 4.56 and 4.68 mM, respectively. Sample: 11 mM CHES, 5.0 mM LiOH.

3. *Influence of the interaction of buffer constituents on the result of electrophoretic separation*

It is well known that the result of electrophoretic separation is extremely sensitive to the selection of a buffer and its pH or ionic strength. Thus, the change of BGE properties connected

with the complexation of buffer constituents with the complexation agent present in BGE might have significant impact on the results of electrophoretic separation. To demonstrate this behavior we performed separations of a mixture of amino acids (namely Leu, Gly, Gln, Ser, Asn) in 10 mM ethanolamine/ 5 mM Tricine and 10 mM CHES/ 5 mM LiOH buffers, both pH 9.41 and IS 5 mM. The separations were performed both in cyclodextrin free buffer and after addition of 10 mM β-CD. The pH of ethanolamine/ Tricine buffer did not change substantially after the addition of β-CD, while the pH of the CHES buffer decreased to the value of 8.86. It confirms that the ethanolamine/ Tricine buffer does not interact with β-CD remarkably, while the CHES buffer complexes strongly. The comparison of the obtained electropherograms is shown in Figure 7A and 7B, respectively. While the electropherograms obtained in ethanolamine/ Tricine buffer before and after the addition of β-CD are almost the same, in the case of the CHES buffer not only position but also the shape of the separated peaks changed significantly after the addition of β-CD. The resolution deteriorated substantially in the latter system. The explanation could be either the complexation of analytes with β-CD or the changes in BGE properties connected with the complexation of buffer constituents. The former possibility is not probable, because no similar effect was observed in the non-interacting ethanolamine/ Tricine buffer. It means that it is the complexation of buffer constituents that should be the major reason for the presented changes.

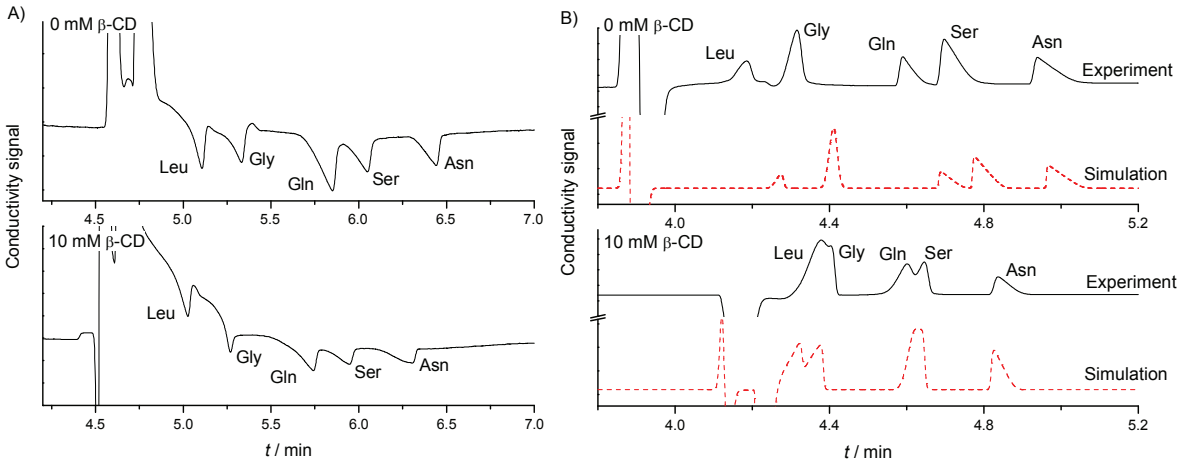

Figure 7. Comparison of the separation of a set of amino acids (Leu, Gly, Gln, Ser, Asn) in A) 10 mM ethanolamine/ 5 mM HCl buffer; and B) 10 mM CHES/ 5 mM LiOH buffer, both pH 9.41 and IS 5 mM. Upper picture, pure buffer marked as 0 mM β-CD; Lower picture: 10 mM concentration of β-CD. Black solid curves: Experiment; Red dashed curve simulations obtained by PeakMaster and Simul 5 Complex, for cyclodextrin free BGE and BGE at a 10 mM concentration of β-CD, respectively. Individual aminoacids are labeled by their respective abbreviation.

To prove these assumptions we mimicked the experiments in the CHES buffer using our simulation software Simul 5 Complex. Complexation constants of CHES determined in Part I of this series of papers were corrected for actual ionic strength and used as input data for simulations, and the complexation of amino acids with β-CD was neglected. The comparison of simulated and experimental profiles is shown in Figure 7B. A very good agreement between the theoretical predictions and measured electropherograms was obtained. It was confirmed that the interaction of the CHES buffer with the complexation agent had a fatal impact on the separation and that ethanolamine/ Tricine buffer should be the buffer of choice for this separation.

We proved that the complexation of buffer constituents with the complexation agent present in BGE might significantly influence the result of separation as it affects the BGE properties *e.g.* pH and IS changes. The possible interaction of BGE constituents with the selected complexation agent must always be considered.

CONCLUSION

In this Part II of this series of papers we illustrate the practical impact of the complexation of buffer constituents with the complexation agents present in BGE. Three highly relevant aspects of electrophoresis were inspected. First, it was shown that the complexation constants of analytes interacting with the complexation agent resulting from ACE measurements can be completely incorrect if the buffer constituents concurrently interact with the agent. The stronger the concurrent interaction, the bigger the effect on the complexation constant value. Moreover, the final effect depends on both the type of the buffer and its concentration and it can lead to virtually abnormal behavior of weak acidic or alkaline analytes. Among the buffers tested, the highest impact was attributed to the CHES buffer if β-CD was used as the complexation agent. Second, the influence of the complexation of buffer constituents with the complexation agent on the development of system peaks and their behavior was demonstrated depending on the complexation agent concentration by experiment, and further confirmed by simulation using our simulation software Simul 5 Complex. Perfect agreement of the simulation and experimental data was achieved, showing that system peaks can substantially change their mobilities and that an additional system peak of non-zero mobility can develop in the system even if a neutral agent is added into the interacting buffer. Last but not least, the substantial effect of the complexation of BGE constituents on the result of CE separation was demonstrated on a mixture of 5 amino acids. It was clearly shown that changes of the BGE properties, that could moreover be different

for different buffers, must be considered in method development procedures. This importantly applies to all analytes in a sample, even those not supposed to interact with the agent themselves.

ASSOCIATED CONTENT

Supporting Information. Additional information as noted in text. This material is available free of charge via the Internet at http://pubs.acs.org.

ACKNOWLEDGMENT

The support of the Grant Agency of the Czech Republic, Grant No. P206/12/P630, Grant Agency of Charles University, Grant No. 323611, the project Kontakt LH11018, and the long-term research plan of the Ministry of Education of the Czech Republic (MSM0021620857), are gratefully acknowledged.

ABBREVIATIONS

ACE, affinity capillary electrophoresis, BGE, background electrolyte, CCD, contactless conductivity detector, CD, cyclodextrin, CE, capillary electrophoresis, CHES, *N*scyclohexyl-2-aminoethanesulfonic acid, DAD, diode array detector, DMSO, dimethylsulfoxide, DM-β-CD, heptakis(2,6-di-*O*-methyl)-β-cyclodextrin, EMD, electromigration dispersion, EOF, electroosmotic flow, HP-β-CD, (2-hydroxypropyl)-β-cyclodextrin, HVL function, Haarhoff -Van der Linde function, IS, ionic strength, L_{CCD}, L_{DAD}, capillary length to CCD /DAD detector, L_{tot}, total capillary length, MES, 2-(*N*-morpholino)ethanesulfonic acid, MOPS, 3-morpholinopropane-1-sulfonic acid, *R*-FLU, (*R*)-(-)-2-fluoro-α-methyl-4-biphenylacetic acid (*R*-flurbiprofen), TAPS, 3-[[1,3-dihydroxy-2-(hydroxymethyl)propan-2-yl]amino]propane-1-sulfonic acid, Tricine, [Tris(hydroxymethyl)methyl]glycine, Tris, Tri(hydroxymethyl)aminomethane

REFERENCES

(1) Kalikova, K.; Riesova, M.; Tesarova, E. *Cent. Eur. J. Chem.* **2012,** *10*, 450-471.

(2) Wren, S. A. C.; Rowe, R. C. *J. Chromatogr.* **1992,** *603*, 235-241.

(3) Rawjee, Y. Y.; Staerk, D. U.; Vigh, G. *J. Chromatogr.* **1993,** *635*, 291-306.

(4) Rawjee, Y. Y.; Williams, R. L.; Vigh, G. *J. Chromatogr., A* **1993,** *652*, 233-245.

(5) Breadmore, M. C.; Quirino, J. P.; Thormann, W. *Electrophoresis* **2009,** *30*, 570-578.

(6) Dubrovcakova, E.; Gas, B.; Vacik, J.; Smolkova-Keulemansova, E. *J. Chromatogr.* **1992,** *623*, 337-344.

(7) Dubsky, P.; Tesarova, E.; Gas, B. *Electrophoresis* **2004,** *25*, 733-742.

(8) Dubsky, P.; Svobodova, J.; Gas, B. *J. Chromatogr., B: Anal. Technol. Biomed. Life Sci.* **2008,** *875*, 30-34.

(9) Dubsky, P.; Svobodova, J.; Tesarova, E.; Gas, B. *J. Chromatogr., B: Anal. Technol. Biomed. Life Sci.* **2008,** *875*, 35-41.

(10) Svobodova, J.; Dubsky, P.; Tesarova, E.; Gas, B. *Electrophoresis* **2011,** *32*, 595-603.

(11) Tesarova, E.; Sevcik, J.; Gas, B.; Armstrong, D. W. *Electrophoresis* **2004,** *25*, 2693-2700.

(12) Hruska, V.; Benes, M.; Svobodova, J.; Zuskova, I.; Gas, B. *Electrophoresis* **2012,** *33*, 938-947.

(13) Breadmore, M. C.; Kwan, H. Y.; Caslavska, J.; Thormann, W. *Electrophoresis* **2012,** *33*, 958-969.

(14) echmet.natur.cuni.cz

(15) Svobodova, J.; Benes, M.; Hruska, V.; Uselova, K.; Gas, B. *Electrophoresis* **2012,** *33*, 948-957.

(16) Svobodova, J.; Benes, M.; Dubsky, P.; Vigh, G.; Gas, B. *Electrophoresis* **2012,** *33*, 3012-3020.

(17) Poppe, H. *Anal. Chem.* **1992**, *64*, 1908–1919.

(18) Stedry, M.; Jaros, M.; Hruska, V.; Gas, B. *Electrophoresis* **2004**, *25*, 3071-3079.

(19) Jaros, M.; Hruska, V.; Stedry, M.; Zuskova, I.; Gas, B. *Electrophoresis* **2004**, *25*, 3080-3085.

(20) Hruska, V.; Svobodova, J.; Benes, M.; Gas, B. *J. Chromatogr., A* **2012,** *1267*, 102-108.

(21) Rawjee, Y. Y.; Williams, R. L.; Vigh, G. *Anal. Chem.* **1994,** *66*, 3777-3781.

(22) Chen, Y. R.; Ju, D. D.; Her, G. R. *J. High Resolut. Chromatogr.* **2000,** *23*, 409-412.

(23) Fang, L.; Yin, X. B.; Wang, E. *Anal. Lett.* **2007,** *40*, 3457-3471.

(24) Evans, C. E.; Stalcup, A. M. *Chirality* **2003,** *15*, 709-723.

(25). Riesova, M.; Svobodova, J.;Tosner, Z.; Benes, M.; Tesarova, E.; Gas, B. Part I of this series of papers, submitted to *Anal. Chem.*

(26) Tanaka, Y.; Terabe, S. *J. Chromatogr., B: Anal. Technol. Biomed. Life Sci.* **2002,** *768*, 81-92.

(27) Uselova-Vcelakova, K.; Zuskova, I.; Gas, B. *Electrophoresis* **2007,** *28*, 2145-2152.

(28) Jiang, C. X.; Armstrong, D. W. *Electrophoresis* **2010,** *31*, 17-27.

(29) Benes, M.; Zuskova, I.; Svobodova, J.; Gas, B. *Electrophoresis* **2012,** *33*, 1032-1039.

(30) Haarhoff, P. C.; Van der Linde, H.J. *Anal. Chem.* **1966,** *38*, 573-582.

(31) Erny, G. L.; Bergstrom, E. T.; Goodall, D. M. *J. Chromatogr., A* **2002,** *959*, 229-239.

(32) Hruska, V.; Riesova, M.; Gas, B. *Electrophoresis* **2012,** *33*, 923-930.

(33) Riesova, M.; Hruska, V.; Gas, B. *Electrophoresis* **2012,** *33*, 931-937.

(34) Gelb, R. I.; Schwartz, L. M.; Johnson, R. F.; Laufer, D. A. *J. Am. Chem. Soc.* **1979,** *101*, 1869-1874.

For TOC only

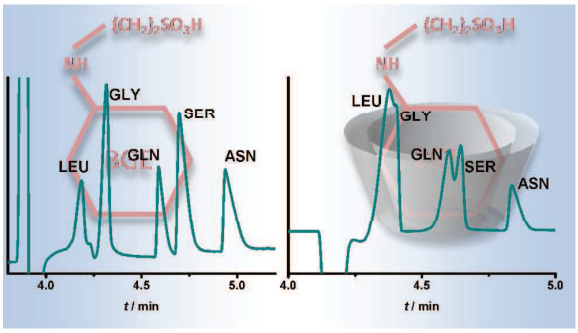
GLY
SER
LEU
GLN
ASN
4.0
4.5
5.0
t / min
LEU
GLY
GLN
SER
ASN
4.0
4.5
5.0
t / min

4.3 Využití kapilární elektroforézy a softwaru PeakMaster v praxi

Analytický chemik musí v praxi při vývoji nové separační metody pro novou sadu analytů zvážit mnoho faktorů, které stojí za volbou vhodného separačního systému. Samozřejmostí je volba vhodného pH pufru. Ladění dalších parametrů, které mohou výsledky separace značně ovlivnit (iontová síla, mobilita složek základního elektrolytu, pozice systémových zón) může být velmi zdlouhavé a metoda pokus-omyl či dodržovaní empiricky stanovených optimalizačních protokolů nemusí vždy vést k nalezení optimálních separačních podmínek. Program PeakMaster je v tomto ohledu nezastupitelný. Umožňuje velmi rychle vyzkoušet mnoho separačních podmínek a predikovat výsledky separace ve stále komplikovanějších systémech.

Příkladem využití kapilární elektroforézy a programu PeakMaster v analytické praxi je vývoj metody pro separaci sady benzodiazepinů (Obrázek 7). Všechny separované látky jsou si strukturně velmi podobné a většinou jsou si blízké i jejich disociační konstanty.

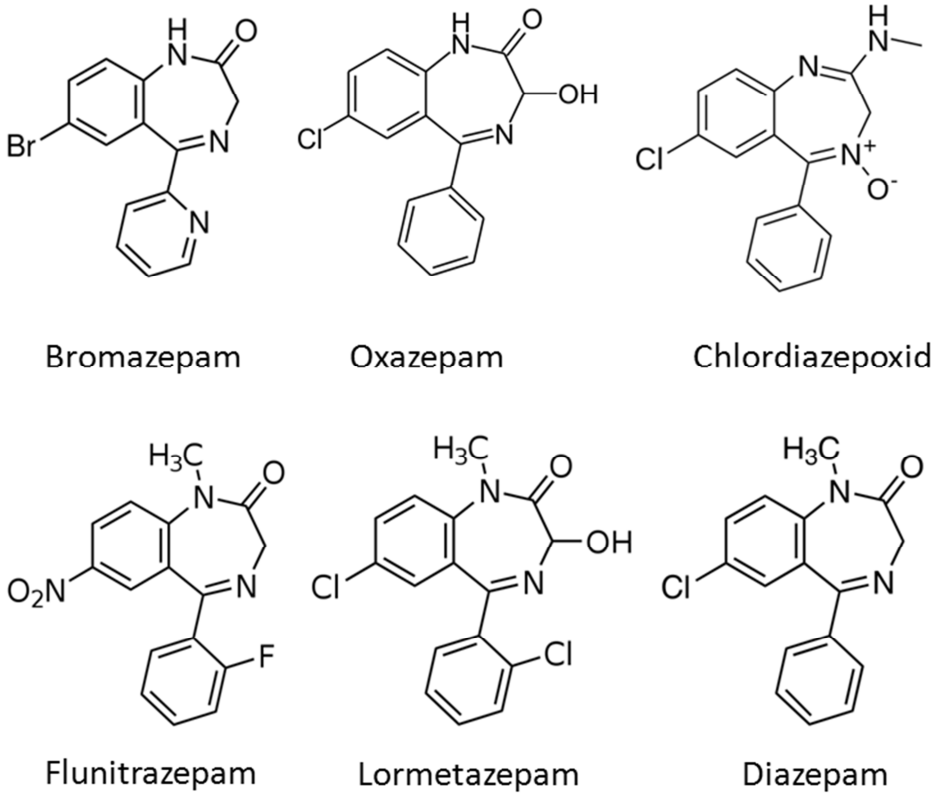

Obrázek 7 *Struktury benzodiazepinů separovaných kapilární elektroforézou za separačních podmínek vybraných a optimalizovaných programem PeakMaster*

Pro separaci bylo zvoleno velmi nízké pH (pH = 2). Pro výpočty v programu PeakMaster jsou zapotřebí hodnoty limitních mobilit a disociačních konstant analytů. Disociační konstanty nebo jejich odhady lze získat výpočtem ve speciálních softwarech [62,63]. Pro odhady limitních mobilit je pak vhodné naměřit při zvoleném pH a známé iontové síle efektivní mobilitu jednotlivých analytů a z té pak limitní mobilitu odhadnout. Pro optimalizaci separace tak bylo zapotřebí jen velmi malé množství experimentů. Po zjištění hodnot efektivních mobilit při dané iontové síle a pH pak pokračovalo ladění podmínek pouze v programu PeakMaster. Tím byly separační podmínky optimalizovány velmi rychle, například ve srovnání s vysokoúčinnou kapalinovou chromatografií, kde podobné softwarové pomůcky nejsou téměř dostupné.

Optimalizovaná metoda pro separaci sady benzodiazepinů byla validována a je tak připravena pro praktické využití při analýze těchto farmaceuticky hojně používaných psychoaktivních látek.

Publikace 6

Separation and Quantification of 1,4-benzodiazepines: HPLC versus CZE

*K. Kalíková, **M. Riesová**, R. Chudoba, M.G. Schmid, E. Tesařová*

Croatica Chemica Acta, 2011, 84, 367-373

CROATICA CHEMICA ACTA
CCACAA, ISSN 0011-1643, e-ISSN 1334-417X
Croat. Chem. Acta **84** (3) (2011) 367–373.
CCA-3484

Original Scientific Article

Separation and Quantification of 1,4-benzodiazepines: HPLC *versus* CZE†

Květa Kalíková,[a,*] Martina Riesová,[a] Richard Chudoba,[a] Martin G. Schmid,[b] and Eva Tesařová[a]

[a]*Department of Physical and Macromolecular Chemistry, Faculty of Science, Charles University in Prague, 128 43 Prague 2, Albertov 2030, Czech Republic*
[b]*Department of Pharmaceutical Chemistry, Institute of Pharmaceutical Sciences, Karl-Franzens-University Graz, Universitätsplatz 1, A-8010 Graz, Austria*

RECEIVED AUGUST 12, 2010; REVISED JANUARY 4, 2011; ACCEPTED FEBRUARY 4, 2011

Abstract. The goal of the present study was to separate a set of benzodiazepines, namely bromazepam, oxazepam, nitrazepam, chlordiazepoxide, flunitrazepam, lormetazepam and diazepam by analytical scale HPLC and CZE. The both methods for separation of these seven compounds from the 1,4-benzodiazepine group were optimized and compared. LODs and LOQs were determined under the optimized conditions in the both methods. The corresponding LOD and LOQ values are approximately three orders of magnitude lower in HPLC than in CZE. As expected, elution order was found to be different for the both techniques. As a result of a critical collation of all the parameters considered, RP-HPLC was found to be more suitable for determination of the set of benzodiazepines. A real sample analysis was performed under optimized conditions to demonstrate applicability of the proposed analytical methods. (doi: 10.5562/cca1738)

Keywords: RP-HPLC, CZE, benzodiazepines, pharmaceuticals

INTRODUCTION

1,4-benzodiazepines (BZDs) are a well-known class of psychoactive drugs; they are known primarily for their hypnotic and sedative effects.[1] This pharmaceutical group is also used as anxiolytics, anticonvulsants and muscle relaxants.[2] They are still widely prescribed but also abused.[3,4] Many studies on these drugs can be found in the literature.[5–8] Diverse analytical methods for determination of benzodiazepines in various matrices have been published,[9,10] *e.g.* potentiometry,[11] immunoassays,[12] spectrophotometry[13] and also separation techniques that represent a clear majority of the reported methods because they allow determination of individual compounds in often rather complicated mixtures. While HPLC remains the most common technique for the analysis of benzodiazepines,[7,9,14,15] mainly in reversed phase (RP) mode, several capillary zone electrophoresis (CZE) methods have recently been developed.[2,16,17] CZE represents an interesting alternative to HPLC for determination of pharmaceuticals, in general,[18,19] mainly because of its higher efficiency in comparison with HPLC.[20]

The aim of this work was to develop and optimize separation conditions for a set of seven 1,4-BZDs in RP-HPLC and CZE with UV detection and compare these methods in terms of efficiency, analysis time, resolution, elution order and basic validation parameters. The results aimed to answer the question if CZE is really a suitable alternative to RP-HPLC for the resolution/analysis of BZDs.

EXPERIMENTAL

Chemicals

Acetonitrile (ACN) for HPLC and methanol (MeOH) for HPLC were obtained from Sigma-Aldrich (Steinheim, Germany). Glacial acetic acid (HAc, purity > 99.5 %), sodium dihydrogen phosphate anhydrous (purity ≥ 99 %) and mesityl oxide were purchased from Fluka (Buchs, Switzerland). Sodium hydroxide solution (0.1 mol/l) was from Agilent Technologies (Waldbronn, Germany). *Ortho*-phosphoric acid (85 %) was obtained from Lachema (Brno, Czech Republic). 1,4-benzodiazepines, namely oxazepam, nitrazepam, lormetazepam, chlordiazepoxide, flunitrazepam, diazepam and bromazepam, were obtained from Sigma-Aldrich (Steinheim, Germany). The tablets of Diazepam Slova-

† Presented at the *10th International Symposium and Summer School on Bioanalysis* within the CEEPUS Network CII-HU-0010-04-0910, Zagreb, Croatia, July 2010.

* Author to whom correspondence should be addressed. (E-mail: kveta.kalikova@centrum.cz)

kofarma® 5 mg were product of Zentiva (Hlohovec, Slovakia) and Lexaurin® 3 (bromazepamum 3 mg) was product of KRKA (Novo mesto, Slovenia). Water was prepared with a Milli-Q water purification system (Millipore, Milford, MA, USA). Stock solutions of the analyzed compounds were prepared in concentration of 1 mg/ml using MeOH as a solvent.

Equipment and Measurement Conditions

All chromatographic measurements were performed on a Waters Breeze HPLC system (Waters Chromatography, Milford, MA, USA) consisting of a 1525 binary pump, a 717 plus autosampler, a column heater and a 2487 dual λ absorbance detector. A Breeze software was used for process control and data handling. Columns used for separations were a Zorbax SB-C8 (column size 150 mm × 4.6 mm i.d., particle size 5 μm) and Zorbax SB-C18 (column size 150 mm × 4.6 mm i.d., particle size 5 μm), both purchased from Agilent Technologies (USA). The columns were thermostated at 25 °C. Flow rate was 2 ml/min. Detection was carried out at the wavelength of 240 nm. Mobile phases were composed of ACN/deionised water with acetic acid, pH 3.0, in various ratios. Injected sample volume was 10 μL. Individual measurements were repeated three times.

Electrophoretic experiments were performed using an Agilent ^{3D}CE equipment operated under control of a ChemStation software (Agilent Technologies, Waldbronn, Germany). Detection was performed with a diode array detector at the detection wavelength of 240 nm. A bare fused-silica capillary of 50 μm i.d. and 363 μm o.d. was product of Polymicro Technologies (Phoenix, USA). Total length of the capillary was 63.7 cm and length to the detector was 55.2 cm. The capillary was thermostated at 25 °C. Driving voltage was +27 kV (with cathode at the detector side). Samples were injected hydrodynamically: 50 mbar × 5 s. Mesityl oxide was used as an electroosmotic flow (EOF) marker. Stock solutions of sodium dihydrogen phosphate and ortho-phosphoric acid at a concentration of 50 mM were used for preparation of background electrolyte (BGE). The running buffer was prepared by mixing of appropriate amounts of the stock solutions and addition of water to obtain BGE with final composition of 6 mM sodium dihydrogen phosphate and 33 mM orthophosphoric acid. pH value of the BGE was 2.0. The capillary was rinsed with pure water for 10 min, with 0.1 mM NaOH for 10 min, 10 min with pure water again and 20 min with running buffer before use. Prior to each measurement the capillary was washed with the running buffer for 4.5 min. All measurements were carried out in triplicates.

Procedures

Real Sample Preparation

Aliquots of powdered tablet samples were dissolved in methanol to concentration of 1 mg/ml. The samples were sonicated for 20 min to provide complete dissolution. Appropriate volumes of clear supernatants were diluted with methanol to concentration of 0.01 mg/ml and with BGE to concentration of 0.05 mg/ml for HPLC and CZE analyses, respectively. The prepared samples were filtered through a 0.45 μm filter before injection. The total amounts of the drugs were then determined using the optimized HPLC and CZE methods.

Statistical Data Evaluation

One-way analysis of variance (ANOVA) statistical method was used for robustness testing. Parameters, which could become significant sources of errors in practice, were chosen as variables. The significance level (α) was set at 0.05. The one-way analysis of variance compares the medians of two or more groups in order to determine if at least a median value of one group is different from the others. The tests are nondirectional as the null hypothesis specifies that all medians are equal and the alternative hypothesis simply states that at least one median value is different.[21] If the statistical *p*-value is higher than the chosen significance level, the null hypothesis of the equal medians is accepted.

RESULTS AND DISCUSSION

Optimization of the Chromatographic Separation Conditions

Optimization of separation conditions for seven drugs from 1,4-benzodiazepine group – bromazepam, oxazepam, nitrazepam, chlordiazepoxide, flunitrazepam, lormetazepam and diazepam - was carried out in RP-HPLC system.[2,7,14,15] The first column tested was Zorbax SB-C8 packed with an endcapped octyl-silica gel stationary phase. The most suitable mobile phase composition found in isocratic elution mode was ACN/deionised water with acetic acid, pH 3.0, 30/70 (*v*/*v*). Baseline resolution of all seven analytes was achieved within 20 minutes – see Figure 1A. Compared to mobile phase composed just of ACN and deionised water the acidified mobile phase enhanced peak symmetry. Various linear gradient elution types were tested to decrease the analysis time. To preserve baseline resolution of a critical pair of flunitrazepam and lormetazepam the acetonitrile gradient could not be applied before 11th minute. As the result of application of the gradient shorter analysis time was reached while the peak symmetry was preserved. However, the isocratic mode is more suitable for routine (repeated) measurements because it does not require column equilibration before each analysis.

Using column with more hydrophobic stationary phase octadecyl-silica gel SP – Zorbax SB-C18 – the analysis time was substantially reduced because a mo-

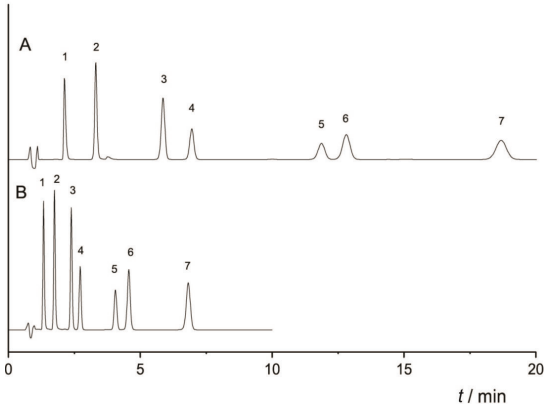

Figure 1. Chromatograms of 1,4-benzodiazepines separation. Chromatogram A: Zorbax SB-C8 column; mobile phase: ACN/water with HAc, pH 3.0, 30/70 (*v/v*); 2 ml/min; 25 °C; 240 nm. Chromatogram B: Zorbax SB-C18 column; mobile phase: ACN/water with HAc, pH 3.0, 40/60 (*v/v*); 2 ml/min; 25 °C; 240 nm. Elution order: 1-chlordiazepoxide, 2-bromazepam, 3-oxazepam, 4-nitrazepam, 5-flunitrazepam, 6-lormetazepam, 7-diazepam.

bile phase with higher ACN content (40 volume percent) could be applied while the separation was still preserved. The baseline resolution of all seven 1,4-BZDs was achieved within 7 min (Figure 1B). Linear gradient elution was also tested. Using the Zorbax SB-C18 column and mobile phase composed of ACN/water with HAc, pH 3.0, 40/60 (*v/v*) and a linear gradient to volume fraction φ = 90 % of acetonitrile applied from 2nd to 3rd minute, the analysis time was reduced to 4.5 minute. The results obtained under isocratic versus gradient elution conditions are summarized in Table 1 for comparison. The peak symmetry was similar under the both studied conditions. Therefore, the isocratic elution was selected as the optimized separation mode. The efficiency, expressed as plate number/meter of column, ranged under optimized isocratic conditions from 2.05×10^4 to 6.00×10^4 while under gradient elution conditions this parameter rendered higher values, from 1.97×10^4 to 3.55×10^5.

Optimization of the Electrophoretic Separation Conditions

The software PeakMaster[22] was utilized for selection of an initial BGE composition, pH and separation conditions. The optimized BGE composition for the analysis of BZDs was 6 mM sodium and 39 mM phosphate ions. According to PeakMaster calculations the optimized BGE had pH 2.0, ionic strength 17.2 mM and buffering capacity 48 mM. Nitrazepam was excluded from the studied set of analytes because of its instability in the buffer of the low pH. Using 6 mM phosphate buffer of higher pH the compounds were not baseline resolved. Baseline separation of six BZDs was obtained within 36 minutes with the BGE of pH 2.0. To reduce the analysis time additional pressure of 50 mbar was applied in 10th min. Then the analysis time decreased to 17 minutes with baseline separation preserved – see Figure 2. The additional pressure could not be used earlier (before the 10th min) because it would not allow baseline resolution of the first three compounds (bromazepam, diazepam and chlordiazepoxide). The efficiency, expressed as plate number / meter, ranged under optimized conditions from 1.11×10^5 to 3.08×10^5. The plate number of the lormetazepam peak was calculated to be an order of magnitude lower in comparison with all the other peaks obtained in the CZE measurements. This is caused by a resonance phenomenon[23,24] that can lead to anomalous dispersion of the analyte´s peak.[25] The resonance can cause false results of analysis. It was described to have also a negative impact on efficiency of separation.[26] Therefore, it is better to avoid using separation conditions at which the resonance occurs.

Table 1. Comparison of retention time (t_R), resolution (R) and peak symmetry (S) for isocratic and gradient elution with Zorbax SB C18 column. Mobile phase compositions: isocratic elution: ACN/deionised water with HAc, pH 3.0, 40/60 (*v/v*); gradient elution: ACN/deionised water with HAc, pH 3.0, 40/60 (*v/v*) in isocratic elution up to 2nd minute and a linear gradient to volume fraction, φ = 90 % of ACN applied from 2nd to 3rd mins

		t_R /min		R		S	
peak number	compound	iso	grad	iso	grad	iso	grad
1	chlordiazepoxide	1.32	1.31			1.21	1.16
2	bromazepam	1.76	1.76	4.44	4.33	1.12	1.14
3	oxazepam	2.41	2.41	5.61	5.60	1.05	1.07
4	nitrazepam	2.74	2.73	2.50	2.53	1.05	1.06
5	flunitrazepam	4.09	3.90	8.39	10.03	1.03	0.99
6	lormetazepam	4.60	4.06	2.65	1.75	1.01	1.04
7	diazepam	6.83	4.40	9.07	4.36	1.02	1.01

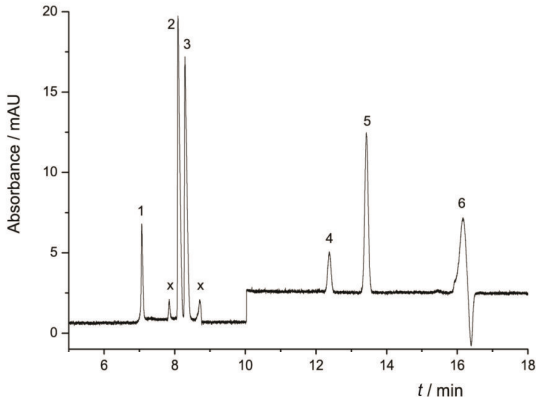

Figure 2. Electropherogram of 1,4-benzodiazepines separation. BGE: 6 mM phosphate buffer, pH 2.0; +27 kV; 25 °C; 240 nm. Elution order: 1-bromazepam, 2-diazepam, 3-chlordiazepoxide, 4-flunitrazepam, 5-oxazepam, 6-lormetazepam in coincidence with stationary system peak, x-impurities. Baseline "jump" at 10th min is caused by application of pressure.

Validation of the Methods

Stability of Sample Solutions

Stability of the sample solutions (1 mg/ml MeOH) kept at low temperature was tested by the optimized HPLC method during the period of three weeks. Almost all the samples were proved to be stabile over the three weeks period. The only exception was solution of chlordiazepoxide that showed slight instability after five days of storage. However, it was still useful for the purpose of this study.

Precision

In order to evaluate the precision of the HPLC and CZE methods, repeatability and reproducibility of measurements were studied at the wavelength of 240 nm. The repeatability of the retention factors and sample concentrations in HPLC and the effective mobilities and sample concentrations in CZE were determined as relative standard deviations (R.S.D.) for 10 consecutive injections of the set of 1,4-benzodiazepines at the concentrations of 0.01 mg/ml and 0.05 mg/ml in HPLC and CZE, respectively. The reproducibility of the chromatographic and electrophoretic data (retention factor, effective mobility, sample concentration) of the tested set of analytes was measured in the period of 3 days by different scientists. The R.S.D. values for precision of the both methods are shown in Table 2. The results suggest that the HPLC and CZE methods are suitable for both qualitative and quantitative analysis of the 1,4-BZDs.

Linearity

The linearity was tested over the concentration range 0.001 to 0.1 mg/ml and 0.02 to 0.1 mg/ml in HPLC and CZE, respectively. Measurements at all concentration levels were carried out in triplicate at six concentration levels and all values of peak areas were subjected to linear regression. Linear relationships between the peak areas in HPLC or the corrected peak areas (peak area/migration time) in CZE and the concentrations of individual 1,4-benzodiazepines were observed – see Table 3.

Table 2. Precision, expressed as relative standard deviation values of concentrations, retention factors and effective mobilities, of the developed HPLC and CZE methods for analysis of 1,4-BZDs

	HPLC				CZE			
	Repeatability		Reproducibility		Repeatability		Reproducibility	
	R.S.D.(c) %	R.S.D.(k) %	R.S.D.(c) %	R.S.D.(k) %	R.S.D.(c) %	R.S.D.(μ_{eff}) %	R.S.D.(c) %	R.S.D.(μ_{eff}) %
chlordiazepoxide	0.965	0.229	1.66	0.635	3.94	0.950	14.7	2.06
bromazepam	0.999	0.188	1.81	0.262	4.11	0.743	9.09	1.11
oxazepam	0.985	0.108	1.37	0.245	4.74	0.732	8.12	0.326
nitrazepam	0.943	0.145	1.18	0.313	x	x	x	x
flunitrazepam	1.24	0.131	1.30	0.261	4.11	0.486	8.87	0.439
lormetazepam	1.14	0.123	1.70	0.227	x	x	x	x
diazepam	1.07	0.132	2.20	0.362	4.10	0.903	11.2	1.19

c, concentration; *k*, retention factor; μ_{eff}, effective mobility; R.S.D, relative standard deviation.
repeatability – the R.S.D. values were calculated from ten consecutive injections of the mixture of analytes.
reproducibility – the R.S.D. values were calculated from measurements obtained by different scientists within a period of 3 days.

Table 3. Linearity – parameters of the obtained linear regression equations

	HPLC				CZE			
	slope / 10^3 mV s ml mg^{-1}	intercept / mV s	R	S.D.	slope / mAU ml mg^{-1}	intercept / 10^{-3} mAU	R	S.D. / 10^{-3}
chlordiazepoxide	2.85	−56	0.9992	41.5	2.85	5	0.9919	14.5
bromazepam	2.80	−7.2	0.9999	4.41	1.09	5	0.9949	3.79
oxazepam	23.32	−4.7	0.9999	3.37	1.19	1	0.9987	2.62
nitrazepam	15.93	4	0.9999	7.54	x	x	x	x
flunitrazepam	13.49	−3.6	0.9999	3.04	0.41	0.4	0.9956	1.38
lormetazepam	21.77	−10	0.9999	12.0	x	x	x	x
diazepam	26.9	5	0.9998	11.8	2.34	3	0.9982	5.40

Table 4. LOD and LOQ data under optimized separation conditions – see the text

	HPLC		CZE	
	LOD / ng ml^{-1}	LOQ / ng ml^{-1}	LOD / μg ml^{-1}	LOQ / μg ml^{-1}
chlordiazepoxide	8.68	28.9	1.63	5.44
bromazepam	7.89	26.3	4.27	14.3
oxazepam	8.91	29.7	2.98	9.94
nitrazepam	17.1	56.8	x	x
flunitrazepam	26.7	89.0	11.2	37.3
lormetazepam	17.8	59.2	x	x
diazepam	22.8	75.9	1.57	5.22

x - not quantified.

Limit of Detection and Limit of Quantification

The limit of detection (LOD), expressed as a concentration at a signal-to-noise ratio 3:1, was calculated on the basis of the baseline noise, which was evaluated by recording the detector response over a period of approximately ten times the widths of the peaks. The signal-to-noise ratio of 10:1 was used to determine the limit of quantification (LOQ). LODs and LOQs were calculated for all seven 1,4-benzodiazepines under the optimized isocratic HPLC conditions. Under the optimized separation conditions in CZE LODs and LOQs were determined for the five separated BZDs. It was not possible to quantify the peak of lormetazepam because its mobility (at the pH of the BGE) was very close to zero and therefore close to the mobility of the stationary system peak. The observed resonance substantially changed the peak height (area), which could not be used anymore for quantification of the analyte. The LODs and LOQs data are summarized in Table 4.

Robustness Studies

One-way ANOVA statistical method was used for robustness testing. The selected variable parameters of the HPLC method were: column temperature (24 °C, 25 °C and 26°C), pH of the aqueous part of the mobile phase (2.8, 3.0 and 3.2) and acetonitrile content in the mobile phase (40 % ± 2 %). The tested parameters of the CZE method were: temperature (24 °C, 25 °C and 26 °C) and background electrolyte pH (2.0 ± 0.2 pH units). The robustness was determined from triplicate injections of 0.01 mg/ml of the set of seven 1,4-BZDs and of 0.05 mg/ml of the set of five 1,4-BZDs in HPLC and CZE, respectively, for every change of the tested parameters. The effect of the method parameters on retention factors or effective mobilities and analytes concentrations was calculated. The hypothesis that errors resulted from a normal distribution was tested first. This hypothesis was accepted in all cases (at α = 0.05). Consequently, the robustness of the method was examined using the one-way ANOVA - see Experimental. The null hypothesis

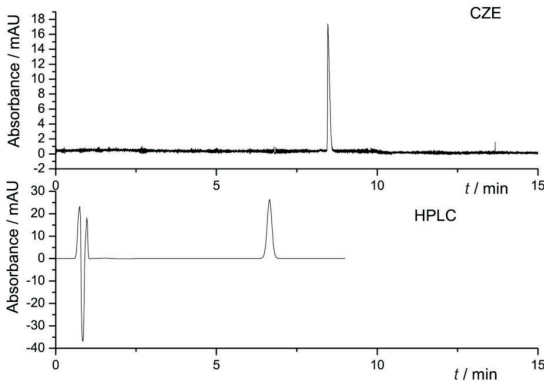

Figure 3. Reports of diazepam tablets analyses under optimized CZE and HPLC conditions. For details see captions to Figures 1 and 2 or Experimental.

was accepted in almost all cases (obtained *p*-values were higher than 0.05), so the robustness of the selected parameters of the methods was verified. An exception was the background electrolyte pH. The effect of an increase of the BGE pH value on the effective mobility and concentration of chlordiazepoxide and diazepam could not be evaluated by one-way ANOVA due to their co-migration.

Real Sample Analysis – Accuracy

Two different tablets containing 10 mg of diazepam and 3 mg of bromazepam were analyzed three times in concentrations of 0.01 mg/ml and 0.05 mg/ml using the optimized HPLC and CZE methods, respectively. Accuracy of the methods, regarded as the closeness of agreement between the claimed contents of tablets and the found values, were 103.2 % for bromazepam and 102.9 % for diazepam by the HPLC method. Accuracy of the CZE analyses were 109.8 % for bromazepam and 103.2 % for diazepam. The reports of the analyses of diazepam are shown in Figure 3. The same results can be achieved for other pharmaceutical preparations containing BZDs.

Comparison of HPLC and CZE Methods

RP-HPLC and CZE methods for separation of 1,4-benzodiazepines were developed and optimized. The HPLC analysis under isocratic elution conditions can be achieved within 7 mins, application of mobile phase gradient can reduce the analysis time to 4.5 minutes. Separation of 1,4-benzodiazepines requires separation time of 17 minutes in the optimized CZE system if additional pressure is applied. The LOD and LOQ values are approximately three orders of magnitude lower in HPLC than in CZE. There are two reasons for these quantification results in CZE: (i) the baseline noise is much higher in CZE than in HPLC, and (ii) lower sample volume is injected in CZE (6 nl) in comparison with HPLC (10 µl). On the other hand the plate number / meter is an order of magnitude higher in CZE than in HPLC. Narrower profiles of peaks obtained in capillary zone electrophoresis can make easier and more reliable quantification from the peak height (compare the analyte´s peaks in Figure 3).

CONCLUSION

HPLC and CZE were proved to be suitable methods for separation of benzodiazepines and for their qualitative and quantitative analyses in pharmaceutical formulations. From the results obtained it is obvious that the method of first choice is RP-HPLC.

Acknowledgements. Financial supports of the Grant Agency of the Czech Republic, grant No. 203/08/1428, CEEPUS, grant No. CII-HU-0010-04-0910, the Grant Agency of the Charles University, grant No. 51009 and the long-term research plan of the Ministry of Education of the Czech Republic, No. MSM 0021620857 are gratefully acknowledged. The authors want to express their gratitute Renata Gilar for language corrections.

REFERENCES

1. L. A. Berrueta, B. Gallo, and F. Vicente, *J. Pharm. Biomed. Anal.* **10** (1992) 109–136.
2. S. McClean, E. O'Kane, J. Hillis, and W. F. Smyth, *J. Chromatogr. A* **838** (1999) 273–291.
3. A. EL Mahjoub and C. Staub, *J. Chromatogr. B* **742** (2000) 381−390.
4. E. Lavie, M. Fatséas, C. Denis, and M. Auriacombe, *Drug Alcohol Depend.* **99** (2009) 338–344.
5. Z. Es´haghi, L. Daneshvar, P. Salari, and S. Bandegi, *Chemija* **20** (2009) 180–185.
6. T. Ishida, Y. Obara, and C. Kamei, *J. Pharmacol. Sci.* **111** (2009) 44–52.
7. L. Mercolini, R. Mandrioli, M. Amore, and M. A. Raggi, *J. Sep. Sci.* **31** (2008) 2619–2626.
8. S. J. Marin, R. C. M. Merrell, and G. A. McMillin, *J. Anal. Toxicol.* **32** (2008) 491–498.
9. V. F. Samanidou, A. P. Pechlivanidou, and I. N. Papadoyannis, *J. Sep. Sci.* **30** (2007) 679–687.
10. O. F. Drummer, *J. Chromatogr. B* **713** (1998) 201–225.
11. A. A. Salem, B. N. Barsoum, and E. L. Izake, *Anal. Chem. Acta* **498** (2003) 79–81.
12. K. H. Beyer and S. Martz, *Arch. Pharm.* **324** (1991) 933–935.
13. A. Elbrashy, F. A. Aly, and F. Belal, *Microchim. Acta* **110** (1993) 55–60.
14. O. Quintela, F.-L. Sauvage, F. Charvier, J.-M. Gaulier, G. Lachatre, and P. Marquet, *Clin. Chem.* **52** (2006) 1346–1355.
15. P. R. Puopolo, M. E. Pothier, S. A. Volpicelli, and J. A. Flood, *Clin. Chem.* **37** (1991) 701–706.
16. G. McGrath, S. McClean, E. O'Kane, W. F. Smyth, and F. Tagliaro, *J. Chromatogr. A* **735** (1996) 237–241.
17. R. Webb, P. Doble, and M. Dawson, *Electrophoresis* **28** (2007) 3553–3565.
18. T. K. Natishan, *J. Liq. Chromatogr.* RT **28** (2005) 1115–1160.
19. A. Jouyban and E. Kenndler, *Electrophoresis* **29** (2008) 3531−3551.
20. M. C. V. Mamani, J. A. Farfán, F. G. R. Reyes, and S. Rath, *Talanta* **70** (2006) 236–243.

21. J. L. Hintze, NCSS User's Guide II, NCSS, Kaysville, UT, USA, 2007.
22. B. Gaš, M. Jaroš, V. Hruška, I. Zusková, and M. Štědrý, *LC GC Europe* **18** (2005) 282–288.
23. M. Štědrý, M. Jaroš, and B. Gaš, *J. Chromatogr. A* **960** (2002) 187–198.
24. B. Gaš, V. Hruška, M. Dittmann, F. Bek, and K. Witt, *J. Sep. Sci.* **30** (2007) 1435–1445.
25. J. L. Beckers, P. Gebauer, and P. Boček, *J. Chromatogr. A* **916** (2001) 41–49.
26. B. Gaš and E. Kenndler, *Electrophoresis* **25** (2004) 3901−3912.

5. Závěr

Předkládaná práce byla zaměřena na zlepšení možností predikce systémových píků v kapilární zónové elektroforéze a na vyšetření vlastností elektroforetických systémů, kde se uplatňují komplexační rovnováhy.

Za účelem predikce tvarů systémových píků byl odvozen nový nelineární model elektromigrace, který byl implementován do nové verze programu PeakMaster 5.3. Funkčnost a správnost PeakMasteru 5.3 byla potvrzena porovnáním jeho výpočtů se simulacemi numerického simulátoru Simul 5. Dále byly vybrány tři typy elektroforetických systémů, u kterých byly sledovány změny tvarů a amplitud systémových píků v závislosti na složení dávkovaného vzorku a také tvaru dávkované zóny. Shoda predikcí PeakMasteru 5.3 a získaných experimentů potvrdila, že PeakMaster 5.3 je schopný správně predikovat tvary a amplitudy systémových píků a může tak výrazně zlepšit jejich identifikaci v reálných elektroforetických záznamech. Zároveň je možné s použitím PeakMasteru 5.3 optimalizovat složení dávkované zóny právě s ohledem na tvary a polaritu systémových píků elektroforetického systému.

Ve své druhé části se práce zabývala elektroforetickými systémy, ve kterých dochází ke komplexaci pufrující složky s přítomným komplexačním činidlem. Bylo prokázáno, že v důsledku zmíněné komplexace může i přídavek neutrálního komplexačního činidla zapříčinit výraznou změnu vlastností základního elektrolytu, což má za důsledek vážné zkreslení různých elektroforetických výsledků. Vyšetřen byl dopad na hodnotu stanovovaných komplexačních konstant metodou afinitní kapilární elektroforézy a negativní vliv komplexujícího pufru byl také demonstrován na separaci sady aminokyselin. Bylo prokázáno, že chování systémových píků v systémech s neutrálním komplexačním činidlem se neřídí lineární teorií elektromigrace v té formě, jak jsme ji doposud vyvinuli. V důsledku vzniku komplexu složka pufru – komplexační činidlo vzniká v daných systémech nový systémový pík, který může mít výraznou mobilitu a zasahovat tak do oblasti migrace analytů. Rovněž se mění i mobility stávajících systémových píků. Chování systémových píků v komplexujících systémech nemohou být zatím efektivně vyšetřovány pomocí stávajících predikčních programů.

Měření změn pH po přídavku komplexačního činidla do roztoku BGE bylo navrženo jako snadná a spolehlivá metoda k odhalení nechtěných komplexací v elektroforetických systémech.

V závěru práce byl zařazen příklad využití programu PeakMaster v běžné analytické praxi. Na základě několika málo experimentů a s využitím PeakMasteru byl vybrán vhodný separační systém pro separaci sady benzodiazepinů.

6. Literatura

[1] Cassidy, R. M.; Fraser, M. *Chromatographia* **1984,** *18*, 369-373

[2] Levin, S.; Grushka, E. *Analytical Chemistry* **1986,** *58*, 1602-1607

[3] Jackson, P. E.; Haddad, P. R. *Journal of Chromatography* **1985,** *346*, 125-137

[4] Melander, W. R.; Erard, J. F.; Horvath, C. *Journal of Chromatography* **1983,** *282*, 229-248

[5] Foret, F.; Fanali, S.; Ossicini, L.; Bocek, P. *Journal of Chromatography* **1989,** *470*, 299-308

[6] Lokajova, J.; Hruska, V.; Tesarova, E.; Gas, B. *Electrophoresis* **2008,** *29*, 1189-1195

[7] Hage, D. S.; Tweed, S. A. *Journal of Chromatography B* **1997,** *699*, 499-525

[8] Dvorak, M.; Svobodova, J.; Benes, M.; Gas, B. *Electrophoresis* **2013,** *34*, 761-767

[9] Gebauer, P.; Beckers, J. L.; Bocek, P. *Electrophoresis* **2002,** *23*, 1779-1785

[10] Beckers, J. L.; Bocek, P. *Electrophoresis* **2003,** *24*, 518-535

[11] Gas, B.; Kenndler, E. *Electrophoresis* **2004,** *25*, 3901-3912

[12] Gas, B.; Hruska, V.; Dittmann, M.; Bek, F.; Witt, K. *Journal of Separation Science* **2007,** *30*, 1435-1445

[13] Thormann, W.; Breadmore, M. C.; Caslavska, J.; Mosher, R. A. *Electrophoresis* **2010,** *31*, 726-754

[14] Hruska, V.; Jaros, M.; Gas, B. *Electrophoresis* **2006,** *27*, 984-991

[15] Mao, Q. L.; Pawliszyn, J.; Thormann, W. *Analytical Chemistry* **2000,** *72*, 5493-5502

[16] Bercovici, M.; Lele, S. K.; Santiago, J. G. *Journal of Chromatography A* **2009,** *1216*, 1008-1018

[17] Bercovici, M.; Lele, S. K.; Santiago, J. G. *Journal of Chromatography A* **2010,** *1217*, 588-599

[18] Longsworth, L. G. *Journal of the American Chemical Society* **1945,** *67*, 1109-1119

[19] Alberty, R. A. *Journal of the American Chemical Society* **1950,** *72*, 2361-2367

[20] Beckers, J. L. *Journal of Chromatography A* **1994,** *662*, 153-166

[21] Beckers, J. L. *Journal of Chromatography A* **1995,** *693*, 347-357

[22] Beckers, J. L. *Journal of Chromatography A* **1995,** *696*, 285-294

[23] Beckers, J. L. *Journal of Chromatography A* **1996,** *741*, 265-277

[24] Beckers, J. L. *Journal of Chromatography A* **1997,** *764*, 111-126

[25] Gebauer, P.; Bocek, P. *Journal of Chromatography A* **1997,** *772*, 73-79

[26] Mikkers, F. E. P. *Analytical Chemistry* **1997,** *69*, 333-337

[27] Gebauer, P.; Bocek, P. *Analytical Chemistry* **1997,** *69*, 1557-1563

[28] Gebauer, P.; Caslavska, J.; Thormann, W.; Bocek, P. *Journal of Chromatography A* **1997,** *772*, 63-71

[29] Beckers, J. L. *Journal of Chromatography A* **1999,** *844*, 321-331

[30] Beckers, J. L. *Electrophoresis* **2001,** *22*, 2684-2690

[31] Gebauer, P.; Borecka, P.; Bocek, P. *Analytical Chemistry* **1998,** *70*, 3397-3406

[32] Gebauer, P.; Pantuckova, P.; Bocek, P. *Analytical Chemistry* **1999,** *71*, 3374-3381

[33] Desiderio, C.; Fanali, S.; Gebauer, P.; Bocek, P. *Journal of Chromatography A* **1997,** *772*, 81-89

[34] Macka, M.; Haddad, P. R.; Gebauer, P.; Bocek, P. *Electrophoresis* **1997,** *18*, 1998-2007

[35] Beckers, J. L.; Gebauer, P.; Bocek, P. *Electrophoresis* **2001,** *22*, 3648-3658

[36] Poppe, H. *Analytical Chemistry* **1992,** *64*, 1908-1919

[37] Poppe, H. *Journal of Chromatography A* **1999,** *831*, 105-121

[38]Bruin, G. J. M.; Vanasten, A. C.; Xu, X. M.; Poppe, H. *Journal of Chromatography* **1992,** *608*, 97-107

[39] Sellmeyer, H.; Poppe, H. *Journal of Chromatography A* **2002,** *960*, 175-185

[40] Stedry, M.; Jaros, M.; Gas, B. *Journal of Chromatography A* **2002,** *960*, 187-198

[41] Stedry, M.; Jaros, M.; Vcelakova, K.; Gas, B. *Electrophoresis* **2003,** *24*, 536-547

[42] Stedry, M.; Jaros, M.; Hruska, V.; Gas, B. *Electrophoresis* **2004,** *25*, 3071-3079

[43] Hruska, V.; Jaros, M.; Gas, B. *Electrophoresis* **2006,** *27*, 513-518

[44] Riesova, M.; Hruska, V.; Kenndler, E.; Gas, B. *Journal of Physical Chemistry B* **2009,** *113*, 12439-12446

[45] Hruska, V.; Stedry, M.; Vcelakova, K.; Lokajova, J.; Tesarova, E.; Jaros, M.; Gas, B. *Electrophoresis* **2006,** *27*, 4610-4617

[46] Jaros, M.; Hruska, V.; Stedry, M.; Zuskova, I.; Gas, B. *Electrophoresis* **2004,** *25*, 3080-3085

[47] echmet.natur.cuni.cz

[48] Onsager, L.; Fuoss, R.M., *Journal of Physical Chemistry* **1932**, *36*, 2689-2778

[49] Vcelakova, K.; Zuskova, I.; Porras, S. P.; Gas, B.; Kenndler, E. *Electrophoresis* **2005,** *26*, 463-472

[50] Hruska, V.; Svobodova, J.; Benes, M.; Gas, B., *Journal of Chromatography A* **2012,** *1267*, 102-108

[51] Benes, M.; Svobodova, J.; Hruska, V.; Dvorak, M.; Zuskova, I.; Gas, B. *Journal of Chromatography A* **2012,** *1267*, 109-115

[52] Hruska, V.; Benes, M.; Svobodova, J.; Zuskova, I.; Gas, B. *Electrophoresis* **2012,** *33*, 938-947

[53] Breadmore, M. C.; Kwan, H. Y.; Caslavska, J.; Thormann, W. *Electrophoresis* **2012,** *33*, 958-969

[54] Caldwell, J. *Journal of Chromatography A* **1996**, *719*, 3-13

[55] FDA'sPolicy StatementfortheDevelopmentof New Stereoisomeric Drugs, *Chirality* 1992, *4*, 338-340

[56] Wren, S. A. C.; Rowe, R. C. *Journal of Chromatography* **1992,** *603*, 235-241

[57] Rawjee, Y. Y.; Staerk, D. U.; Vigh, G., *Journal of Chromatography* **1993,** *635*, 291-306

[58] Rawjee, Y. Y.; Williams, R. L.; Vigh, G. *Journal of Chromatography A* **1993,** *652*, 233-245

[59] Chen, Y. R.; Ju, D. D.; Her, G. R. *Journal of High Resolution Chromatography* **2000,** *23*, 409-412

[60] Fang, L.; Yin, X. B.; Wang, E. *Analytical Letters* **2007,** *40*, 3457-3471

[61] Gas, B.; Zuska, J.; Coufal, P.; van de Goor, T. *Electrophoresis* **2002**, *23*, 3520-3527

[62] Sparc online calculator, https://archemcalc.com/sparc.html

[63] MarvinSketch, ChemAxon, http://www.chemaxon.com/products/marvin/

Přílohy

A. Seznam publikací

1. Electromigration Oscillations Occurring in Ternary Electrolyte Systems with Complex Eigenmobilities, as Predicted by Theory and Ascertained by Capillary Electrophoresis
M.Riesová, V. Hruška, E. Kenndler, B. Gaš
The Journal of Physical Chemistry B, 2009, 113, 12439–12446

2. Polyaniline synthesis with iron(III) chloride-hydrogen peroxide catalyst system: Reaction course and polymer structure study
M. Bláha, **M. Riesová**, J. Zedník, A. Anžlovar, M. Žigon, J. Vohlídal
Synthetic Metals, 2011, 161, 1217-1225

3. Separation and Quantification of 1,4-benzodiazepines: HPLC versus CZE
K. Kalíková, **M. Riesová**, R. Chudoba, M.G. Schmid, E. Tesařová
Croatica Chemica Acta, 2011, 84, 367-373

4. Recent chiral selectors for separation in HPLC and CE
K. Kalíková, **M. Riesová**, E. Tesařová
Central European Journal of Chemistry, 2012, 10, 450-471

5. Nonlinear Electrophoretic Model for PeakMaster: I. Mathematical Model
V. Hruška, **M. Riesová**, B. Gaš
Electrophoresis, 2012, 33, 923-930

6. Nonlinear Electrophoretic Model for PeakMaster: II. Experimental Verification
M. Riesová, V Hruška, B. Gaš
Electrophoresis, 2012, Vol. 33, 931-937

7. Complexation of buffer constituents with neutral complexation agents: Part I. Impact on common buffer properties
M. Riesová, J. Svobodová, Z. Tošner, M. Beneš, E. Tesařová, B. Gaš
Analytical Chemistry (*v době podání práce úspěšně prošlo 1. kolem recenzního řízení)*

8. Complexation of buffer constituents with neutral complexation agents: Part II. Practical impact in capillary zone electrophoresis
M. Beneš, **M. Riesová**, J. Svobodová, E. Tesařová, P. Dubský, B. Gaš
Analytical Chemistry *(v době podání práce úspěšně prošlo 1. kolem recenzního řízení)*

B. Seznam konferenčních příspěvků

Přednášky:

1. Seeking for ampholytes for oscillating electrolytes in CZE
M. Riesová, L. Maliňáková, V. Hruška, B. Gaš
10th International Symposium and Summer School on Bioanalysis, září 2011, Graz, Rakousko

2. Influence of complexation on basic properties of background elektrolyte
M. Riesová, J. Svobodová, P. Dubský, B. Gaš
12th International Symposium and Summer School on Bioanalysis, červenec 2012, Cluj-Napoca, Rumunsko

3. Vliv komplexace na vlastnosti základného elektrolytu v kapilární elektroforéze
M. Riesová, J. Svobodová, P. Dubský, B. Gaš
64. Sjezd chemických společností, červen 2012, Olomouc

4. System Peak Bahavior in Complexing Background Electrolytes
M. Riesová, J. Svobodová, M. Beneš, Z. Tošner, E. Tesařová, B. Gaš
13th International Symposium and Summer School on Bioanalysis, červenec 2013, Debrecen, Maďarsko

Plakátová sdělení:

1. Electrophoretic Systems with Complex System Mobilities – Oscillating Electrolytes
M. Riesová, V. Hruška, B. Gaš
15th International Symposium on Separation Sciences & 8th Balaton Symposium, září 2009, Siofok, Maďarsko

2. Oscillating Electrolytes in Electrophoresis
M. Riesová, V. Hruška, B. Gaš
9th International Symposium and Summer School on Bioanalysis, září 2009, Blagoevgrad, Bulharsko

3. Electromigration Oscillations Occuring in Ternary Electrolyte Systems
M. Riesová, V. Hruška, B. Gaš
25th International Symposium on Microscale BioSeparation, březen 2010, Praha

4. System Peaks in Capillary Zone Electrophoresis: PeakMaster 6.0
M. Riesová, V. Hruška, B. Gaš
16th International Symposium on Separation Science, září 2010, Řím, Itálie

5. New Version of PeakMaster: Shapes and Amplitudes of System Peaks
M. Riesová, V. Hruška, B. Gaš
10th International Symposium and Summer School on Bioanalysis, červenec 2010, Záhřeb, Chorvatsko

6. Searching for Ampholytes Suitable for Oscillating Electrolytes in CZE
M. Riesová, L. Maliňáková, B. Gaš
36th International Symposium on High-Performance Liquid Phase Separations and Related Techniques, červen. 2011, Budapešť, Maďarsko

7. Shapes and Aplitudes of System Peak
M. Riesová, V. Hruška, B. Gaš
18th International Symposium on Electro- and Liquid phase-separation techniques, srpen 2011, Tbilisi, Gruzie

8. Impact of Complexation on Basic Characteristics of BGE in Capillary Electrophoresis
M. Riesová, J. Svobodová, P. Dubský, B. Gaš
Advances in chromatography and electrophoresis & Chiranal 2012, červen 2012, Olomouc
BEST POSTER AWARD

9. Effect of Complexation on Properties of BGE in Capillary Electrophoresis
M. Riesová, J. Svobodová, P. Dubský, B. Gaš
29th Interanational Symposium on Chromatography and 18th International Symposium on Separation Sciences, září 2012, Toruń, Polsko